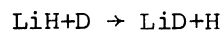
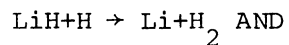


STUDIES OF VALENCE-BOND BASED QUANTUM MECHANICAL

POTENTIAL-ENERGY SURFACES: PART I: $H_2 + D_2$

EXCHANGE REACTION - PART II:



REACTIONS

By

BART HAROLD FREIHAUT
II

Bachelor of Science in Engineering Chemistry
Christian Brothers College
Memphis, Tennessee
1965

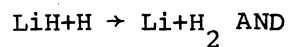
Submitted to the Faculty of the Graduate College
of the Oklahoma State University
in partial fulfillment of the requirements
for the Degree of
DOCTOR OF PHILOSOPHY
December, 1975



STUDIES OF VALENCE-BOND BASED QUANTUM MECHANICAL

POTENTIAL-ENERGY SURFACES: PART I: $H_2 + D_2$

EXCHANGE REACTION - PART II:



REACTIONS

Thesis Approved:

Leon M. Raff

Thesis Adviser

John E. Moore

Herbert A. Pohl

Neci Pundic

J. Paul Devlin

N. N. Durbin

Dean of the Graduate College

964146

ACKNOWLEDGEMENTS

I would first like to express my unbounded love and everlasting gratitude to my wife, Letty, and our twin girls, Beverly and Lorraine, for her and their understanding and patience at times when discouragement in this work was so eminent in my mind. My parents and brother, Jim and sister, Mary Ann also helped me immeasurably thru various difficult periods during my graduate life, and to them my deepest love goes.

I would also like to express my grateful thanks to my thesis advisor, Dr. Lionel M. Raff, who never doubted in my ability and was also there with timely suggestions when research impasses were encountered.

I would also like to thank Oklahoma State University for financial assistance during this work along with the access to university computer facilities. Dr. Ronald Oines is acknowledged for the use of his plotting routines and also Dr. Jerald Hinkel whose matrix diagonalization routine was used in this study.

Finally, I would like to thank the fellow graduate students for their friendship during this study.

TABLE OF CONTENTS

Chapter	Page
PART I: $H_2 + D_2$ EXCHANGE REACTION	
I. ABSTRACT.	2
II. INTRODUCTION.	4
III. HISTORICAL.	7
IV. METHOD.	28
V. RESULTS AND DISCUSSION.	38
VI. CONCLUSIONS AND RECOMMENDATIONS	69
PART II: $LiH + H \rightarrow Li + H_2$ AND $LiH + D \rightarrow LiD + H$ REACTIONS	
VII. INTRODUCTION.	71
VIII. HISTORICAL.	73
IX. METHOD.	80
X. RESULTS AND DISCUSSION.	86
XI. CONCLUSIONS AND RECOMMENDATIONS	109
A SELECTED BIBLIOGRAPHY	111
APPENDIX A. FOR H_4 SYSTEM STUDY.	116
APPENDIX B. FOR H_4 STUDY	118
APPENDIX C. FOR $Li + H + H$ SYSTEM STUDY.	119

LIST OF TABLES

Table	Page
I. List of the Seventeen Matrix Elements One Solves for in the H_4 System.	35
II. Comparison of Results for Two Separate H_2 Molecule Limit	39
III. Comparison of Minimal-Basis VB Computations With Previously Reported Results	49
IV. Comparison of VB and Huckel Results for Trans, T, and Y Conformations.	67
V. Results for the $Li-H_2$ and $LiH-H$ System Limits.	87
VI. Barrier Height Energies and Saddle Points for $LiH+H \rightarrow Li+H_2$ and $Li+H_2 \rightarrow LiH+H$ Reactions for Various Configurations	94
VII. Comparison of VB and CI Results for $Li+H+H$ Collinear Surface.	97
VIII. Well Energies and Associated Points for Various $H-Li-H$ Configurations	98
IX. Energy Contour Values for Figures 24 and 25.	99
X. Contour Values for Figures 26 Thru 30.	100

LIST OF FIGURES

Figure	Page
1. H_4 System Depicting Protons and Electrons in System. . . .	29
2. Contour Plot of H_4 in Unsymmetric "T" Configuraation . . .	43
3. Contour Plot of H_4 in Symmetric "T" Configuration. . . .	44
4. Contour Plot of H_4 in Symmetric 120° "Y" Configuration . .	45
5. Contour Plot of H_4 in Unsymmetric 90° "Y" Configuration. .	46
6. Contour Plot of H_4 in Symmetric 90° "Y" Configuration. . .	47
7. Contour Plot of H_4 in Symmetric Linear Configuration . . .	48
8. Contour Plot of H_4 in a 30° Parallelogram Configuration. .	49
9. Contour Plot of H_4 in a 60° Parallelogram Configuration. .	50
10. Contour Plot of H_4 in Rectangular Configuration.	51
11. Contour Plot of H_4 in a 60° Symmetric Trapezoridal Config- uration.	52
12. Contour Plot of H_4 in 90° Symmetric Kite Configuration . .	53
13. 3-D Plot of H_4 in Unsymmetric "T" Configuration.	54
14. 3-D Plot of H_4 in Symmetric "T" Configuration.	55
15. 3-D Plot of H_4 in Symmetric 120° "Y" Configuration	56
16. 3-D Plot of H_4 in Unsymmetric 90° "Y" Configuration. . . .	57
17. 3-D Plot of H_4 in Symmetric 90° "Y" Configuration.	58
18. 3-D Plot of H_4 in Symmetric Linear Configuration	59
19. 3-D Plot of H_4 in a 30° Parallelogram Configuration. . . .	60
20. 3-D Plot of H_4 in a 60° Parallelogram Configuration. . . .	61
21. 3-D Plot of H_4 in Rectangular Configuration.	62

LIST OF FIGURES (Continued)

Figure	Page
22. 3-D Plot of H_4 in a 60° Symmetric Trapezoidal Configurations.	63
23. 3-D Plot of H_4 in a 90° Symmetric Kite Configuration . . .	64
24. PES for Li-H-H Linear Configuration.	90
25. PES for Li-H-H in 135° Obtuse Triangle Configuration . . .	91
26. 135 Degree VB Surface for Li-H-H	92
27. 90 Degree VB Surface for Li-H-H.	93
28. 135 Degree VB Surface for H-Li-H	101
29. Collinear VB Surface for H-Li-H.	102
30. 90 Degree VB Surface for H-Li-H.	103
31. 3-D Plot of Li-H-H in Linear Configuration	104
32. 3-D Plot of Li-H-H in 135 Obtuse Triangle Configuration. .	105
33. 3-D Plot of Li-H-H in Right Triangle Configuration	106
34. 3-D Plot of Li-H-H in 45 Acute Triangle Configuration. . .	107

PART I: $\text{H}_2 + \text{D}_2$ EXCHANGE REACTION

CHAPTER I

ABSTRACT

A near ab initio potential energy surface for the $H_2 + D_2 \rightarrow 2HD$ four-body exchange reaction was calculated using a perfect pairing valence-bond formalism for various geometries. The results indicate that the saddle point (lowest barrier height) for the system compatible with a four-body mechanism is achieved in the square configuration with the magnitude of the barrier height energy in close agreement with prior full molecular-orbital self-consistent-field configuration-interaction (MO-SCF-CI) studies. This value, however, is not in good accord with the experimental activation energy for the four-body exchange reaction and possible reasons for the discrepancies are discussed such as O_2 impurities in experimental studies and vibrational excitation mechanisms. The results of the perfect-pairing VB calculations for a "Y" to "T" to "Y" reaction pathway for the four-body exchange, which an extended Huckel calculation indicated was a very plausible one, showed that such a reaction pathway could not yield an activation energy in accord with the experimental results.

The quantum mechanical potential energy surfaces for the $LiH + H \rightleftharpoons Li + H_2$ and $LiH + D \rightarrow LiD + H$ were found as a function of various probable reaction geometries using a valence bond (VB) formalism with ionic terms representing the ionic character of the LiH bond included. This was done for the doublet spin state of the (Li,H,H) sys-

tem. Mulliken's approximation is used to simplify three center integrals and two center exchange integrals. The linear configuration for the $\text{LiH} + \text{H} \rightarrow \text{Li} + \text{H}_2$ gave the lowest barrier height energy of all the configurations tested. The linear barrier height energy was in good agreement with previous studies. The PES for the $\text{LiH} + \text{D} \rightarrow \text{LiD} + \text{H}$ reaction showed a slight potential well for H-Li-D bond angles of 180° to 90° . This is an artifact of the VB method from the use of Mulliken's approximation. Overall the VB method showed good agreement with a full CI calculation on the system.

CHAPTER II

INTRODUCTION

Purpose of Investigation and General Remarks

The $\text{H}_2 + \text{D}_2 \rightarrow 2\text{HD}$ reaction is of considerable interest to both theoretical and experimental chemists in that, it is the simplest illustration of an elementary gas phase kinetic process in which two atoms (H and D) are exchanged in the collision of a pair of molecules (H_2, D_2). Therefore, it is the prototype of more complicated bimolecular exchange reactions, if indeed, this exchange reaction does proceed thru a four-body intermediate. To relate experimental kinetic data on this system to theoretical values and mechanistic models, an accurate quantum mechanical potential-energy surface (PES) for the (H_2, D_2) system is needed. This study is involved with the calculation of such a surface for the $\text{H}_2 + \text{D}_2$ pathways.

The purpose of this work is to calculate a near ab initio quantum mechanical PES for the (H_2, D_2) system for various geometries and determine the geometry of the saddle-point along with its corresponding energy, in order to ascertain whether these values are compatible with the observed activation energy for the exchange process. Two and three-dimensional potential-energy contour maps are given for various geometries of the (H_2, D_2) system. The surfaces and selected energy values are critically compared with other quantum mechanical methods for

obtaining such a surface. Special emphasis is given to comparing the surfaces for a $Y \rightarrow T \rightarrow Y$ type reaction intermediate geometry (1) for the (H_2, D_2) system with one calculated from less stringent theoretical concepts (2).

Theoretical calculations of experimentally determinable quantities, such as activation energy and rate constants, need an accurate quantum mechanical PES in order to be evolved from absolute rate (3) or quasi-classical trajectory analysis (4,5). This PES is especially needed in the region of the saddle-point configuration in order to critically determine if either of these two methodologies can predict results that are in accord with the experimental kinetic data for the $H_2 + D_2 \rightarrow 2HD$ exchange reaction.

The barrier height for the system, which is the energy difference between the saddle-point energy of the PES and the energy of two isolated H_2 molecules, must fall in the near neighborhood of the exchange reactions experimental activation energy in order to have any likelihood of success in obtaining acceptable correlation with experimental kinetic results. Also implied in the above is that the saddle-point geometry also be compatible with a four-body exchange mechanism. That is to say, for a given reaction coordinate to be a viable mechanistic pathway, the saddle-point geometry must be accessible to the reactants. Another situation that might arise is that the saddle-point for a certain geometry might correspond to a three-body intermediate rather than a four-body reaction intermediate which might be inconsistent with experimental observation.

At the present time the mechanistic pathway to $H_2 - D_2$ exchange is very uncertain. The following historical subsection, which states the

experimental work achieved on the (H_2, D_2) system and other PES type calculations on the system, presents the reasons for this situation. It is the purpose of this investigation to attempt to resolve the present paradoxical problem.

CHAPTER III

HISTORICAL

Experimental

Bauer and Ossa (6) have experimentally studied the $\text{H}_2\text{-D}_2 \rightleftharpoons 2\text{HD}$ gas-phase reaction in the temperature range of 1100-1500°K employing a single-pulse shock tube method. In their experimental apparatus a Pyrex tube with end hooked up to pressure transducers and the pressure signals produced by incident and reflected shock waves were measured by means of an amplifier-oscilloscope setup. The average residence time, used in arriving at an empirical power rate expression, was estimated experimentally from the measured time between the arrival of the reflected shock waves at the transducer farther from the end plate of the shock tube and the arrival of the cooling wave at the same point. This, in turn, was used to calculate, from the ideal shock equation, the reaction temperature and corresponding gas densities. The different species' concentrations ($\text{H}_2, \text{D}_2, \text{HD}$) were calculated from the initial and final compositions of the gas mixtures and the corresponding molar densities before and during the reaction. A rather large excess of argon (89 to 98%) was used in the $\text{H}_2\text{-D}_2 \rightarrow 2\text{HD}$ reaction in order to insure low concentrations of H_2 and D_2 (1 to 10%). This minimized the reverse reaction of 2HD to $\text{H}_2\text{-D}_2$. In order to avoid the dissociation of H_2 or D_2 by hot walls of the reactor, which from previous work (7,8) led to

production of HD by a three-body atom displacement chain (H-D_2 or D-H_2) mechanism, gas dynamical methods were used for heating the gaseous system to the high temperature of the four-body exchange reaction in a very short time (10^{-8} sec) under conditions which kept the walls of the reactor essentially at room temperature. Having the reactor walls at essentially room temperature also would seem to exclude the possibility that heterogeneous surface catalysis may produce H and D radicals which then might proceed to give HD thru a nonbimolecular exchange mechanism (9).

Bauer and Ossa (6) arrived at the following empirical rate expression from analysis of data from 62 runs:

$$\frac{\Delta \text{HD}}{\Delta T} = K_p [\text{Ar}]^{.98} [\text{D}_2]^{.66} [\text{H}_2]^{.38} \quad (1)$$

using the Arrhenius type equation:

$$K_p = AT^{\frac{1}{2}} e^{-E_a/RT} \quad (2)$$

where K_p is the rate constant, A is the preexponential factor, T is the reaction temperature, R is the gas law constant, the activation energy (E_a) for the exchange reaction was obtained. The K_p for various runs at different temperature was calculated from (1) having determined reaction orders of Ar, H, D, from the data for that run. A plot of $\log (K_p T^{-\frac{1}{2}})$ vs. $\frac{1}{T}$ yielded a value of E_a equal to $-42.26 \frac{\text{Kcal}}{\text{mole}}$. As will be seen later in the semiempirical and ab initio calculation subsections of the historical portion and the result section of this thesis, E_a is markedly lower than the barrier height energies found from quantum mechanical potential-energy surface calculation for geometric configurations that are compatible with a biomolecular exchange mechanism.

An atom abstraction mechanism based on the homogeneous dissociation of H_2 and D_2 as the first step was dismissed as a viable mechanism due to the fact that under experimental conditions the maximum concentrations of H and D atoms is nine orders of magnitude smaller than number of HD molecules found in the shocked sample under the same conditions. The concentration of the H and D atoms was calculated from the homogeneous rates of H_2 and D_2 dissociation in excess argon (10,11) and quoted values of the rate constants and the magnitude of the equilibrium constants for the dissociation step (12,13).

On comparison with an average rate of HD production calculated in the format of the atom displacement chain mechanism ($H+DD \rightleftharpoons H...D...D \rightarrow HD+D$) and Bauer's experimentally observed magnitude for the average HD production rate ($3 \cdot 10^{-6} \text{ mole cm}^{-3} \cdot \text{sec}^{-1}$), it would require that the atom displacement reaction have a preexponential factor greater than $1.5 \cdot 10^{16} \text{ (cm}^3 \text{ mole}^{-1} \cdot \text{sec}^{-1})$, which is far too great for such a simple bimolecular process. In the above no oxygen contamination was included. Bauer (6) also rules out the possibility of the H atom displacement chain mechanism initiated in the early stages by combustion reactions due to possible impurities of O_2 in their system by calculating that the H atom produced by such a mechanism is very small compared to that which would be needed to explain the overall HD production. Other work indicates that the O_2 impurities, which might be present in the shock tube experiments, imply an extreme increase in H or D atom formation rate so as to present a counter argument to above in terms of a three body atom displacement chain reaction mechanism (14).

Neither the bimolecular exchange mechanism nor the atom displacement chain mechanism explain the difference in the observed (6) reaction

orders relative to H_2 and D_2 (.36 and .66) nor the first-order dependence upon the argon concentration. Also the observed activation energy is higher than expected were the exchange controlled by a combustion process, and it is markedly lower than the barrier-height energies found from PES that are compatible with a bimolecular exchange mechanism (15).

In view of the above and having in-hand the prior investigation of Bauer's (16) on the gas-phase reaction between D_2 and NH_3 where a vibrational excitation mechanism was proposed to explain the results, a similar vibrational excitation mechanism was proposed for the H_2 - D_2 exreaction. In this model Bauer (6) stated that either H_2 or D_2 must first be vibrationally excited to a critical vibrational level by collision with an argon atom. The H_2 or D_2 in turn then will react with a vibrationally unexcited H_2 or D_2 molecule to form 2HD. The slow step in this mechanism is the vibrational excitation of H_2 or D_2 by argon. This might explain the order of Ar, D_2 , H_2 in Equation (1). Bauer (6), using a two-state excitation model and the stationary-state approximation on activated intermediate species, arrived at a rate coefficient (K_v) for this mechanism in terms of the experimental data and in the form of an Arrhenius type equation as:

$$K_v = T^{\frac{1}{2}} e^{-42.65/RT} \text{ mole}^{-1} \text{ cm}^3 \text{ sec}^{-1} \quad (3)$$

with standard deviation in $\log K_v$ vs. $T^{\frac{1}{2}}$ of .084. This model indirectly implies that the relative kinetic energy of the H_2 and D_2 molecules along their lines of the center has little effect on the reaction probability.

As a quantitative test for the vibrational excited mechanism,

Bauer (6) compared the magnitude of the pre-exponential factor of the experimental rate constant (K_v) with that formulated from the measured vibrational relaxation times of deuterium (17,18) in terms of a non-equilibrium, j vibrational state excitation model where the assumptions are that the steady-state condition is imposed for all but the population of the D_2 ground vibrational level and that there is a critical vibrational level (V) for D_2 . Contributions are negligible for all vibrational levels below V because rate coefficients for the exchange reaction from these levels are small even though the population of these levels are significant. Levels higher than V are of negligible contribution to the reaction since their populations are very small compared to equilibrium values due to the depletion of the population in the critical level by reaction which in turn causes depletion of levels higher than V relative to their equilibrium values. From the above an expression for K_v was reached where the vibrational relaxation time for D_2 is in pre-exponential term for K_v . From this analysis the pre-exponential term calculated from vibrational relaxation time data at 1400 °K is approximately one order of magnitude lower than the experimentally derived pre-exponential factor of K_v previously described. Also, from this analysis the vibrational excitation energy is $\approx \frac{\text{Kcal}}{\text{mole}}$ which gives additional plausibility that translational energies of H_2 and D_2 may not be very influential on the possible four-body reaction. Cases of vibrationally excited species of various mineral acids and deuterium at room temperature have also been inferred in reaction with diazomethane (19).

Using a similar single-pulse shock-tube technique as Bauer, Burcat and Lifshitz (20) report a somewhat different observed rate law where the overall reaction order is approximately 2 and the partial order with

respect to argon is $.65 \pm .01$ and that of hydrogen plus deuterium is 1.3 ± 0.1 . The activation energy is $40 \pm 1 \frac{\text{kcal}}{\text{mole}}$. The above values were obtained from analysis of the relation: $K_m t = - \ln (1 - \text{extent of reaction})$ (4) where K_m is the first-order rate coefficient and t is the time after reaction has been initiated. Their overall observations supply strong supporting evidence for Bauer's "vibrational excitation" mechanism. They explain their reaction orders of argon (0.65) and $\text{H}_2 + \text{D}_2$ (1.3) as compared with Bauer's values, for such, which exclude any contribution to the vibrational excitation step by H_2 or D_2 themselves, by the following: They showed thru vibrational relaxation data of H_2 and D_2 (17,18) that indeed excitation of H_2 or D_2 can be accomplished by H_2 or D_2 as well as Ar. They arrive at a calculated value of 1.2 for the total reaction order of $\text{H}_2 - \text{D}_2$ from the previously mentioned vibrational relaxation data which is in good agreement to their experimentally derived value of 1.3 ± 0.1 .

Lewis and Bauer (21) studied the deuterium hydride (HD) self-exchange reaction (reverse reaction of $\text{H}_2 + \text{D}_2 \rightarrow 2\text{HD}$) by the same experimental shock-tube method as reported previously in this section. They reported an activation energy of $35.9 \frac{\text{kcal}}{\text{mole}}$ and a 1.43 reaction order dependence for HD and a 0.57 reaction order for argon.

Poulson (22) used a system of coupled vibrational-relaxation reactions (master equations numerically solved herein with necessitated approximations included) and exchange reactions to describe a theoretical reaction mechanism for the $\text{H}_2 + \text{D}_2 \rightarrow 2\text{HD}$ reactions in presence of excess argon. From her study she concluded that H_2 and D_2 react with a higher probability when the energy for exchange originates in vibrational rather than translational energy mode. Agreement with Bauer's experimental

shock-tube results (6) was reached when the experimental rate constants for vibrational relaxation of H_2 and D_2 (17,18) were used. Poulson reports the minimum energy needed for reaction is about 38 Kcal/mole in addition to zero point vibrational energy and the important elementary reactions are $D_2^{(3)} + H_2^{(1)}$, $D_2^{(2)} + H_2^{(2)}$ and possibly $D_2^{(1)} + H_2^{(2)}$ where the superscripts are the vibrational quantum numbers. The concentration dependence of argon, which from her analysis gave a reaction order of .55 to argon on the reaction rate, was explained in that excitation of H_2 and D_2 by Ar is needed because concentrations of the species ($D_2^{(3)}$ and $H_2^{(2)}$) are depleted below their equilibrium values in the non-equilibrium mechanism. Two major differences between her conclusions and Bauer's are that she states that the translational degree of freedom can contribute part of the necessary energy for reaction to occur and that reactions in which both D_2 and H_2 are vibrationally excited are likely to dominate over those in which one species carries all the activation energy. Also, in contrast to Bauer's implication that the experimentally measured activation energy (E_A) is larger than that necessary for reaction to occur, Poulson concludes that this is true only when either H_2 or D_2 is in the ground vibrational state and in this condition the relative translational energy does not increase the reactivity. In Poulson's mechanism, the theoretical activation energy (36 Kcal/mole) is slightly smaller than the necessary energy (38 Kcal/mole) for reaction to occur and the temperature dependence of vibrational relaxation constants of H_2 and D_2 contribute positively to E_A to enable the reaction to occur in light of classical energy considerations.

Kern and Nika (23) studied the rate of exchange of H_2 and D_2 by using the coupling of a shock tube to a time-of-flight mass spectro-

meter (TOF). Reflected shock waves of equimolar mixtures of H_2 and D_2 (1.5 to 3%) diluted in neon were analyzed at 20 μ sec intervals by the TOF. The temperature range studied was 1800 $^\circ K$ to 3000 $^\circ K$ with a typical measured reaction time being 500 μ sec. For several of the runs at temperatures exceeding 2600 $^\circ K$ equilibrium was reached during the observation time. Reaction profile were fitted to the equation (5):

$$(1-2f_{HD}) = e^{-K[M]t^2} \quad (5)$$

having previously determined from their data that the mole fraction

$$f = \frac{[HD]}{2[H_2]_0} \quad (6)$$

was indeed quadratic with respect to time. In Equation (5) M is the concentration of neon and K is the forward rate constant equal to the form:

$$K = Ae^{-\frac{E_A}{RT}} \quad (7)$$

which from an Arrhenius type analysis of the data yielded

$$A = 10^{16.93 \pm 0.24} \text{ cm}^3 \text{ mole}^{-1} \text{ sec}^{-2} \quad (8)$$

and activation energy

$$(E_A) = 44.37 \pm 2.51 \text{ Kcal/mole} \quad (9)$$

Bauer's data (6) was analyzed in terms of Equation (5) and yielded

$$A = 10^{17.10 \pm 0.15} \text{ cm}^3 \text{ mole}^{-1} \text{ sec}^{-2} \quad (10)$$

and

$$E_A = 43.50 \pm 0.89 \text{ kcal/mole} \quad (11)$$

which was within one standard deviation with respect to both $\log A$ and E_A determined from their own data. They showed that Bauer's critical vibrational excitation mechanism (6), in light of the use of the steady-state approximation in it, is inconsistent with their reported non-linear (quadratic) time dependence for the exchange reaction. In addition, they state that a straight four-center molecular mechanism would predict zero order dependence on the inert gas, a linear time dependence, and a considerably higher activation energy. An atomic mechanism was ruled out in that it would require a combined order dependence of one for reactants expressed on a mole fraction basis and an activation energy of 110 K cal/mole (due principally to dissociation of H_2 to $2H$). They suggest that a solution of the master equation for the vibrational excitation mechanism would be the proper approach. Poulson (22) has attempted such a solution, but in order to obtain numerical solution, a number of approximations were necessary. Her calculations were discussed previously in this subsection in the thesis.

Kern and Nika stated four positive contributions from their work as follows:

- (a) extension of the temperature range to a 2000° interval,
- (b) recording of the exact conversion from zero to equilibrium,
- (c) deduction of a non-linear time dependence for product formation. Previous single-pulse shock experiments (6,20) did not attempt such measurements.

(d) agreement of results (A, E_A) with those obtained from previous shock tube work (6) where absence of gas flow did not complicate the analysis with TOF analysis.

Kern and Nika (24) studied the HD self-exchange reaction using the same shock tube-TOF apparatus as previously mentioned for the $H_2 + D_2$ exchange reaction. The temperature range was 1800 °K to 2800 °K. This work did show consistency with their experimental results reported for the reverse reaction, in that, the activation energy (E_A) for the HD self-exchange reaction was found to be $40.98 \pm 2.25 \frac{\text{kcal}}{\text{mole}}$ compared with $44.37 \pm 2.51 \frac{\text{kcal}}{\text{mole}}$ for the $H_2 - D_2$ reaction. These two activation energies should indeed be of the same magnitude since the overall reaction is almost thermoneutral. In addition, consistency was shown by the HD self-exchange reaction in terms of product formation also being non-linear (quadratic) with respect to time. The equilibrium constant for the overall reaction was obtained using the previously reported (23) rate constant for the forward reaction along with the self-exchange rate constant determined herein and good agreement within experimental errors was obtained with the calculated equilibrium constant.

Recently Bauer and co-workers (25), by use of a stimulated Raman laser (SRL) technique, observed HD production at room temperature from mixtures of H_2 and D_2 . In the SRL technique a pulsed ruby laser was used to stimulate a Stokes field at $10,251 \text{ cm}^{-1}$ with H_2 or $11,415 \text{ cm}^{-1}$ with D_2 in a H_2 or D_2 Raman laser cell which then interacted with a test cell containing a mixture of $H_2 + D_2$ to cause an over-population of $v=1$ vibrational states of either H_2 or D_2 which then led to appreciable occupancy of higher vibrational states of H_2 or D_2 by means of vibrational-vibrational energy transfer between the molecules. This pumping

of higher vibrational levels led to measurable amounts of HD production which Bauer explained in terms of the critical excited vibrational mechanism he had previously proposed (6). This experimental work seemed to provide confirmation for the vibrational excitation mechanism via a four-center process in that diatomic molecules (H_2 or D_2) which had low relative translational velocities (at room temperature) but were vibrationally excited had a high probability for reaction as shown by the measurable amounts of HD production.

Bauer (25) states that the molecular beam experiment of Jaffe and Anderson (26) also adds to the plausibility of a four-center exchange in $H_2 - D_2$ via vibrational excitation mechanism. Jaffe and Anderson (26) showed that when vibrationally unexcited diatomic reactants (HI,DI) collided with rather high kinetic energy of translation (hence high relative translational velocities) ranging from 20 K cal/mole to 110 K cal/mole, which bracketed the anticipated activation energy of about 40 K cal/mole, there was no detectable production of HD. This suggests, from the experimental results of Sullivan (27) for the (H_2, I_2) system, and previously reported theoretical studies (28) that a four-atom center I...H..H....I is possibly involved. Thus, Jaffe and Anderson's negative results for the reverse of the above reaction would imply (by microscopic reversibility) that one or both of the nascent HI molecules are in vibrationally excited states (25). One should note that this story is still not complete and that certain difficulties remain particularly with regards to the shape of the four-center potential-energy surface (29).

Bauer (25) pointed out that an analytical solution necessitated the use of the steady-state approximation in the original critical excited

vibrational mechanism development for $H_2 - D_2$ (6) and that Kern and Nika's (23) observed quadratic time dependence for the exchange reaction was qualitatively reproduced by a computer solution of the master equation using the ten lowest vibrational levels of both H_2 and D_2 . The master equation usage yielded an effective activation energy of 36 to 42 $\frac{\text{kcal}}{\text{mole}}$ along with qualitative agreement for the HD production for both the SRL and shock tube experiments as well as the prediction that the conversion passes thru a maximum similar to that observed in the SRL experiments. The proposals made by Poulson (22) concerning HD formation thru D_2 ($v=2,3$) and H_2 ($v=1,2$) vibrational states needs to be examined by their computer model in that for $V = 1,2$ for H_2 and $V = 2,3$ for D_2 the reaction rate coefficients for those states leading to HD production were assumed to be zero. Bauer (25) did stress the need for a large number of following computer computations to try and quantitatively reproduce the SRL and shock tube results. In terms of the SRL experiments Bauer (25) stated the need to further refine the experimental apparatus so as to eliminate all conceivable heterogenous factors and to test via Lyman-absorption spectroscopy (30) for the possibility of any H atoms present in the test cell by means of the SRL technique.

Semi-Empirical Calculations

The first study to treat the interaction of four hydrogen atoms was done by Eyring (31). It is semiempirical in that in addition to using London's approximate formula (32), he obtained the exchange energy contribution as the difference between the experimental total energy obtained from spectra and the calculated Coulombic terms. By varying the ratio of exchange energy to Coulombic energy, he calculated an activa-

tion energy of 60 Kcal/mole and his transition state from absolute rate theory analysis consisted of H_4 in a square of side length 1.2 Angstroms (.635 a.u.).

Benson (33) employed the semiempirical Benson-Bose semi-ion pair model to calculate the activation energy for the reaction discussed here. He postulated that the reaction would proceed thru a rectangular transition state and that the activation energy was 61.5 K cal/mole. The saddle point was at a distance of 1.74 a.u. between the centers of H_2 and D_2 .

Abrams (34) has used the semiempirical diatomics in molecules method to calculate the H_4 energy in various configurations. The molecular wave function is expanded linearly in terms of a connical set of 16 determinental VB (Valence-Bond) wave functions formed by making all possible spin assignments to the product of the four Slater type 1s orbitals centered at the four nuclei of H_4 . Ionic terms were not included. Various energy matrix elements are approximated in terms of experimental ground and excited state energies of all possible diatomic and monoatomic fragments of the polyatomic along with the use of the overlap integrals between the VB wave functions. Barrier height energies were 52 K cal/mole for the linear case, 67.5 K cal/mole for the square ($R = 2$ a.u.), 98 K cal/mole for the rhombus and 134 K cal/mole for the tetrahedron.

Morokuna and Pederson (35) employed the perfect pair VB formulation along with several semiempirical approximations (36) to study the H_4 reaction surface. Their approximations were:

- (1) The sum of the kinetic energy and $\frac{1}{r}$ terms of the Hamiltonian operator operating on the 1s Slater wave function are set

equal to zero since the isolated hydrogen atom was taken as the zero energy point.

- (2) A Morse-type function (36) was used for the 1E state of H_2 and a Sato-type function (37) for the 3E state of H_2 , both of which are based on the Kolos-Roothaan calculations (38) along with the Heitler-London expression for the singlet ground-state energy (1E) of H_2 and the triplet first excited state (3E) of H_2 . These functions were used to obtain an expression for the Coulombic integrals and single-exchange integrals.
- (3) The double-exchange integrals were obtained from an empirical expression of the form, E, S_1, S_2, S_3 , where E is a defined constant and S_1, S_2, S_3 are overlap integrals.
- (4) Integrals of the type $\langle ab | \frac{1}{r_{12}} | cd \rangle$ are set equal to zero based on the zero differential overlap approximation.
- (5) The screening parameter (δ) in the Slater $1s$ wave function is assumed to be a function of internuclear distance.

On their potential-energy surface (PES) the saddle-point geometry for the exchange reaction is a square of side length 1.970 a.u. with a barrier height equal to 62.7 K cal/mole. In contrast to Bauer's (6) mechanism for the $H_2 + D_2 \rightarrow 2HD$ reaction, their quasiclassical trajectory analysis on the $H_2 - D_2$ system, employing the before-mentioned semi-empirical potential-energy surface, indicated that there is no theoretical evidence for a "vibrational threshold", that is, a critical vibrational excitation for the $H_2 + D_2$ exchange reaction. Their calculations showed that an increase in vibrational energy availability is, by itself, not sufficient to produce such a "vibrational threshold" to occur the translational energy must be significantly, less effective than vibra-

tion energy. Their trajectory calculations did not tend to bear this out. The rate coefficients for the exchange reaction from the trajectory analysis at 1600 °K and 1000 °K were 1.332×10^3 cm³/mole-sec and 1.164×10^3 cm³/mole-sec respectively. The resulting activation energy was 61.64 K cal/mole with a pre-exponential factor of 3.475×10^3 cm³/mole-sec. The absolute rate theory results for the rate coefficients using the same semi-empirical PES were smaller than those from the trajectory treatment (0.643×10^5 cm³/mole-sec at 1600 K and 0.296×10^5 cm³/mole-sec at 1000 K).

Gimarc (2) used an extended Huckel method based on simple MO theory and overlap arguments to suggest a possible pathway for the $H_2 + D_2 \rightarrow 2HD$ reaction. He suggested that a "Y" shaped complex is formed in collision between H_2 and D_2 and that this structure then rearranges through a relatively low-energy pathway, comparable to Bauer's experimental activation energy value, to a "T" structure. Rearrangement in the opposite direction, followed by separation of the "Y" thus formed then leads to the "HD" product.

Ab Initio Calculations

De Boer (39) and Margenau (40,41) both used a VB formalism, similar to the one in this study, but they used only one of the two possible covalent wave functions, to calculate the "exchange energy", along with the quadrupole and Van der Waal's energies, between two H_2 molecules at their equilibrium distances (1.4 a.u.). Their calculated "exchange energy" is analogous to the potential energy of the H_4 system calculated in this study. They both either approximate or neglect all three and four center integrals. Since they both are interested in intermolecular forces, their surface points are not in the range of interest for the

$H_2 + D_2$ reaction study.

Taylor (42) carried out both ab initio molecular orbital (MO) and configuration interaction (CI) calculations on the linear H_4 system with the distances between adjacent atoms being equal to the equilibrium distance of H_2 (1.4 a.u.). He was the first to show that the three- and four-center integrals were of great importance in such a calculation. The screening parameter (δ) of the hydrogenic 1s basis wave functions were set at 1. Also the numerical values of the MO coefficients were not determined with self consistency. Using a single configuration in the MO method, he obtained a value for the energy of the linear H_4 system at 1.4 a.u. of -54.591 e.V. (barrier height = $166 \frac{\text{kcal}}{\text{mole}}$). This energy (-54.591 e.V.) is slightly stable with respect to four isolated hydrogen atoms but not with respect to two isolated H_2 molecules as implied by the barrier height ($166 \frac{\text{kcal}}{\text{mole}}$) being in reference to two isolated H_2 molecules. His CI calculation using six configurations derived from the four molecular orbitals gave an energy of $E = -56.404$ e.V. (barrier height = $125 \frac{\text{kcal}}{\text{mole}}$).

Griffing and Macek (43) used a MO single determinant wave function with hydrogenic 1s basis function ($\delta=1$) to calculate the energy of various square conformations for the H_4 system at selected points and found the quadratic H_4 system to be unstable with respect to 4 H atoms separated at ∞ . The triplet state was found to have the lowest energy values ($R = 1.606$ a.u., $E = -46.0$ e.V. (barrier height = $331 \frac{\text{kcal}}{\text{mole}}$); $R = 2.00$ a.u., $E = -49.9$ e.V. (barrier height = $241 \frac{\text{kcal}}{\text{mole}}$) as compared to singlet-state values.

Griffing and Vanderslice (44) used Roothaan's (45) LCAO-MO-SCF equations for selected points (1.4 a.u., 1.6 a.u., 2.0 a.u., 2.2 a.u.)

on the linearly symmetric H_4 system to calculate the energy for these possible activated complexes for the H_4 system. They found that their energy at $R = 1.4$ a.u. (-55.48 e.V. (barrier height $\approx 48 \frac{\text{kcal}}{\text{mole}}$) was better than Taylor's value (42) using simple MO treatment but poorer than his CI values.

Parker and Eyring (46) compared a non-ionic VB treatment (same as used in this study except that $\delta = 1$ in their Slater atomic orbitals) with the simple MO and limited MO-CI treatment of Taylor (42) for the symmetric linear ($R=1.4$ a.u.) H_4 system. Their values from the VB treatment for the symmetrical linear H_4 using the single covalent structure was -57.02 e.V. (barrier height = $113 \frac{\text{kcal}}{\text{mole}}$) and -58.59 e.V. (barrier height $\approx 77 \frac{\text{kcal}}{\text{mole}}$) using both covalent structures.

Griffing and Ruffa (47) calculated energies for the linear H_4 system as a function of R for various values of r ($H-r-H-R-H-r-H$) using Roothaan's LCAO-MO-SCF method with hydrogenic $1s$ basis functions ($\delta = 1$). Mulliken's approximation (48) was used for three and four-center integrals. A saddle point occurs at $r = R = 1.8$ a.u. with $E = -54.01$ e.V. (barrier height = $65 \frac{\text{kcal}}{\text{mole}}$). Thus, if one looks at this geometry and the associated barrier height energy ($65 \frac{\text{kcal}}{\text{mole}}$) in terms of a four-body reaction intermediate for the $H_2 - D_2$ exchange reaction, one still has the main problem of showing how this linear intermediate can lead to exchange products on geometric arguments. In addition, this barrier height is still approximately 20 K cal/mole higher than the experimental activation energy as reported by Bauer (6) and Kern (23).

Magnasco and Musco have reported both a restricted (49) and full (50) VB treatment of the interaction of two H_2 molecules in their ground state at their equilibrium values of $R = 1.4166$ a.u. as a func-

tion of intermolecular distance between them for various geometries. In the restricted calculations the basic Slater 1s atomic orbitals were symmetrically orthogonalized by means of a Lowdin transformation (51) and all the orthogonalized valence bond (OVb) structures involving formal covalent "long bond", along with the ionic structures arising from overlaps of charge between distant atoms (52), are neglected. The above procedure left nine OVb structures corresponding to the singlet molecular ground state of H_4 . In the full VB treatment all twelve contributing structures resulting from including all covalent and ionic structures were used along with the usage of nonorthogonalized Slater 1s atomic orbitals. In both treatments a basis of four 1s atomic orbitals with $\delta = 1.193$ was used. The full treatment is equivalent to a full CI calculation on this system. The restricted method gave considerably higher interaction energies (difference between the calculated H_4 energy and the energy of two isolated H_2 molecules) than did the unrestricted method. The interaction energy also decreased as the two H_2 molecules changed from a rectangular configuration to the following "staggered" configuration . In the rectangular configuration with side lengths of 1.4166 a.u. and 2.1249 a.u., which is a plausible geometry for a four-body exchange reaction, the interaction energy was .21156 Hartrees (132.7 K cal/mole) which is about three times the experimental activation energy for $H_2 - D_2$ exchange reaction.

Conroy (53) has carried out an ab initio calculation of the PES using a basis set of properly antisymmetrized products of one-electron factors so constructed to give the final wave function cusps at the nuclei of the correct form and such that poles at the nuclei in $\hat{H} \psi$ will be removed. He found the energy of the H_4 system by minimizing the

variance

$$(U)^2 \text{ of } E, U^2 = \frac{\int (\hat{H}\psi - E\psi)^2 dx}{\int \psi^2 dx} \quad (13)$$

The value of E correspond to the point of smallest radius of curvature on the boundary in the plane $[E, U(E)]$. The rectangular-square conformation was the only configuration reported. The saddle point was located at $R = 2.2$ a.u., in the square configuration and the corresponding barrier height energy was 124 ± 6 Kcal/mole.

Schwartz and Schaad (54), using a linear combination of Gaussian orbitals (LCGO)-MO-SCF technique, calculated the energy for the H_4 system in various linear geometries. They obtained lower energy values than Griffing (44,47) who used Slater type 1s orbitals ($\delta = 1$) in a LCAO-MO-SCF treatment that has been previously mentioned. The principal value of Gaussian orbitals used in their study is their ease in integrating as compared with Slater type orbitals although they have wrong functional properties as the nucleus-electron distance approaches zero. A saddle point $R = 1.6$ a.u., for the symmetric linear H_4 system was obtained with an energy value of -2.16686 hartrees which corresponds to a barrier height energy of $65.5 \frac{\text{kcal}}{\text{mole}}$.

Shavitt and Rubenstein (55) carried out an ab initio full CI calculation on the H_4 system using as a basis set eight scaled optimized double-zeta orbitals. The barrier height energies were $43 \frac{\text{kcal}}{\text{mole}}$ for the linear case, 109 Kcal/mole for the rectangle, 142 Kcal for the square, 151 Kcal/mole for the rhombus, and 188 Kcal/mole for the tetrahedron. Such results would appear to indicate that the square configuration cannot be the transition-state for a four-center exchange mechanism for

the required energy (142 Kcal/mole) is even considerably above that needed to dissociate a H_2 or D_2 molecule (110 Kcal/mole) and carry out a three-center exchange type reaction to get 2HD.

Wilson and Goddard (56) have reported a full ab initio CI calculation on H_4 which included all of the 36 possible configurations consistent with the Pauli principle which can be formed from Slater 1s basis functions. The saddle point energy for the square configuration was -2.06 hartrees near $R = 2.6$ a.u. which resulted in a barrier height of 132 ± 20 Kcal/mole for the exchange reaction. The error limits take into account the use of a minimum basis set. Both the symmetric trapezoid and the rhombus had saddle point energies approximately equal to that of the square configuration but their internuclear distances corresponded to the H_3-H system and thus is not a suitable four-body transition-state for the reaction. In a second paper, Wilson and Goddard (57) attempted to use their spin optimized GI (SOGI) wave function to examine the H_2-D_2 exchange reaction. The SOGI wave function is one that transforms as one of the young tableau belonging to the desired representation of the permutation group (58) and one whose electron spin and spatial orbitals have been coupled and optimized. Each spatial orbital in the total SOGI wave function is unique and only one electron is placed in it as in the unrestricted Hartree-Fock (UHF) method. In contrast to the standard MO and VB treatments. The spatial orbitals are determined thru a SCF type calculation on the system. The obtained PES for the H_2+D_2 system in the square configuration was very similar to their previous full CI study. The saddle point for the square is at $R = 2.48$ a.u. with an energy of -2.071 hartrees (barrier height energy equals 132 Kcal/mole). From the shape of the potential surface for the

square configuration, they state that they would expect that only collisions in which nearly all the "classical" activation energy (132 Kcal/mole) is in the vibrational mode would proceed thru this geometry. Thus their conclusion is in qualitative but not quantitative agreement with Bauer's (6) critical vibrational state mechanism interpretation of his own experimental results.

CHAPTER IV

METHOD

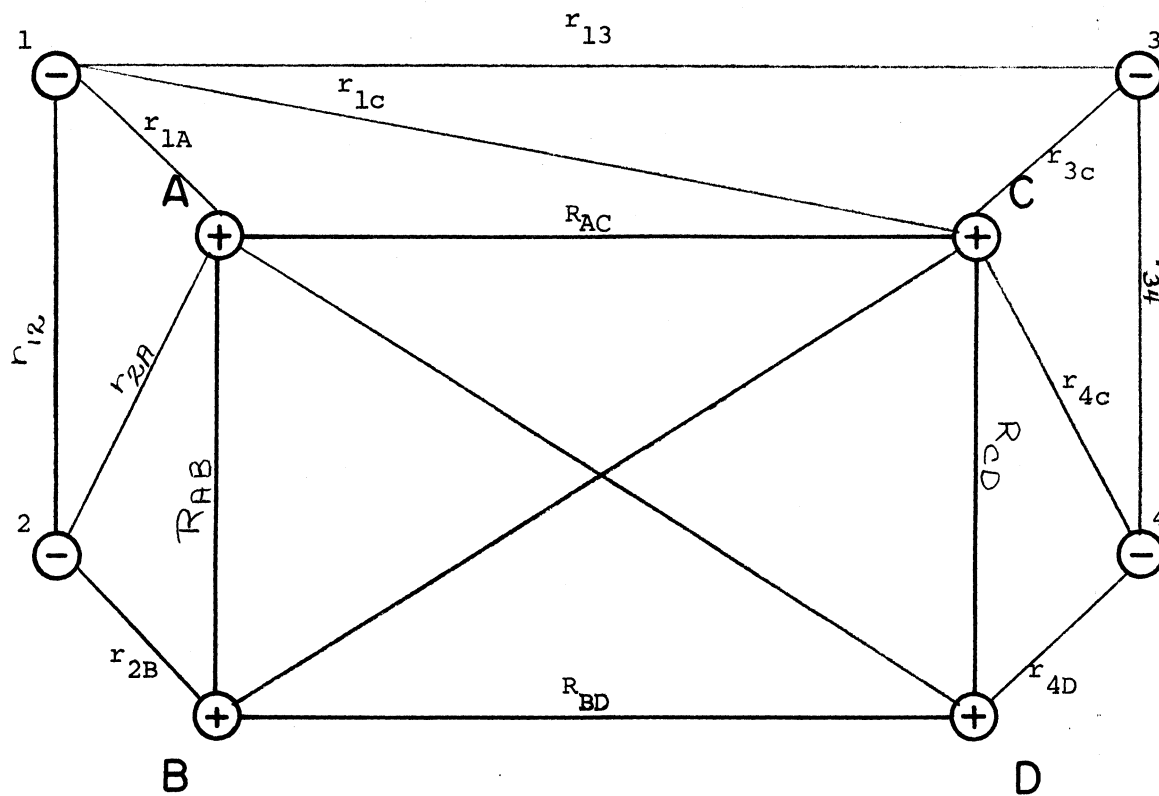
The perfect pairing valence bond (VB) model has been employed to calculate the potential-energy surface, for the H_4 surface (59,60,61).

Four Slater type 1s electron space orbitals (designated a,b,c,d, in Figure 1 depending upon the nuclear center (A,B,C,D) are used. The form of the 1s electron orbitals is:

$$1s = N e^{-\delta r} \quad (14)$$

N is the normalization constant equal to $(\frac{\delta}{\pi})^2$. δ is the screening parameter, r is the distance of an electron from a particular H atom nucleus. These orbitals were used as the minimal-basis set for the four-electron, four-proton H_4 system. Each space orbital is converted into a spin orbital by multiplication by one of the two spin functions, α or β . Thus, there are eight spin orbitals for the H_4 system that serve as the spin included basis set.

A VB term of the complete electronic wave function for the H_4 system would be a product of four-spin orbitals, each electron occupying one spin orbital, permuted in the form of a Slater determinant (ϕ) to give the correct antisymmetry property to the electronic wave function. There are 32 determinants for the H_4 system since each column in the determinant can contain an α or β spin function for a given spatial orbital.



r = distance between electron and H Nucleus
 R = distance between H Nuclei (A,B,C,D)

Figure 1. H_4 System Depicting Protons and Electrons in System

The requirement that the total molecular wave function be an eigenfunction of both \hat{S}^2 and \hat{S}_z (60) in union with the perfect-pairing valence-bond format determines the form of the total molecular wave function used in this study. Perfect pairing in the VB model for H_4 requires that each pair of atoms in the system have their valence electrons paired together such that a chemical bond may exist between them. Thus, if one atom's spin orbital has an α function the other atom spin orbital in the pair must have a β spin function. With H_4 we can form a maximum of two chemical bonds using the above scheme in a given ϕ representation. The six ϕ 's which result from the perfect-pairing VB method applied to H_4 are the following six Slater determinants.

$$\phi_1 = |a(1)\alpha(1)b(2)\alpha(2)c(3)B(3)d(4)B(4)| \quad (15)$$

$$\phi_2 = |a(1)\alpha(1)b(2)B(2)c(3)\alpha(3)d(4)B(4)| \quad (16)$$

$$\phi_3 = |a(1)B(1)b(2)\alpha(2)c(3)\alpha(3)d(4)B(4)| \quad (17)$$

$$\phi_4 = |a(1)\alpha(1)b(2)B(2)c(3)B(3)d(4)\alpha(4)| \quad (18)$$

$$\phi_5 = |a(1)B(1)b(2)\alpha(2)c(3)B(3)d(4)\alpha(4)| \quad (19)$$

$$\phi_6 = |a(1)B(1)b(2)B(2)c(3)\alpha(3)d(4)\alpha(4)| \quad (20)$$

These six ϕ 's all have eigenvalue of \hat{S}_z equal to zero, and they are the only ones of the original 32 determinants that have this eigenvalue. Thus, the secular equation used in the energy calculation reduces to a 6x6 matrix.

The ϕ 's which correspond to a bond between A and B and a bond between C and D are $\phi_2, \phi_3, \phi_4, \phi_5$. A linear combination of these four determinants would thus represent a wave function ψ_{c-d}^{a-b} that would completely include each ϕ that pertains to a perfect pairing ψ_{c-d}^{a-b} VB bonding scheme. By interchanging spins on a and b and then c and d and by making use of the fact that ψ_{c-d}^{a-b} must be antisymmetric, one obtains the fol-

lowing unnormalized linear combination:

$$\psi_1 = \psi_{\substack{a-b \\ c-d}} = \phi_2 - \phi_3 - \phi_4 + \phi_5 \quad (21)$$

In a similar manner, one obtains two other wave functions which consist of a linear combination of the ϕ s that represent two other canonical structures:

$$\psi_2 = \psi_{\substack{a-a \\ b-d}} = \phi_1 - \phi_3 - \phi_4 + \phi_6 \quad (22)$$

$$\psi_3 = \psi_{\substack{a-b \\ c-d}} = \phi_1 - \phi_2 - \phi_4 + \phi_6 \quad (23)$$

Only ψ_1 , and ψ_2 are linearly independent as (60) $\psi_3 = \psi_2 - \psi_1$. Therefore the total perfect-pairing VB wave function for H_4 is as follows:

$$\Psi = C_1\psi_1 + C_2\psi_2 \quad (24)$$

Both ψ_1 and ψ_2 when operated on by \hat{S}^2 gives an eigenvalue of zero which corresponds to a singlet ground state for H_4 . All ionic structures and nonperfect pairing structures are excluded in this VB form of the wave function.

Porter and Raff (62) have shown that this perfect pairing valence-bond wave function (Ψ) contains a considerable amount of configurational mixing. In fact, for the D_{4h} square conformation the configuration coefficients in the VB wave function for the ground state ${}^1B_{1g}$ are very nearly equal to those obtained in a full CI treatment (55,56).

The ground state electronic energy (E) of the H_4 system is given by:

$$E = \frac{\int \Psi^* \hat{H} \Psi d\tau}{\int \Psi^* \Psi d\tau} \quad (25)$$

Variational minimization yields the following expression for the singlet ground state energy of H_4 :

$$E = \frac{1}{X}(-X_2 - (X_2^2 - X_1 X_3)^{\frac{1}{2}}) \quad (26)$$

where

$$X_1 = \langle \Psi | \psi_1 \rangle \langle \psi_2 | \psi_2 \rangle - \langle \psi_1 | \psi_2 \rangle$$

$$X_2 = \langle \psi_1 | \hat{H} | \psi_2 \rangle \langle \psi_1 | \psi_2 \rangle - \frac{1}{2} \langle \psi_1 | \hat{H} \psi_1 \rangle \\ - \langle \psi_2 | \Psi \rangle - \frac{1}{2} \langle \psi_2 | \hat{H} | \psi_2 \rangle - \langle \psi_1 | \Psi \rangle$$

$$X_3 = \langle \psi_1 | \hat{H} | \psi_1 \rangle \langle \psi_2 | \hat{H} | \psi_2 \rangle - \langle \psi_1 | \hat{H} | \psi_2 \rangle^2$$

and ψ_1 and ψ_2 are the wave functions defined previously and \hat{H} is the Hamiltonian operator for the H_4 system. The Hamiltonian for the H_4 system is a 24 term operator if one employs the Born-Oppenheimer approximation (63) and excludes any spin coupling terms:

$$\hat{H} = -\frac{1}{2} \bar{V}^2, -\frac{1}{2} \bar{V}_2^2 - \frac{1}{2} \bar{V}_3^2 - \frac{1}{2} \bar{V}_4^2 - \frac{1}{r_{1A}} - \frac{1}{r_{1C}} - \frac{1}{r_{1D}} \\ - \frac{1}{r_{2A}} - \frac{1}{r_{2B}} - \frac{1}{r_{2C}} - \frac{1}{r_{2D}} - \frac{1}{r_{3A}} - \frac{1}{r_{3B}} - \frac{1}{r_{3C}} - \frac{1}{r_{3D}} \\ - \frac{1}{r_{4A}} - \frac{1}{r_{4B}} - \frac{1}{r_{4C}} - \frac{1}{r_{4D}} + \frac{1}{r_{12}} + \frac{1}{r_{13}} + \frac{1}{r_{14}} + \frac{1}{23} \\ + \frac{1}{r_{24}} + \frac{1}{r_{34}} + \frac{1}{R_{AB}} + \frac{1}{R_{AC}} + \frac{1}{R_{AD}} + \frac{1}{R_{BC}} + \frac{1}{R_{BD}} + \frac{1}{R_{CD}} \quad (27)$$

Thus, one has four kinetic energy terms for the electrons, sixteen terms resulting from nuclear-electron Coulombic interaction, six terms

resulting from electron-electron Coulombic repulsion, and six terms resulting from nuclear-nuclear Coulombic repulsion (see Figure 1).

Since the ψ_1 and ψ_2 are linear combinations of various ϕ 's, integrals of the type $\langle \phi_i | H | \phi_j \rangle$ and $\langle \phi_i | \phi_j \rangle$ result from Equation (25).

Let us take $\langle \phi_1 | \hat{H} | \phi_2 \rangle$ as an example. Due to identical terms in the determinants ϕ_1 and ϕ_2 , $\langle \phi_1 | \hat{H} | \phi_2 \rangle$ yields:

$$Sa(1)2(1)b(2)2(2)c(3)B(3)d(4)B(4) \left| \hat{H} \left(\frac{1}{\sqrt{4!}} \phi_2 \right) \right| d\tau_T \quad (28)$$

where $d\tau$ represents the total spin-spin volume element. Because of the orthogonality of the spin functions α and β , Eq.(28) becomes, upon integration over spin, a sum of only four terms:

$$\begin{aligned} \langle \phi_1 | \hat{H} | \phi_2 \rangle = & Sa(1)b(2)c(3)d(4) \left| \hat{H} | a(1)c(2)b(3)d(4) \right| \\ & + Sa(1)b(2)c(3)d(4) \left| \hat{H} | a(1)c(2)d(3)b(4) \right| d\tau \\ & + Sa(1)b(2)c(3)d(4) \left| \hat{H} | c(1)a(2)b(3)d(4) \right| d\tau \\ & - Sa(1)b(2)c(3)d(4) \left| \hat{H} | c(1)a(2)d(3)b(4) \right| d\tau \end{aligned} \quad (29)$$

It follows that $\langle \phi_1 | \phi_2 \rangle$ is the sum of the same above four integrals where \hat{H} would be replaced by the identity operator 1.

One now uses the facts as long as one does the same permutation to a wave function on the left side of any Hermitean operator (e.g., $\hat{H}, 1$) in a integral such as

$$Sa(1)b(2)c(3)d(4) \left| \hat{H} | c(1)d(2)b(3)a(4) \right| d\tau$$

as one does to the wave function on the right side of the operator the integral remains unchanged in value (59). Using the above and the fact

that real Hermitean operators are used in the integrals it can be shown that, for example:

$$\begin{aligned} & \int a(1)b(2)c(3)d(4) |\hat{H}| c(1)d(2)b(3)a(4) d\tau \\ & \int a(1)b(2)c(3)d(4) |\hat{H}| d(1)c(2)a(3)b(4) d\tau \end{aligned} \quad (30)$$

Using all of the preceding steps on each of the $\langle \phi_i | \hat{H} | \phi_j \rangle$ and $\langle \phi_i | \phi_j \rangle$ integrals where both i and j vary from 1 to 6, it may easily be shown that the energy of the system is a function of 17 different integrals with \hat{H} or 1 as the contained operator. These integrals are listed in Table I.

We now proceed to solve each of the various 24 subintegrals that result from explicitly writing out the 24 term \hat{H} for each of the seventeen independent integrals listed in Table I.

Rosen (64) has given analytic solutions for kinetic energy terms using the fact that,

$$\left(-\frac{1}{2} \nabla^2 - \frac{\delta}{r_{1\Delta}}\right) a(1) = \delta^2 a(1) \quad (31)$$

He also gives analytical expressions for the two-center Coulombic integral of the form:

$$\int a(1)b(2) \left| \frac{1}{r_{12}} \right| a(1)b(2) d\tau$$

The two-center electron exchange integrals of the form:

$$\int a(1)b(2) \left| \frac{1}{r_{12}} \right| b(1)a(2) d\tau$$

were solved analytically by reference to works of Slater (65) and Hastings (66).

TABLE I

LIST OF THE SEVENTEEN INDEPENDENT MATRIX ELEMENTS
ONE SOLVES FOR IN THE H_4 SYSTEM

$\langle a(1) b(2) c(3) d(4) Q a(1) b(2) c(3) d(4) \rangle$
$\langle a(1) b(2) c(3) d(4) Q a(1) d(2) c(3) b(4) \rangle$
$\langle a(1) b(2) c(3) d(4) Q b(1) a(2) c(3) d(4) \rangle$
$\langle a(1) b(2) c(3) d(4) Q a(1) b(2) d(3) c(3) \rangle$
$\langle a(1) b(2) c(3) d(4) Q a(1) c(2) b(3) d(4) \rangle$
$\langle a(1) b(2) c(3) d(4) Q d(1) b(2) c(3) a(4) \rangle$
$\langle a(1) b(2) c(3) d(4) Q c(1) d(2) a(3) b(4) \rangle$
$\langle a(1) b(2) c(3) d(4) Q d(1) c(2) b(3) a(4) \rangle$
$\langle a(1) b(2) c(3) d(4) Q b(1) a(2) d(3) c(4) \rangle$
$\langle a(1) b(2) c(3) d(4) Q c(1) b(2) a(3) d(4) \rangle$
$\langle a(1) b(2) c(3) d(4) Q b(1) d(2) c(3) a(4) \rangle$
$\langle a(1) b(2) c(3) d(4) Q c(1) a(2) b(3) d(4) \rangle$
$\langle a(1) b(2) c(3) d(4) Q d(1) b(2) a(3) c(4) \rangle$
$\langle a(1) b(2) c(3) d(4) Q a(1) c(2) d(3) b(4) \rangle$
$\langle a(1) b(2) c(3) d(4) Q d(1) a(2) b(3) c(4) \rangle$
$\langle a(1) b(2) c(3) d(4) Q c(1) d(2) b(3) a(4) \rangle$
$\langle a(1) b(2) c(3) d(4) Q b(1) d(2) a(3) c(4) \rangle$

$|Q|$ represents the identity operator or the
Hamiltonian operator for the H_4 system.

Overlap integrals, one-electron one-center integrals, one-electron two-center integrals, and one-center two-electron integrals were calculated analytically using confocal elliptical coordinates (See Appendix for functional form of the solutions to above integrals).

The three- and four-center two-electron integrals and the three-center one-electron integrals were approximated by first applying Mulliken's approximation (48):

$$a(1) b(1) = \frac{\langle a(1) | b(1) \rangle}{2} (a(1)^2 - b(1)^2), \quad (32)$$

which reduces the three- and four-center integrals to various two- and one-center integrals. These integrals were then calculated analytically by the methods described above. This overall procedure for three- and four-center integrals is illustrated in the Appendix. Mulliken's approximation is reasonably good (67), especially at the internuclear distances (1 to 5 a.u.), at which calculations were made. In this work all screening parameters (δ) for the four Slater type s orbitals were set equal.

The above procedure yields the perfect pairing VB energy for H_4 as a function of the screening parameter and the six internuclear distances of the system. In each H_4 conformation one can use Equation (26) and vary the screening parameter until the lowest energy is found.

The following numerical checks were employed to insure accuracy. The four H atoms were placed essentially infinitely apart to see that the calculations gave that limit. Two of the H atoms were placed at Wang's equilibrium distance for H_2 given in his work (68) and, using his minimized screening parameter, with other H atoms essentially infinitely far away from the H_2 molecule and from each other the system

energy was computed. The difference between Wang's result and that calculated herein was less than .3% (the one calculated herein being lower in energy). This difference results from the fact that Wang's solution was partly graphical and his values of $\int_x^\infty \frac{1}{u} e^{-u} du$, where u is a dummy integration variable and x is equal to $2\delta R$, that was used in calculating two-electron exchange integrals were not as accurate as the ones used herein from the work of Hasting (66). Essentially twice Wang's energy value was obtained when the conformation of two isolated H_2 molecules was studied using Wang's H_2 equilibrium distance and screening parameter.

The other checks that were run involved putting the H_4 system in a square conformation and also in various rectangle conformations and checking to see that various integrals in Table I were equal to each other as required by consideration of the symmetry of the conformation.

CHAPTER V

RESULTS AND DISCUSSION

The relevant limit of two isolated H_2 molecules obtained in this VB study as regards to energy (-61.801 e.v.) and H_2 equilibrium distance (1.41 a.u.) are listed in the Table II along with two previously reported ab initio CI results and the experimental values for the system. Reasonable agreement with the CI based calculations as well as the experimental values are seen from Table II. The value of the screening constant (δ) contained in the 1s STO basis functions was found for the above energy minimization for the two isolated H_2 molecules to be 1.16 as compared to the $\delta=1$ for the system of four isolated H atoms (-54.42 e.v.). The value of $\delta = 1.16$ for the two isolated H_2 molecule is in agreement with Wang's value (68) for the H_2 system using the same VB format as contained herein.

In the Table III a comparison is presented of the minimal basis VB computation results of this study with previously reported ab initio results on the H_4 system as well as with an extended Huckel calculation result (2) for various geometric conformation. One can readily see the rather good and general accuracy of the present computations when they are compared to the more accurate ab initio results. Comparison with the semiempirical extended Huckel calculation of Gimarc (2) shows considerable differences in energies and this point will be expounded upon in considerable depth later on in this reaction when the proposed

TABLE II
COMPARISON OF RESULTS FOR TWO SEPARATE H₂ MOLECULE LIMIT

Method	Energy* (e.v.)	Equilibrium Distance (a.u.)
VB method presented herein	-61.801	1.41
CI of Wilson and Goddard ^a	-62.471	1.4304
Shavitt and Rubinstein work ^b	-62.637	1.42
Experimental ^c	-63.918	1.4008

*Zero reference point is taken to be four protons and four electrons separated to infinite distance.

^aReference 56.

^bReference 55.

^cReference 91.

TABLE III
 COMPARISON OF MINIMAL-BASIS VB COMPUTATIONS WITH
 PREVIOUSLY REPORTED RESULTS

Conformation		Present Cal.		Previous Ab		Gimarc
Form	Dimensions	ξ	E(ev)	Initio	Results	
				E(ev)	Ref.	E(ev)
Square (D_{4h})	2.25 au	1.03	-55.919	-55.511	56	
				-58.284	53	
	2.46	1.02	-56.111			-58.474
	2.47	1.02	-56.114	-56.461	55	
	2.75	1.01	-56.047	-56.017	56	
Rhombus (D_{2h})	70° ; 2.54 au	1.01	-55.579	-55.473	56	
	70° ; 2.50	1.02	-55.553	-56.080	55	
	60° ; 2.46	1.01	-54.611			-60.637
Rectangle (D_{2h})	2.61 & 2.09 au	1.04	-57.137	-57.93	55	
Tetrahedron (T_d)	2.46 au	1.00	-52.122	-53.699	55	
	3.80	1.01	-54.408	-54.474	55	
Linear ($D_{\infty h}$)	1.60 au	1.12	-59.636	-59.892	56	
	1.70	1.10	-59.755	-60.787	55	
	1.80	1.08	-59.725	-60.156	56	
	2.46	1.01	-57.988			-63.630
Equilateral Triangle (D_{3h})	2.46 au	1.02	-54.365	-54.858	56	-59.726

four-body exchange mechanism of Gimarc for the (H_2, D_2) exchange reaction is discussed in light of his and the present results.

The data of Table III also illustrated that the VB computations qualitatively predict the relative conformation energies in agreement with the ab initio results as given by the following inequality: linear < rectangle < square < rhombus < equilateral triangle < tetrahedron. For shorter bond distances of 2.2 a.u. between outer points on the equilateral triangle surface, the present VB computations predict nearly equal stability for the equilateral triangle and tetrahedron. At even shorter distances the last inequality (equilateral triangle < tetrahedron) reverses itself.

The best minimized screening parameter used in this study's various geometric conformations was 1.02. This value is used throughout this work unless stated otherwise. The linear configuration used a minimized screening parameter of 1.10 when the internuclear separation was greater than 2.2 a.u. The energy minimization was very sensitive to a change in δ of .05 units or less.

It is also of interest to notice in Table III is that for the square and the 70° rhombus conformations the VB energies are lower than the previous cited ab initio results of Wilson and Goddard (56) which is in violation of the variation theorem. This is due to Mulliken's approximation being used in the VB case herein for the three- and four-center integrals. Mulliken's approximation imparts added stability to all the conformations studied but it is evident only in the square and 70° rhombus for following reason. Porter and Raff (62) showed that for the square conformation the configuration coefficients in the VB wave function for the ground state are very nearly equal to those obtained by

Wilson and Goddard (56) in their full CI treatment. This implies that the VB ground-state energies of both the square and its close geometric brother, the 70° rhombus, would be in close agreement with the CI results on these. Thus, when Mulliken's approximation is used, the increased stability gives rise to a lower energy than the ab initio CI results. Generally though, as can be seen by averaging the VB results with the previous ab initio results in Table III, the present VB formulation underestimates the conformation stability by about 0.5 eV.

The added stability resulting from Mulliken's approximation was verified to be indeed the case. Analytical values of the three- and four-center integrals, involving 1s STO, given by Magnasco (49) for the rectangular conformation of side lengths 1.4166 au and 2.8332 au were used in calculating the ab initio VB energy at that point. This result was compared with that obtained using Mulliken's approximation for the three- and four-center integrals for the same rectangular point. Mulliken's approximation gave an energy stabilization of ≈ 0.6 eV as compared to the result not using it.

In Figures 2 thru 12 are pictured two-dimensional energy contour plots of the H_4 interaction system for various geometries. The corresponding three-dimensional plots are seen in Figures 13 thru 23. From these plots, as well as from the values in Table III, it is apparent that only the linear configuration possesses interaction energies (contour energy values minus the $2 H_2$ limit of -61.801 eV) on its surface that lie in the range of the previously discussed experimental activation energy (6). A four-body exchange mechanism for the (H_2, D_2) system implies that points on the pathway represent those associated with four-body interactions and not points representing systems such as

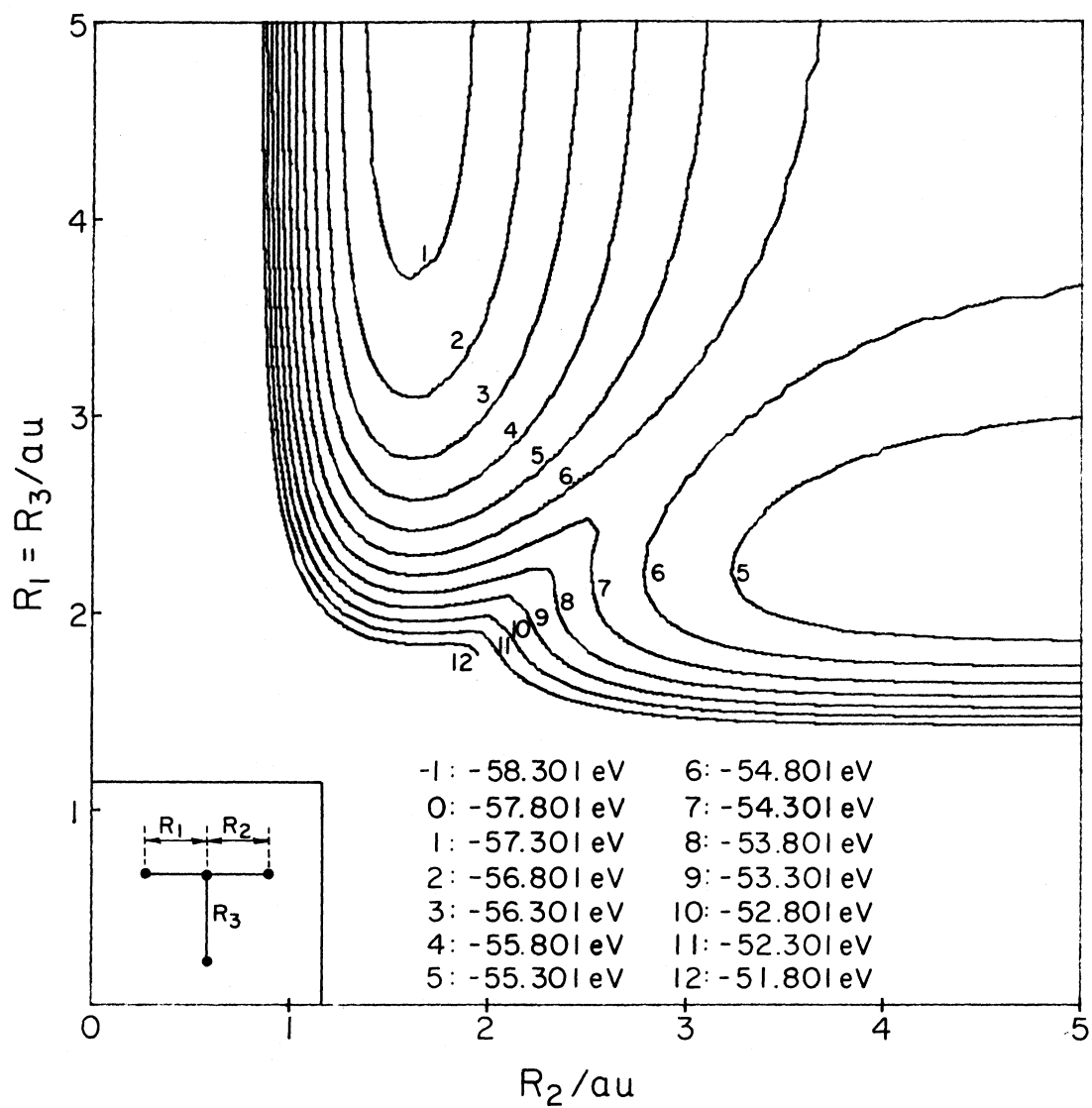


Figure 2. Contour Plot of H_4 in Unsymmetric "T" Configuration

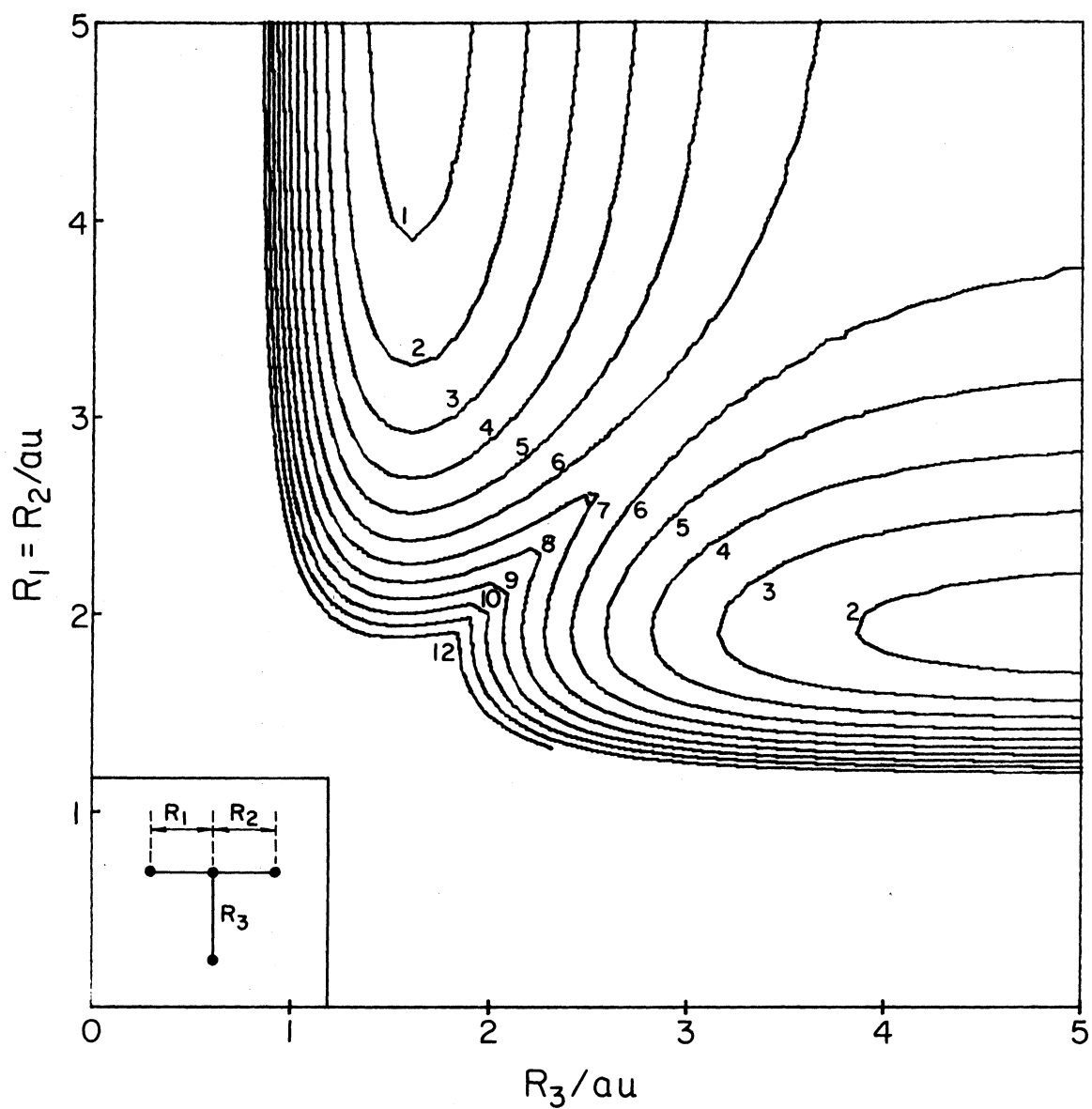


Figure 3. Contour Plot of H_4 in Symmetric "T" Configuration

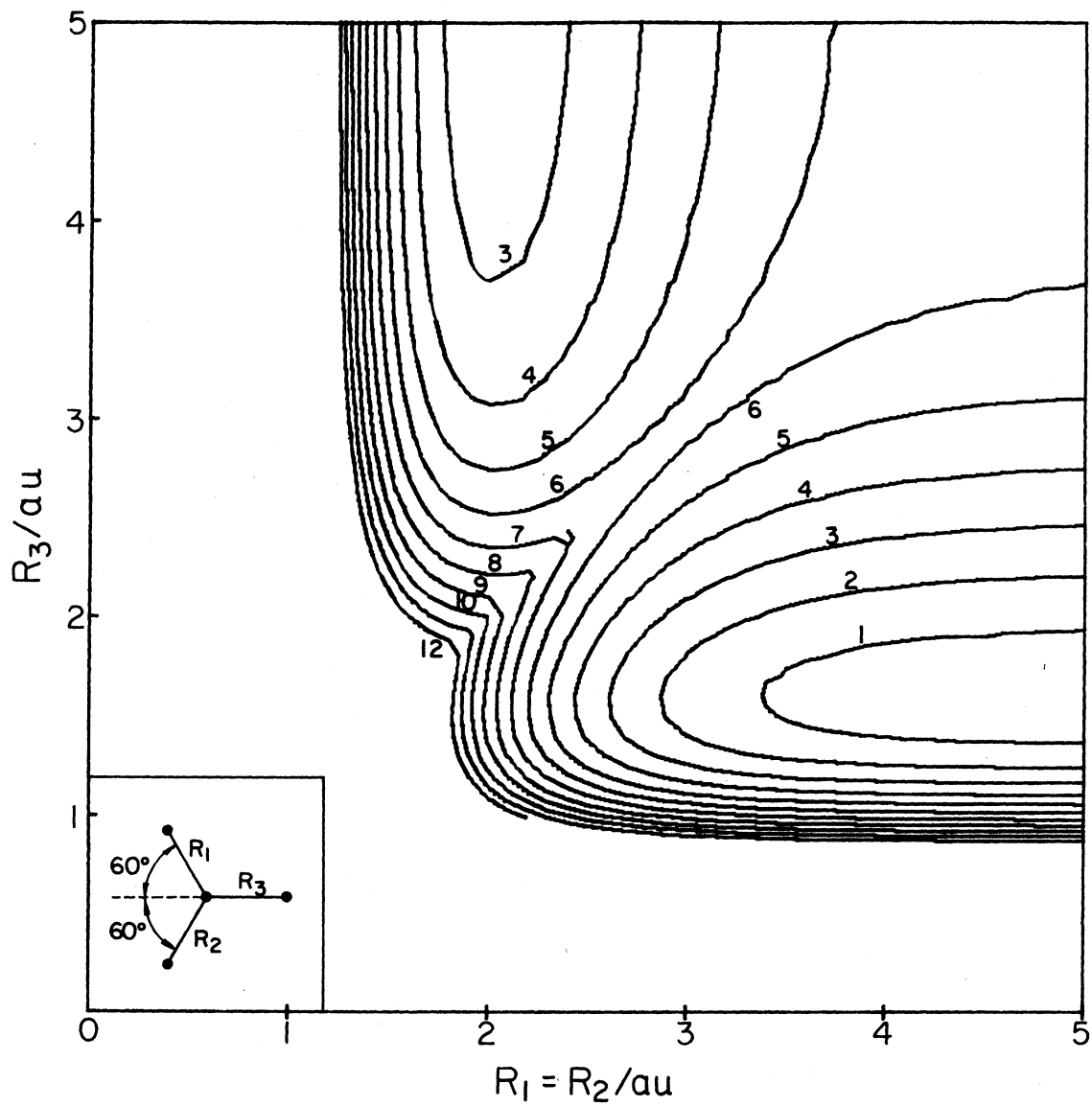


Figure 4. Contour Plot of H_4 in Symmetric 120° "Y" Configuration

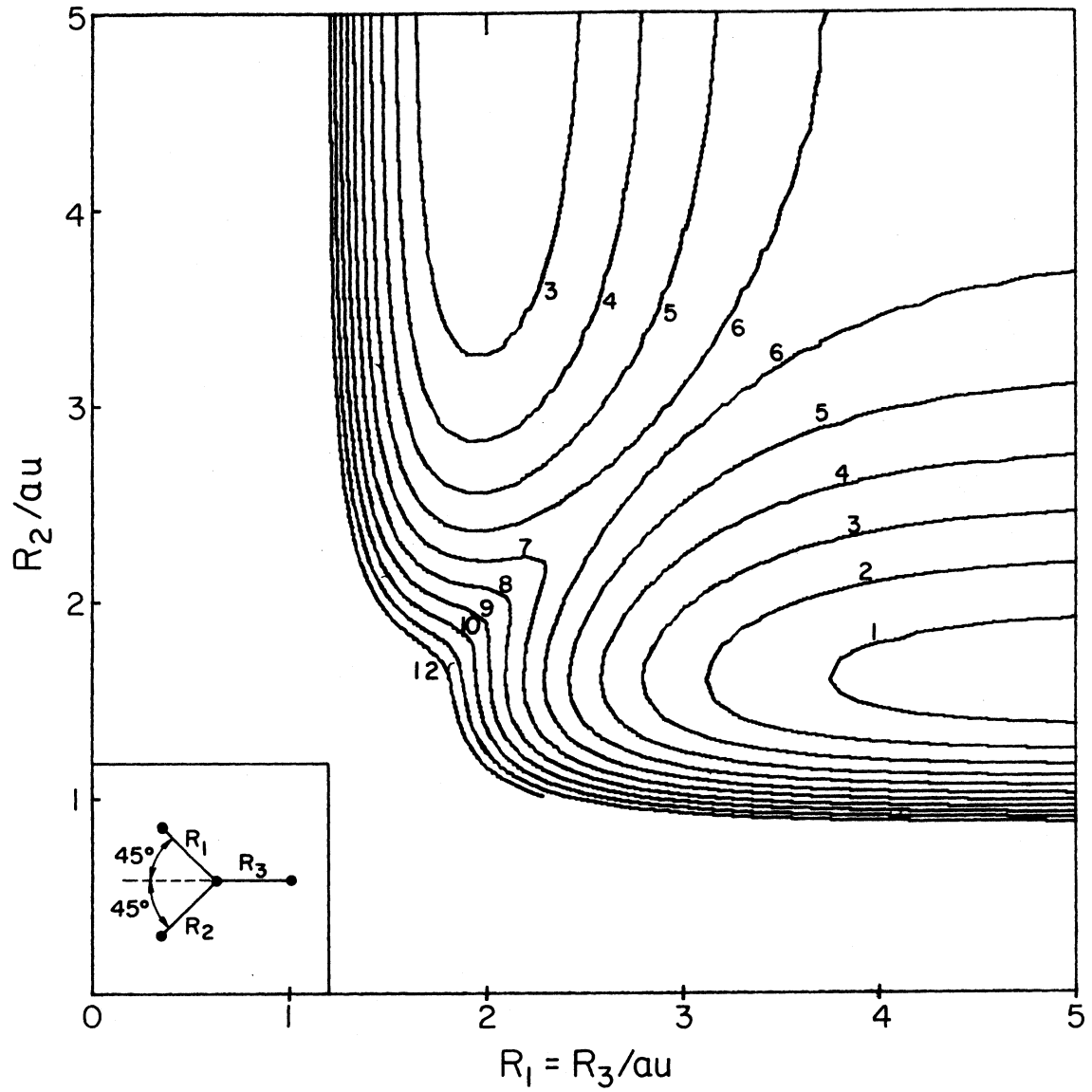


Figure 5. Contour Plot of H_4 in Unsymmetric 90° "Y" Configuration

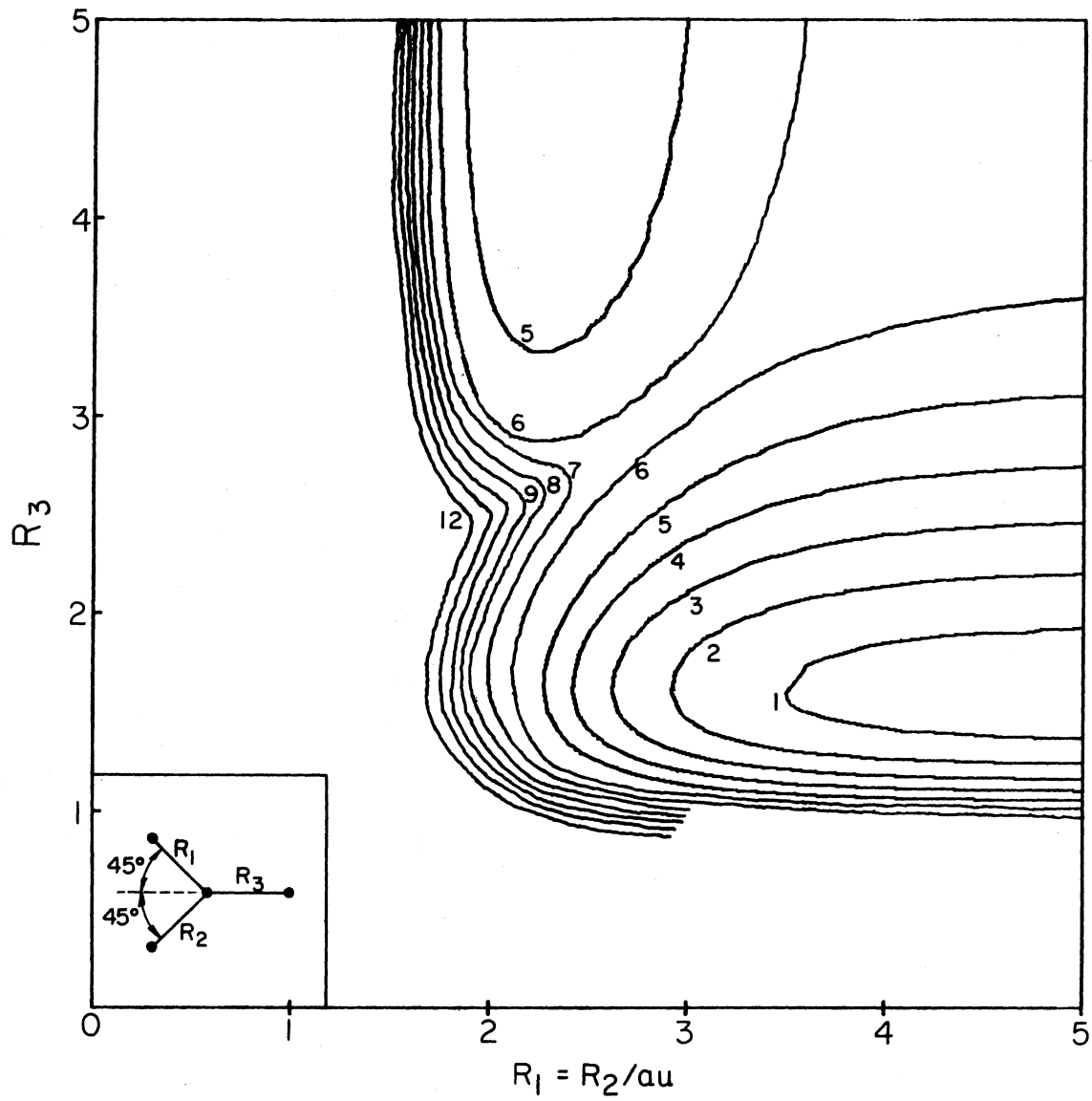


Figure 6. Contour Plot of H_4 in Symmetric 90° "Y" Configuration

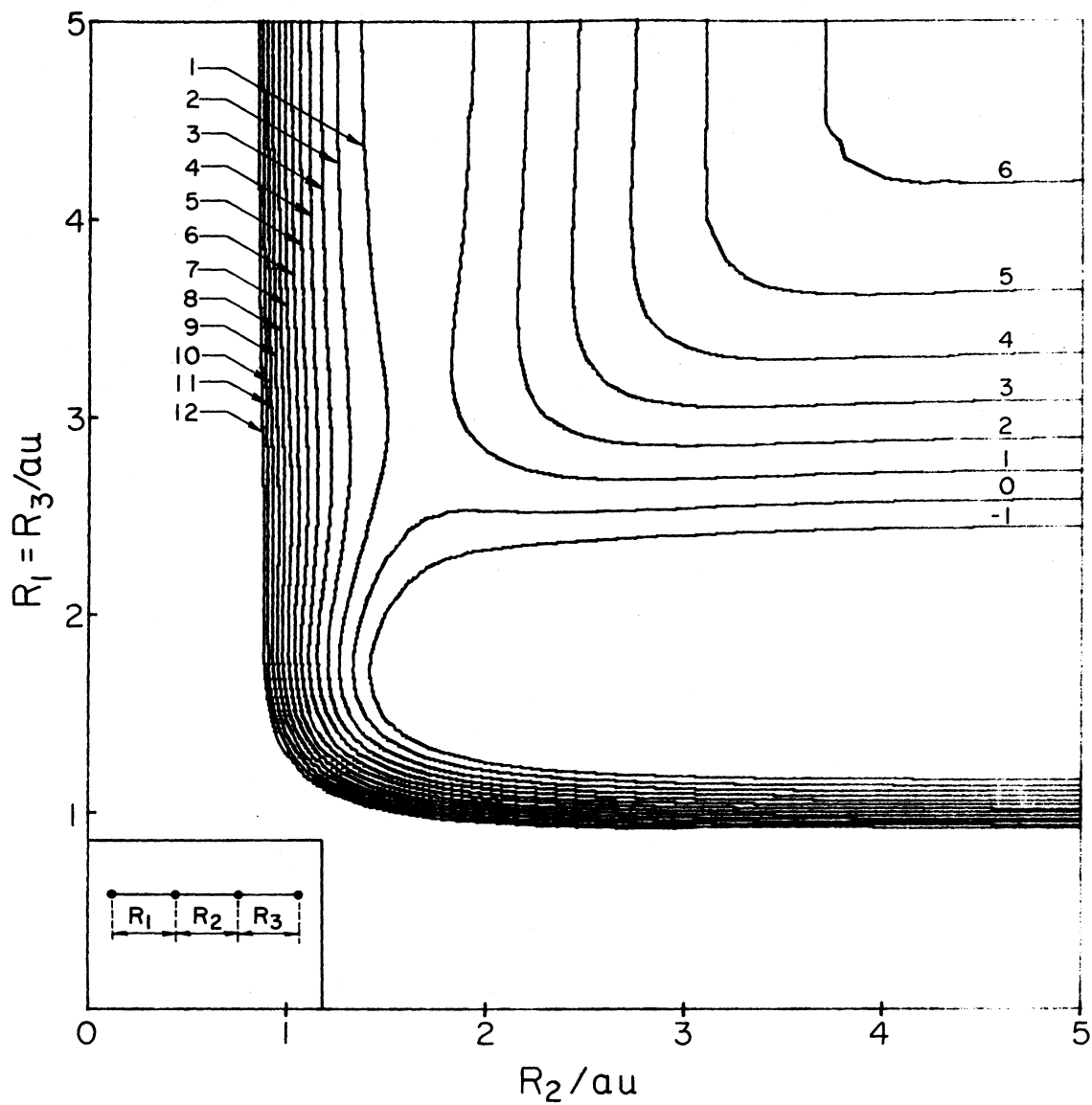


Figure 7. Contour Plot of H_4 in Symmetric Linear Configuration

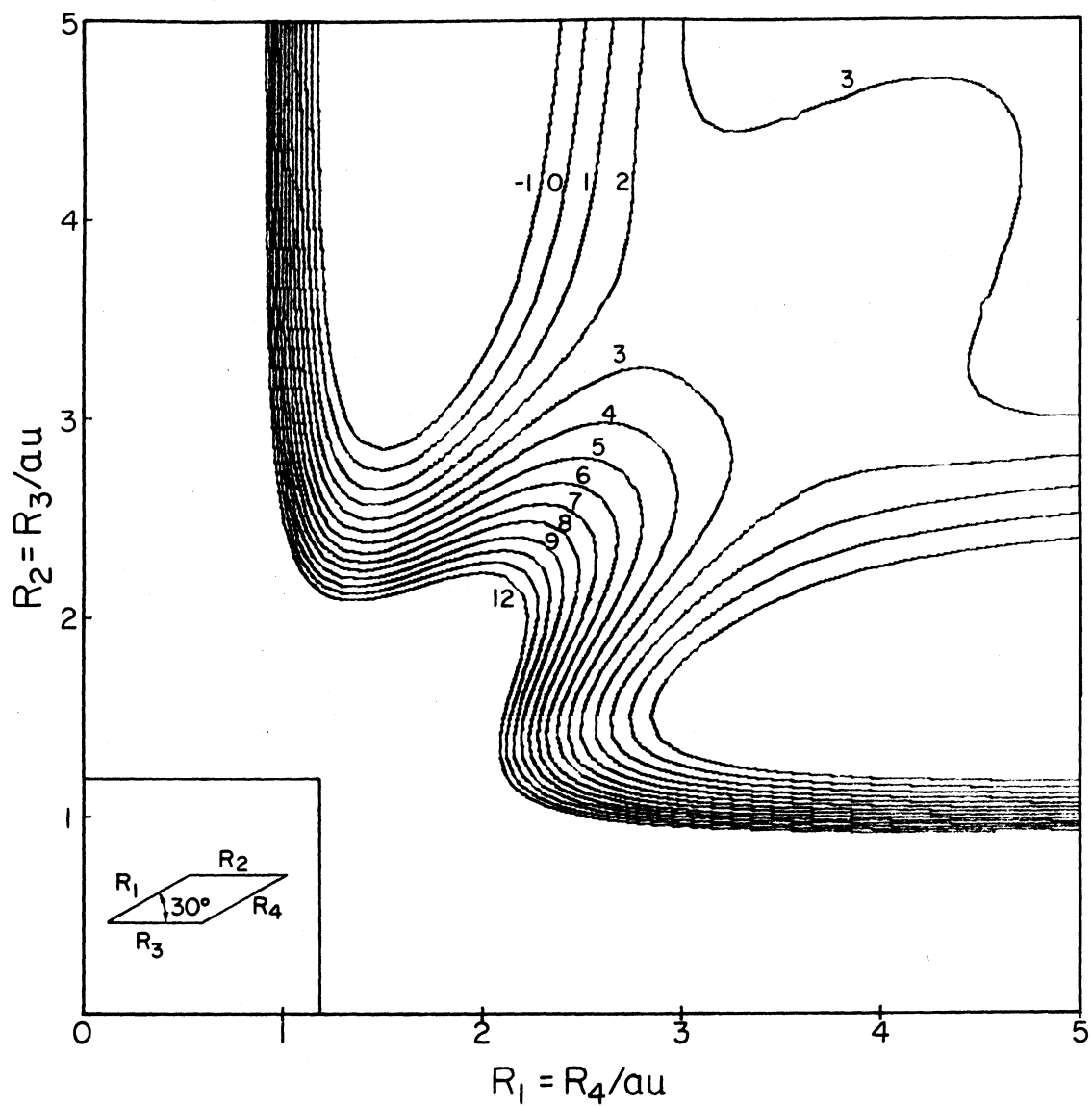


Figure 8. Contour Plot of H_4 in a 30° Parallelogram Configuration

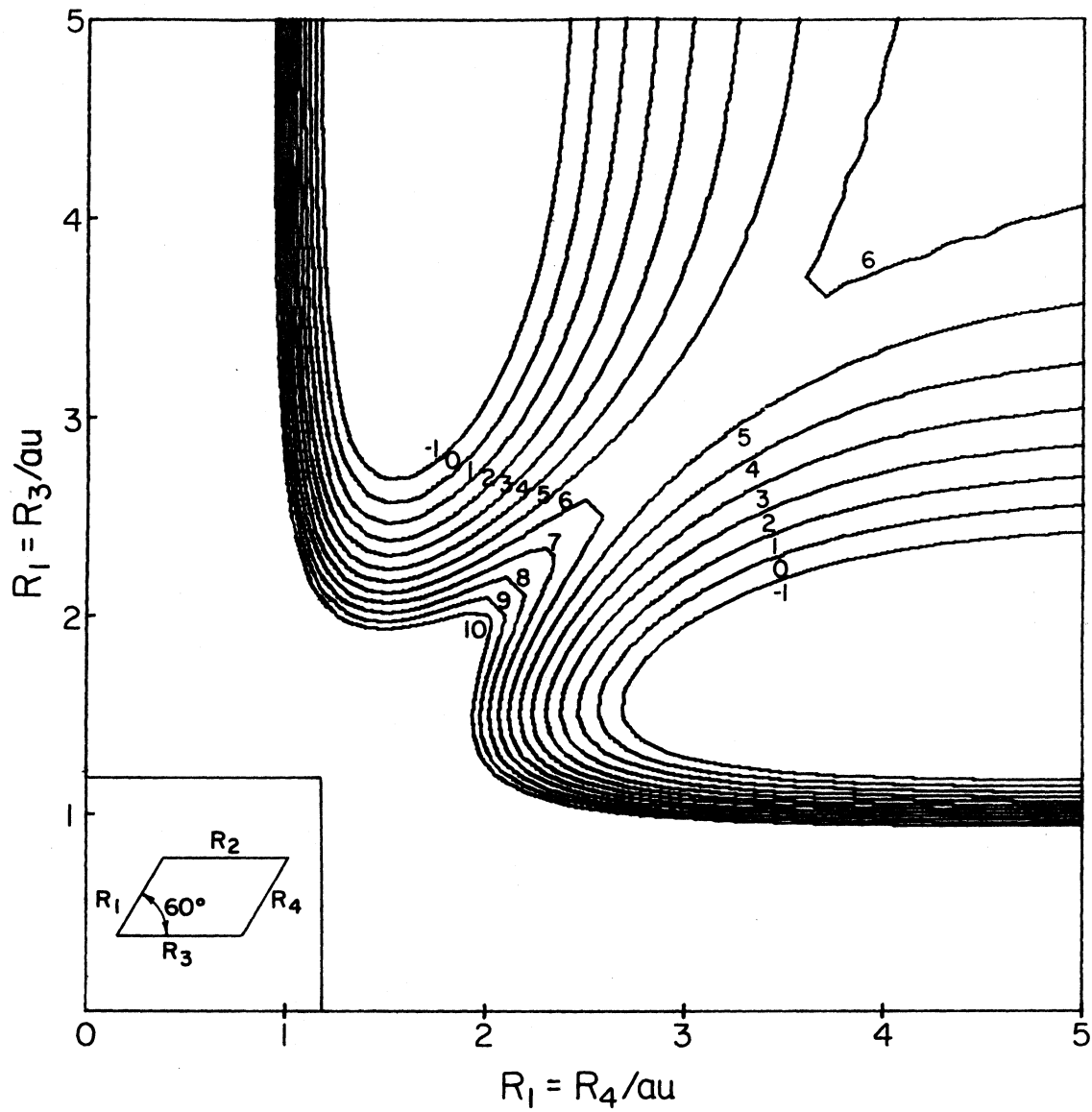


Figure 9. Contour Plot of H_4 in a 60° Parallelogram Configuration

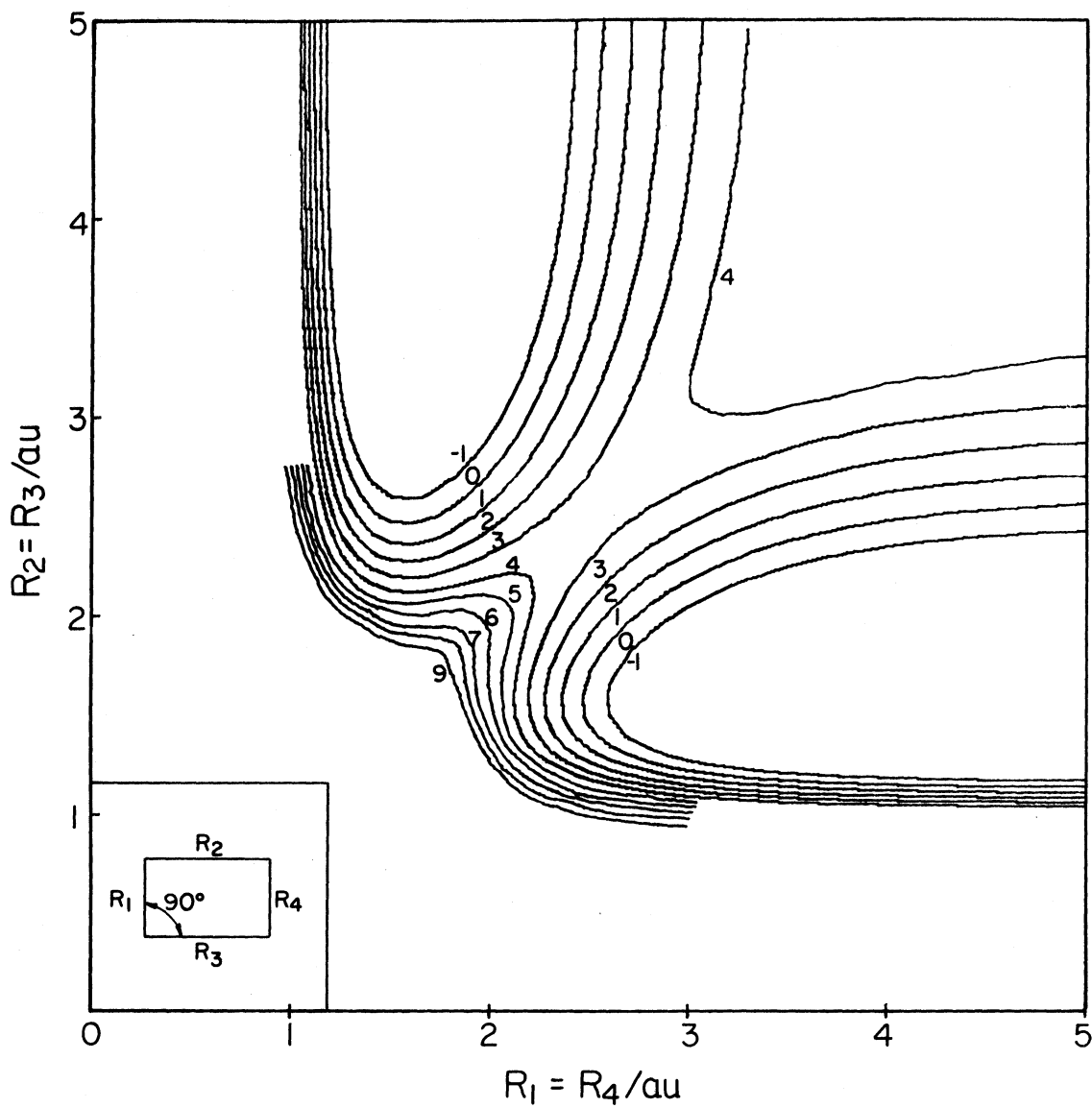


Figure 10. Contour Plot of H_4 in Rectangular Configuration

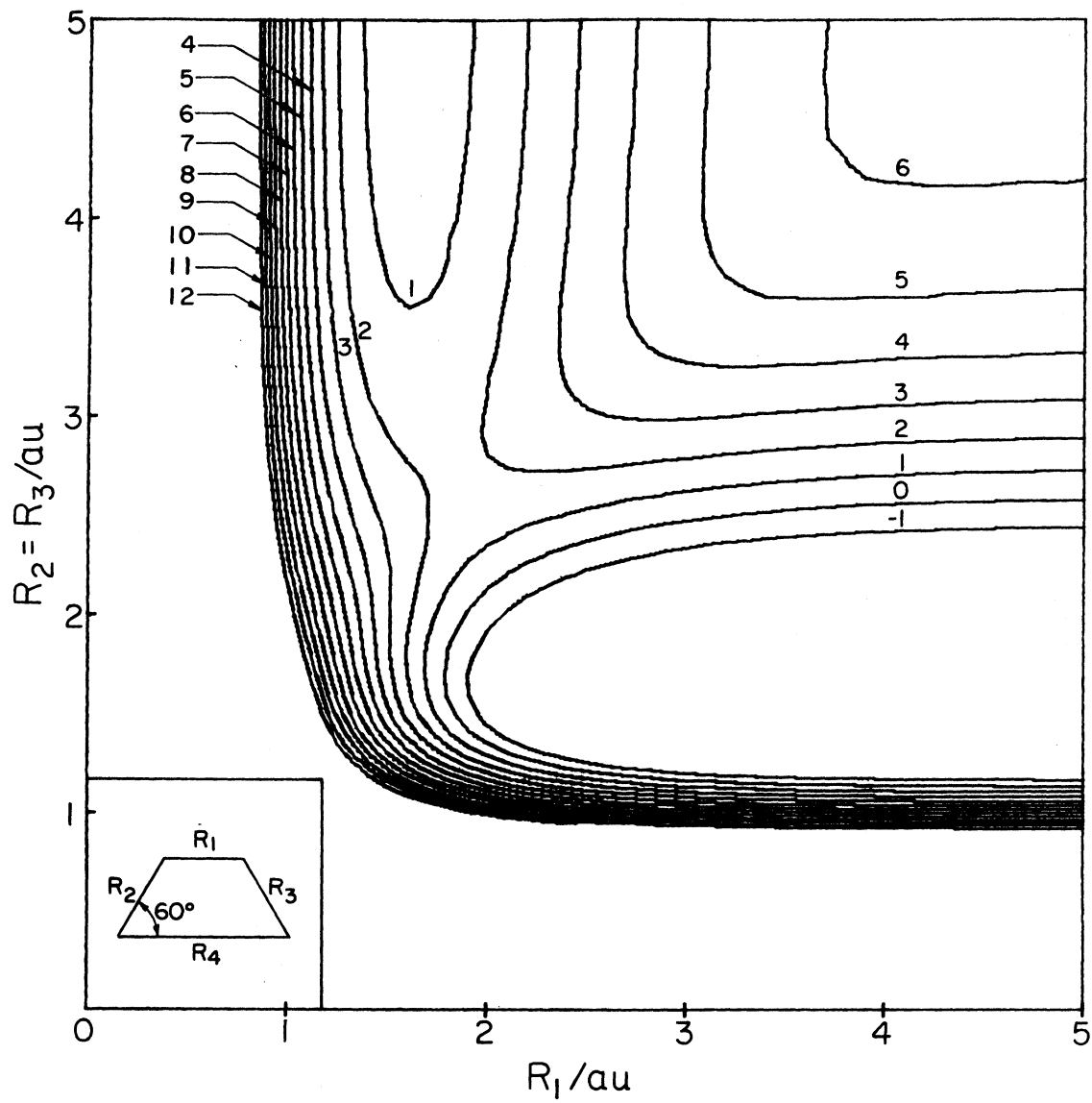


Figure 11. Contour Plot of H_4 in a 60° Symmetric Trapezoidal Configuration

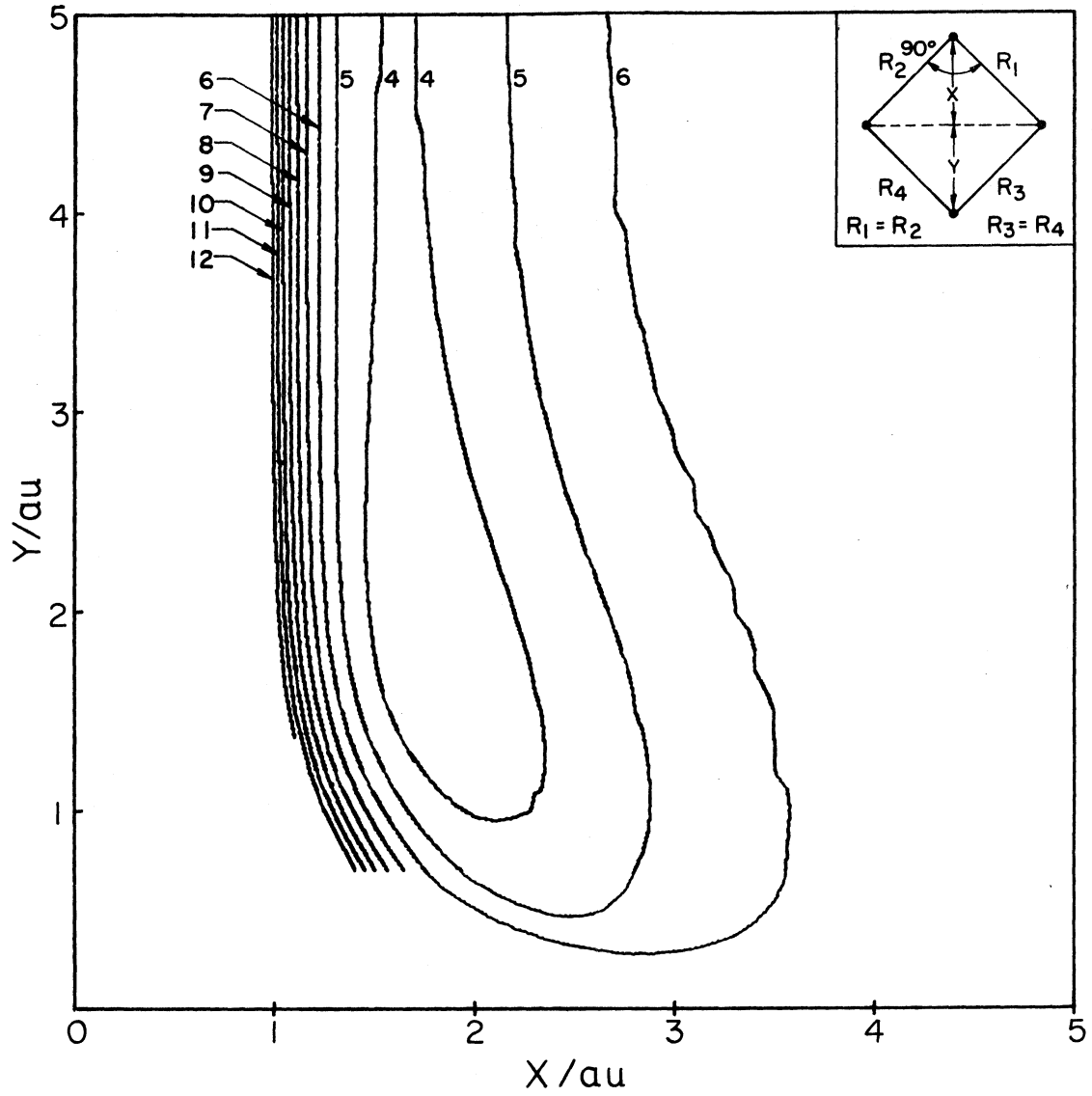


Figure 12. Contour Plot of H_4 in 90° Symmetric Kite Configuration

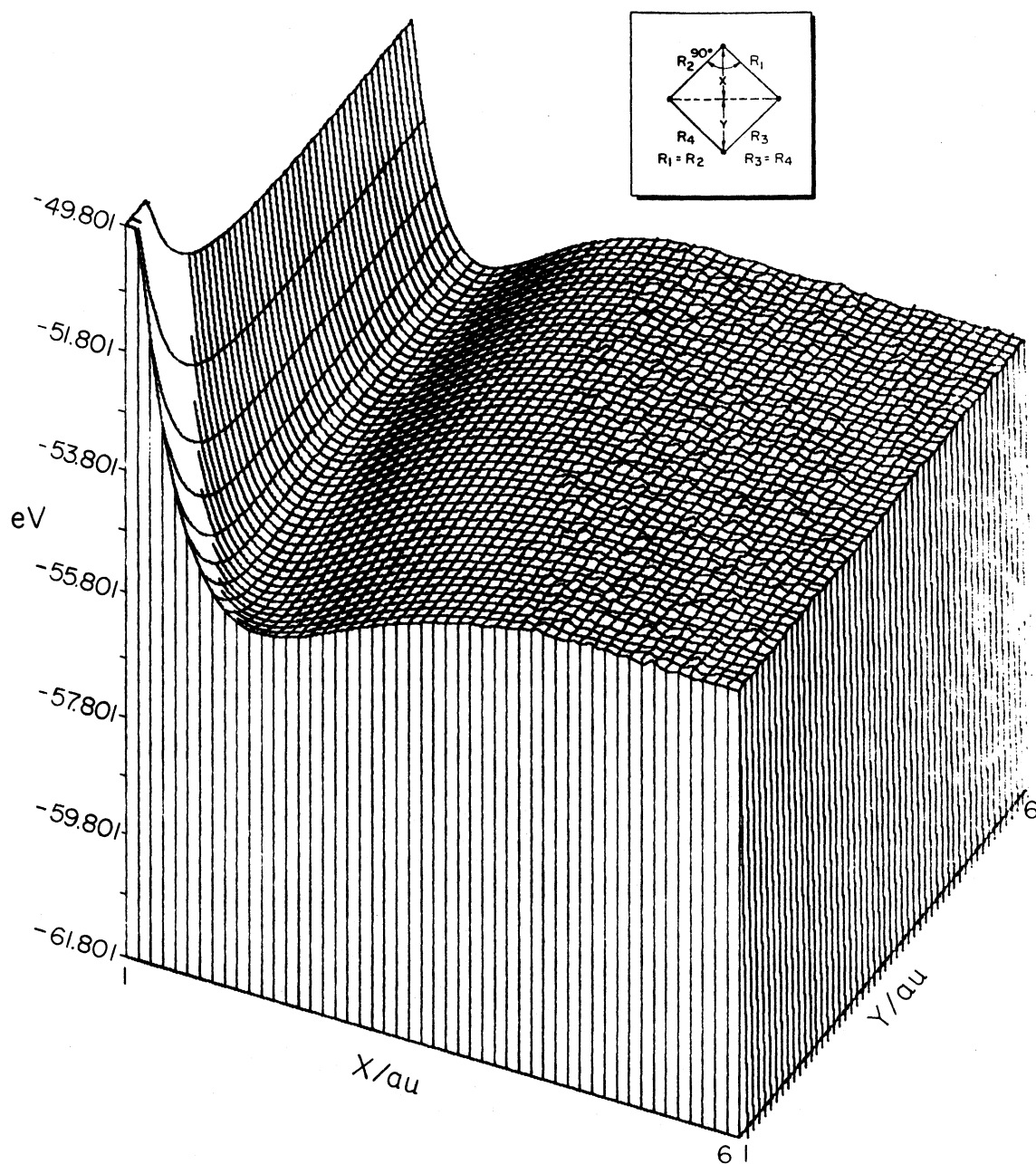


Figure 13. 3-D Plot of H_4 in Unsymmetric "T" Configuration

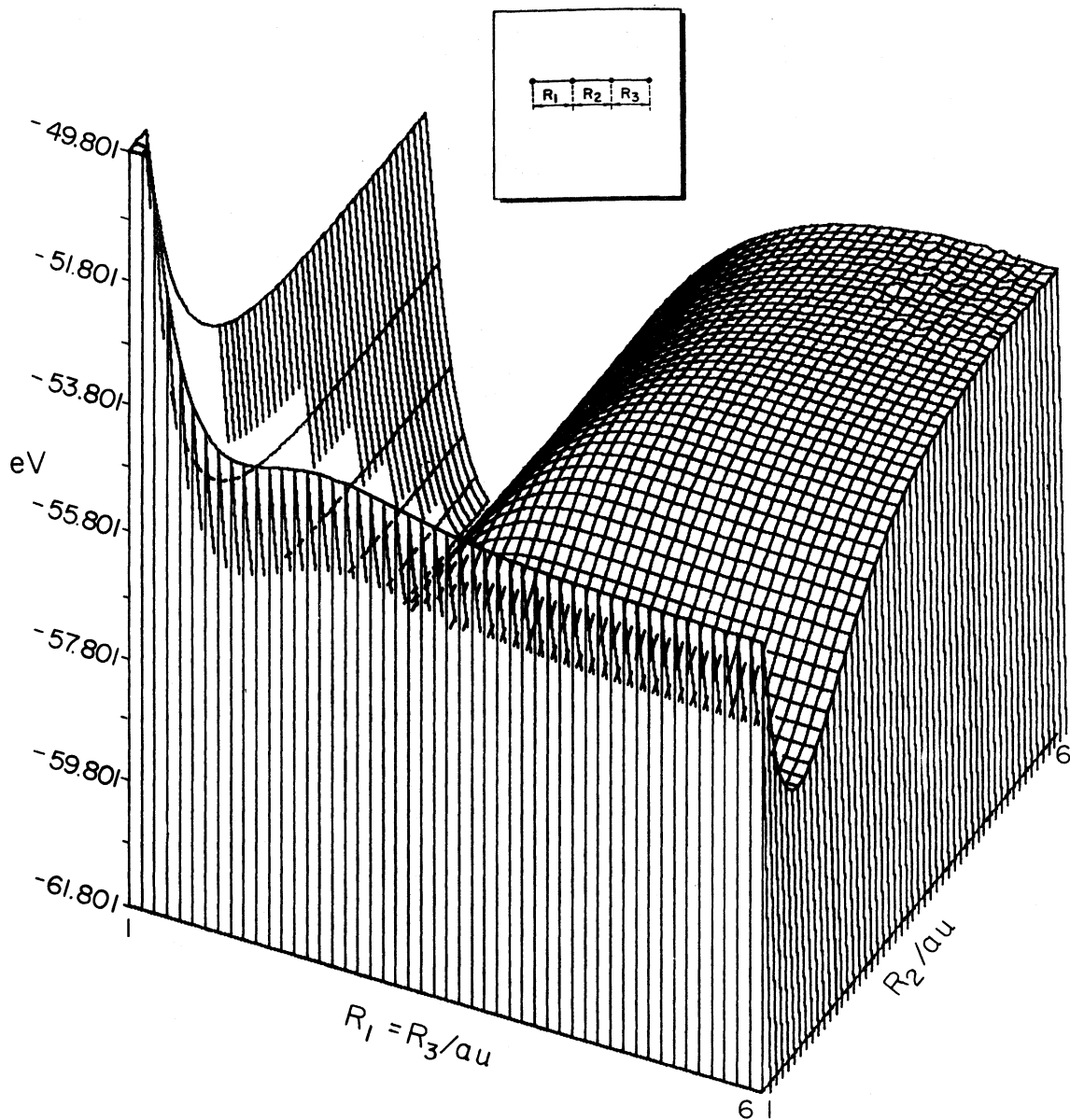


Figure 14. 3-D Plot of H_4 in Symmetric 120° "y" Configuration

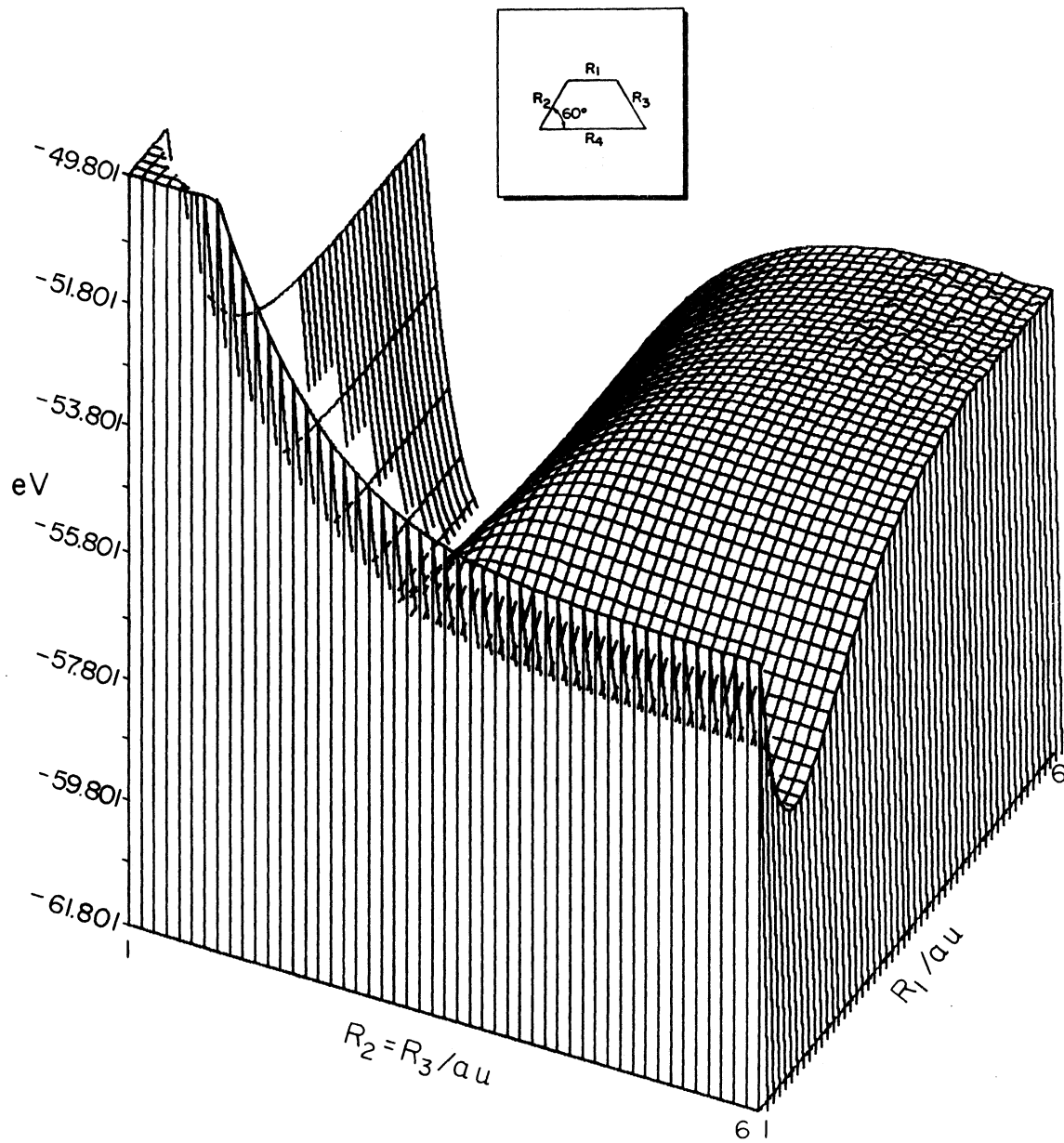


Figure 15. 3-D Plot of H_4 in Unsymmetric 90° "y" Configuration

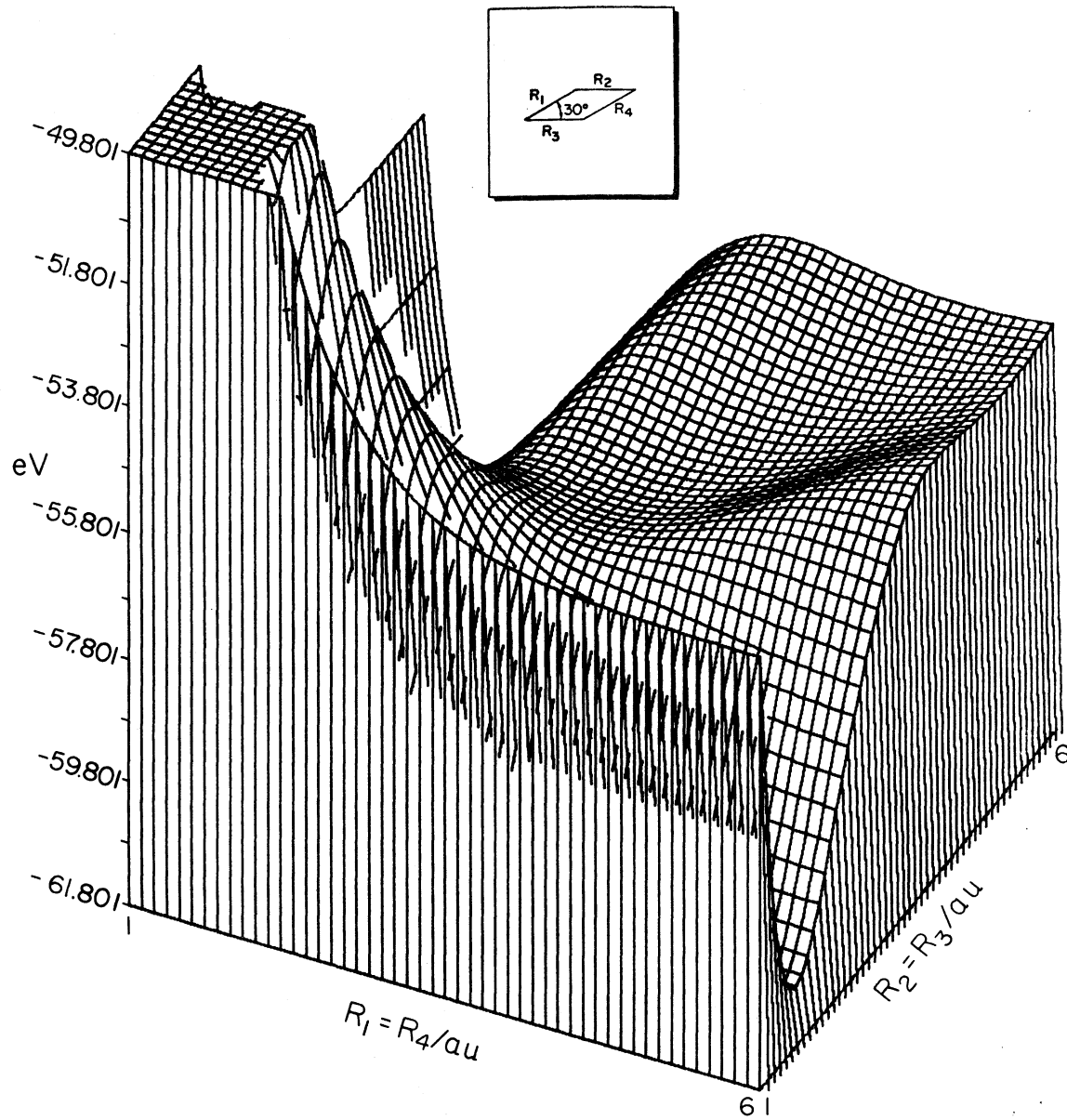


Figure 16. 3-D Plot of H_4 in Symmetric 90° "Y" Configuration

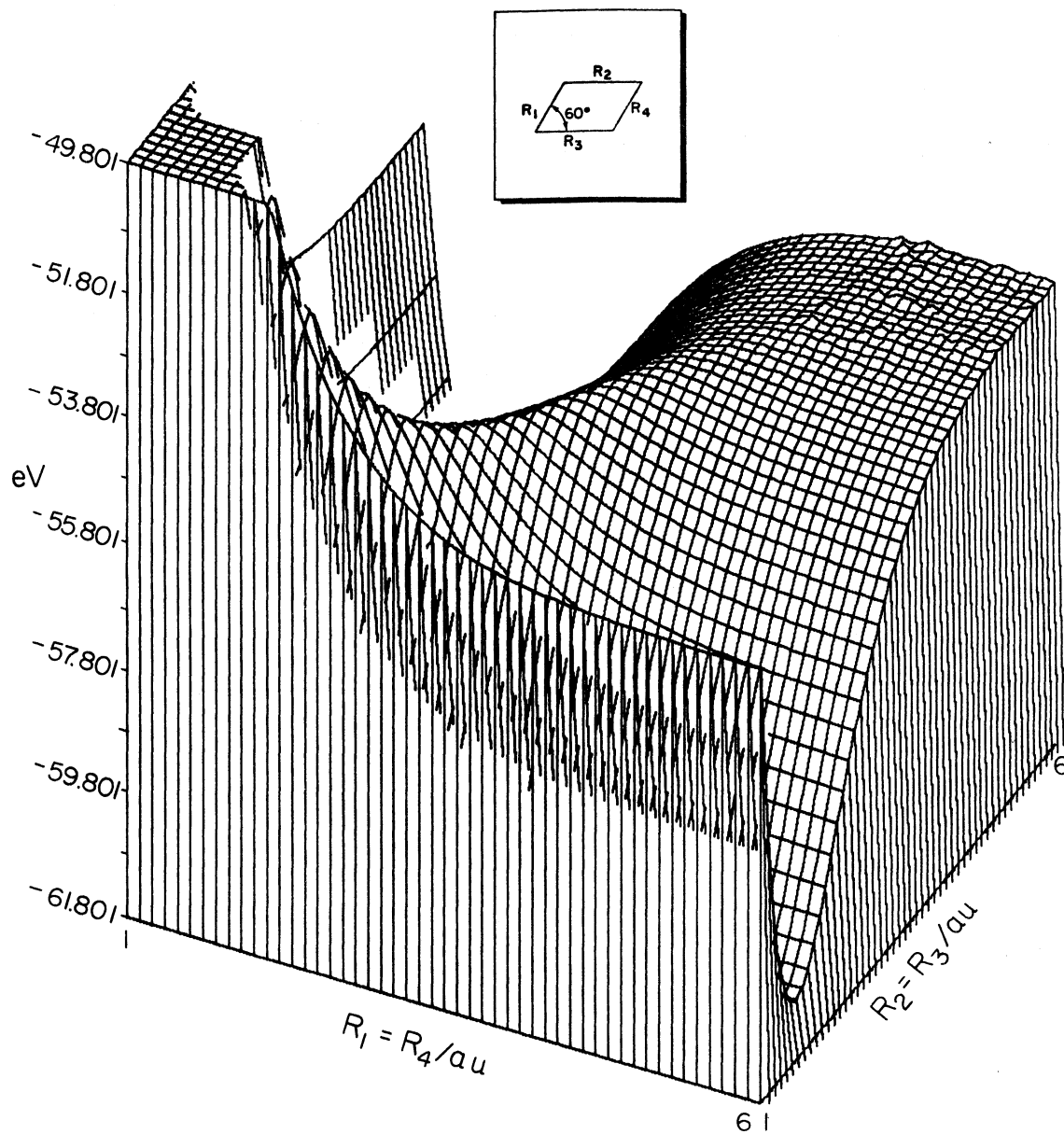


Figure 17. 3-D Plot of H_4 in Symmetric Linear Configuration

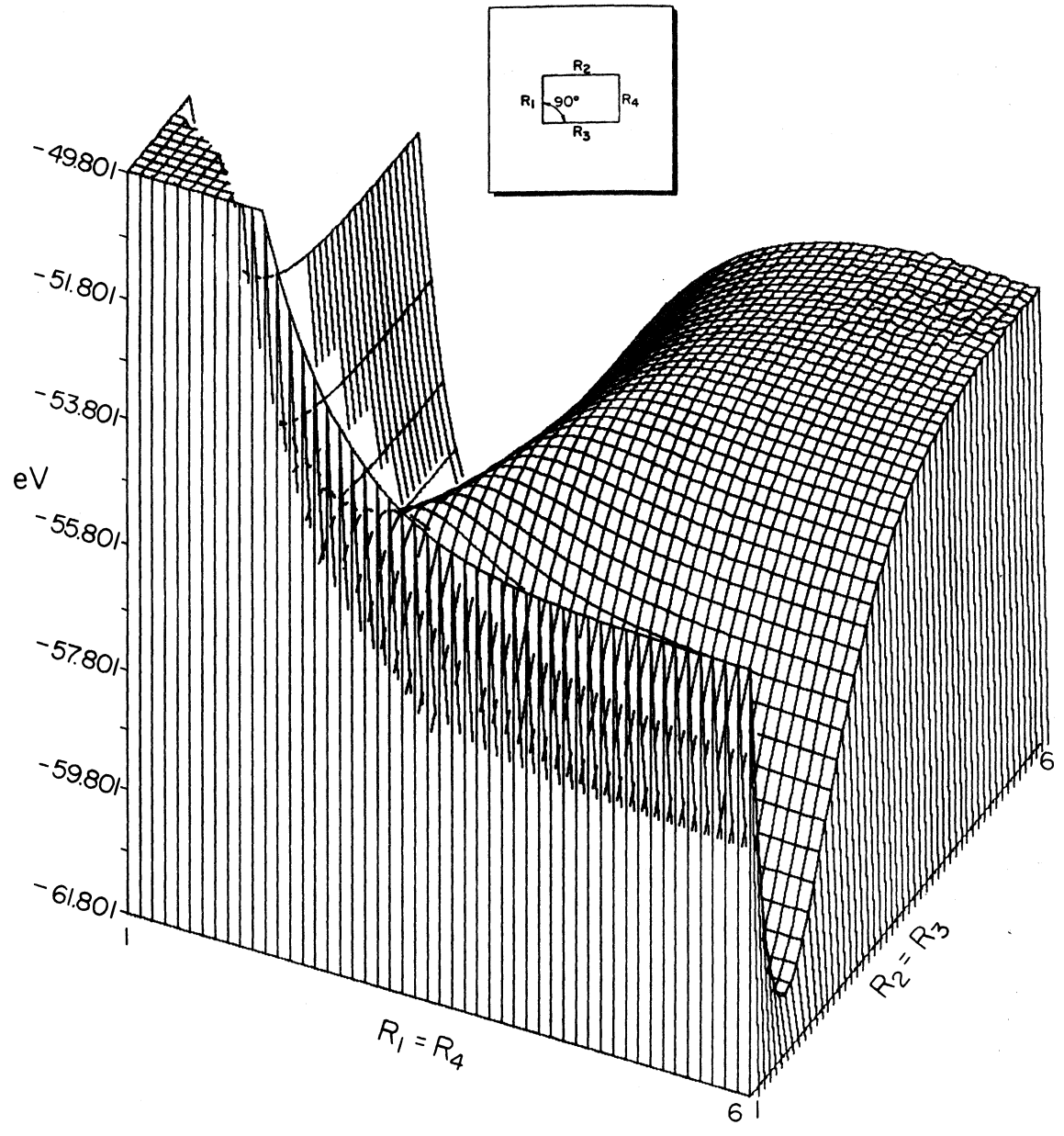


Figure 18. 3-D Plot of H_4 in a 30° Parallelogram Configuration

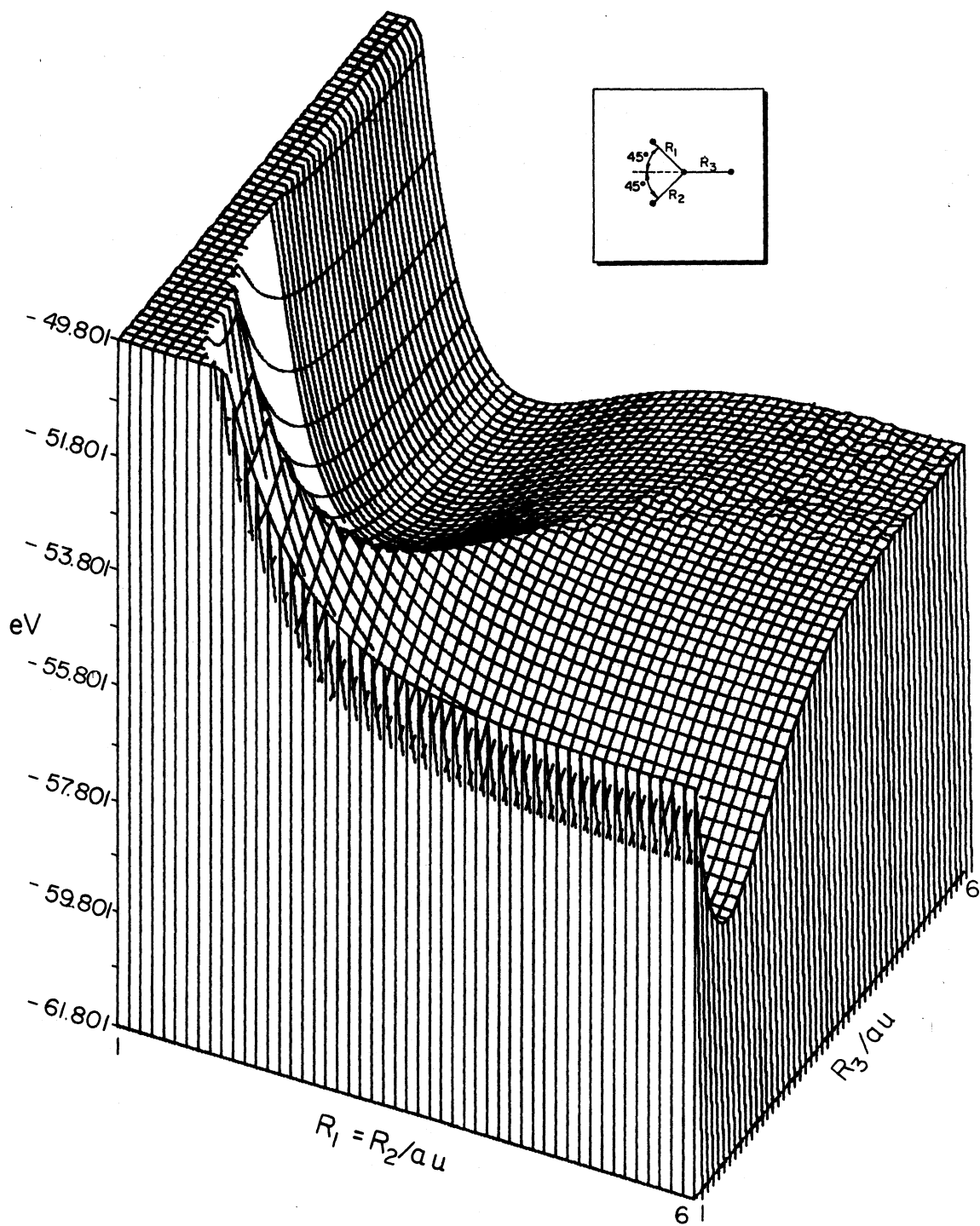


Figure 19. 3-D Plot of H_4 in a 60° Parallelogram Configuration

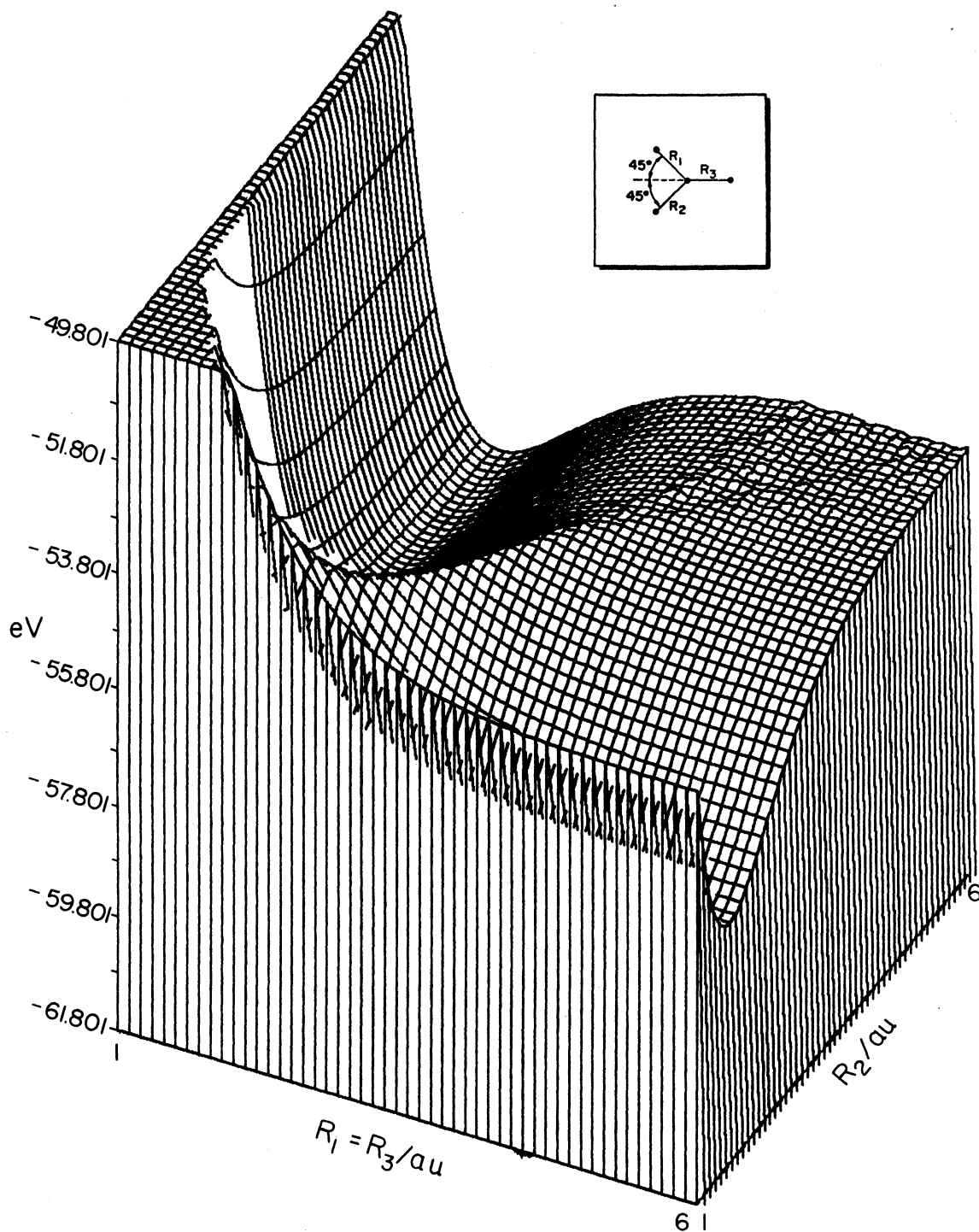


Figure 20. 3-D Plot of H_4 in Rectangular Configuration

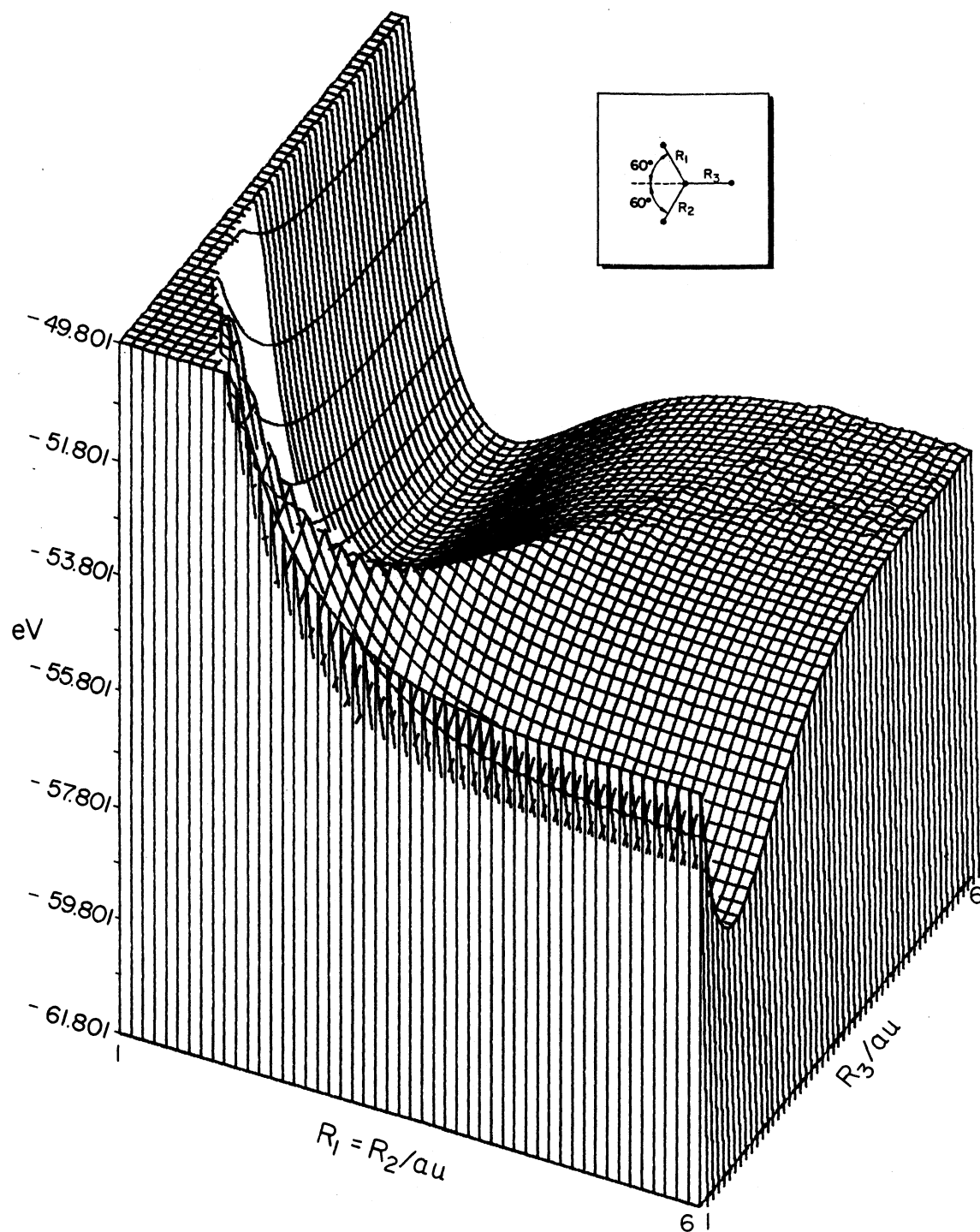


Figure 21. 3-D Plot of H_4 in a 60° Symmetric Trapezoidal Configuration

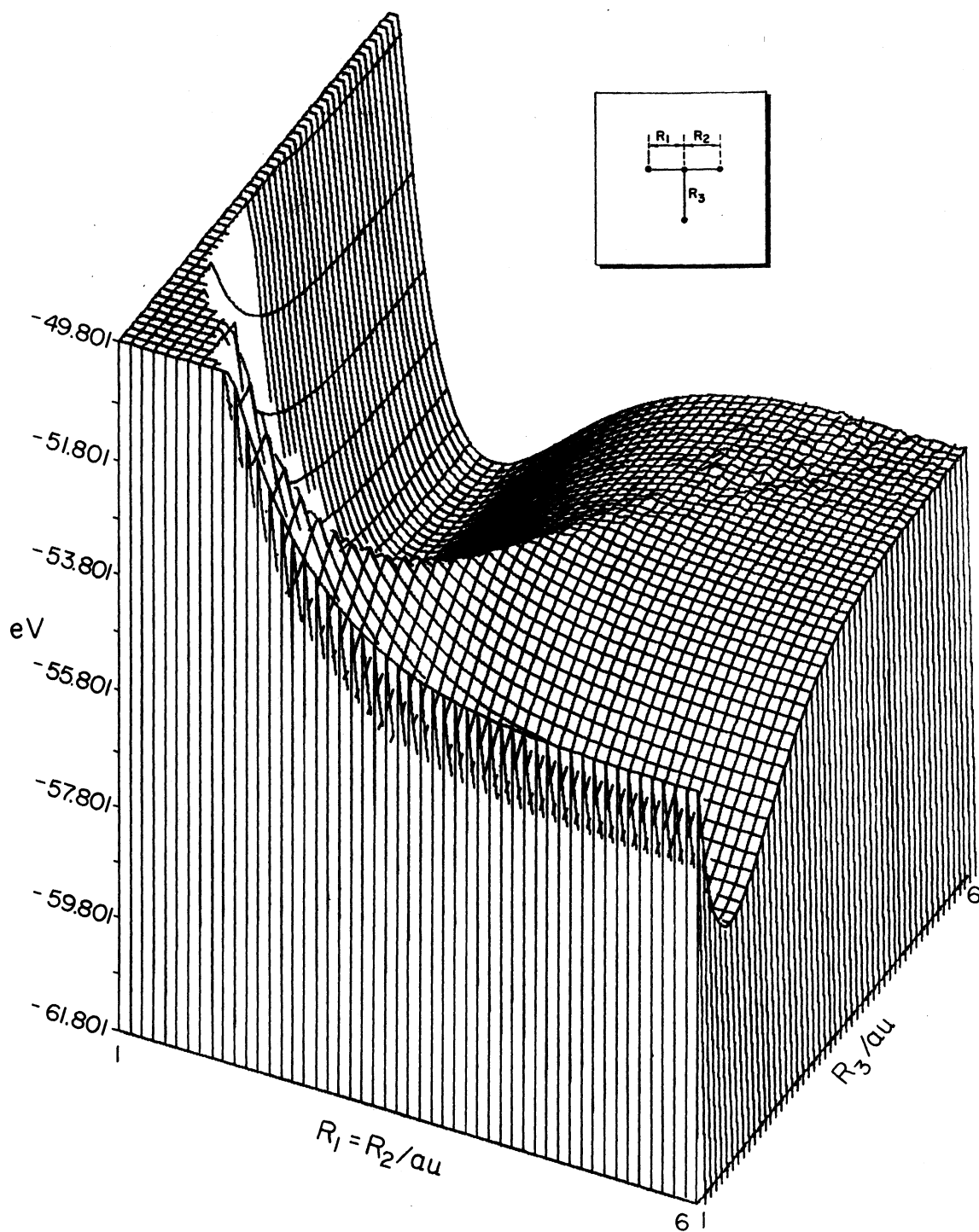


Figure 22. 3-D Plot of H_4 in a 90° Symmetric Kite Configuration

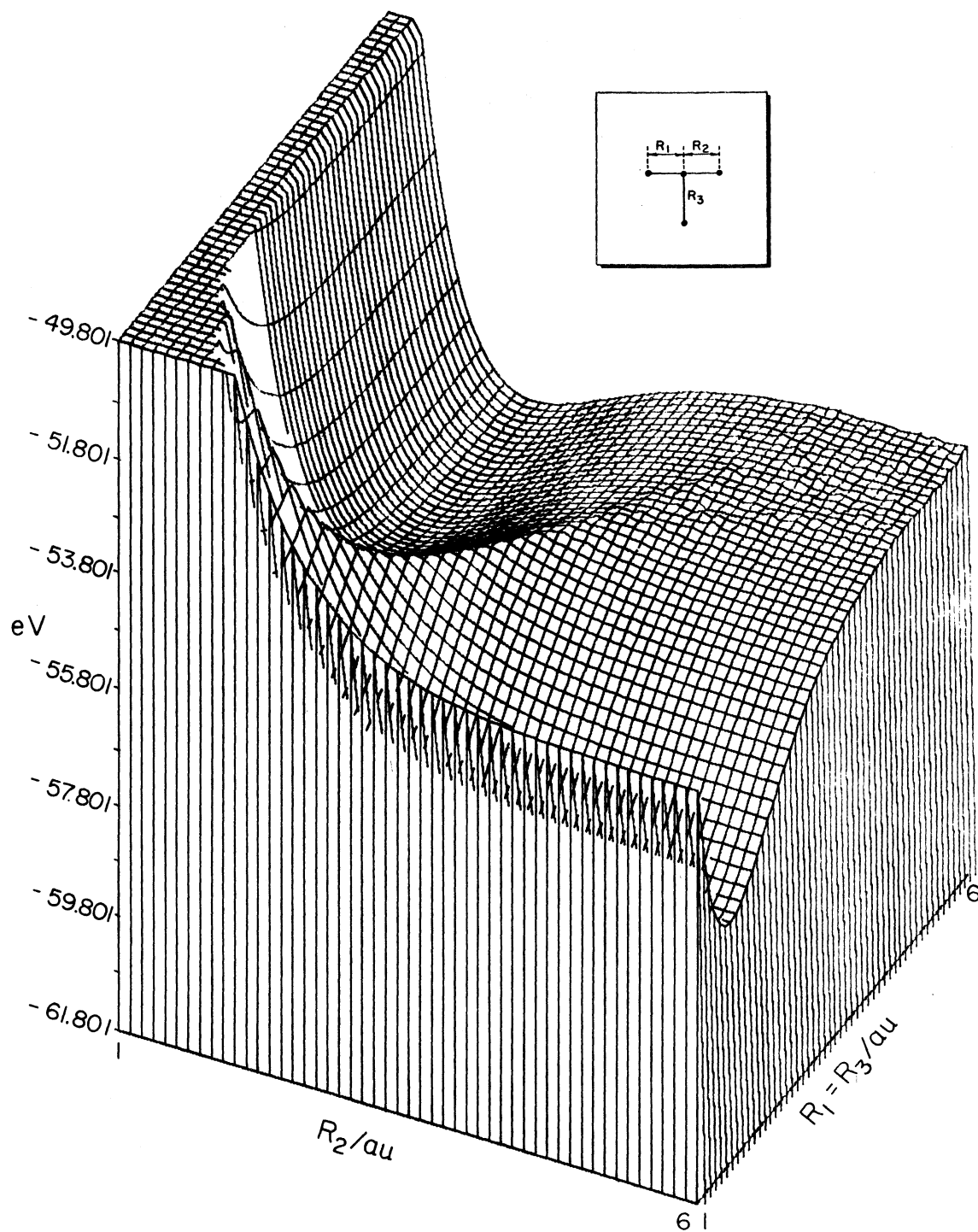


Figure 23. PES for Li-H-H Linear Configuration

$D_2, +2H, H_2$ $D+D, H_2+2D$. Unfortunately, the linear configuration cannot be a pathway for a four-body exchange mechanism without it rearranging into another conformation such as one of the parallelograms pictured in Figures 2-12 which would be compatible on geometric grounds for a four-body intermediate but not so in terms of barrier-height energies for these conformations. The lowest barrier-height energies for the various conformations given in Figures 2 thru 12 and Table III, that are compatible to a four-body intermediate being formed, are in the range of 130 kcal/mole and up. The square configuration yielded the lowest-valued saddle point ($E = -56.19$ e.v., $R = 2.49$) of any conformation compatible with four-body interaction mechanism. This agrees quite well with Wilson and Goddard's (56) results which showed that the square at $R = 2.6$ a.u., $E = -56.053$ e.v. represented the lowest saddle point energy of any geometrically compatible conformation they studied. This again reinforces the concept discussed by Porter and Raff that the minimal basis VB wavefunction contains a significant amount of configuration mixing especially in the square conformation. Their remains, even with the inclusion of possible vibrational preexcitation energy ($31 \frac{\text{kcal}}{\text{mole}}$) as discussed by Bauer and Ossa (6), the essential paradox between the experimental activation energy for the (H_2, D_2) exchange system and the barrier height energies found for likely four-body reaction conformations thus far investigated. All transition conformation energies studied are all higher than that of the H_2+2H system energy. This rules out these conformations as reasonable geometries for (H_2, D_2) exchange system since the experimental activation energy is less than half the energy required to break the H_2 bond. This brings this study to the point where a $Y \rightarrow T \rightarrow Y$ four-body reaction mechanism proposed by Gimarc (2) for

the H_2-D_2 exchange reaction is analyzed in terms of the VB method used herein. Gimarc's study used the semiempirical extended Huckel method. Comparison of VB and Hückel results for trans, T, and Y conformation are presented in Table IV. As in Table III the difference in energies between the two methods is quite pronounced with the extended Huckel results yielding the much more stable energy values. From the energy values for the Y and T conformations obtained by the semiempirical extended Huckel results Gimarc postulated a $Y \rightarrow T \rightarrow Y$ exchange mechanism for the (H_2, D_2) system. The barrier height based on the extended Huckel results in Gimarc's mechanism (dependent on the "T" structure) is in the near neighborhood of the experimental activation energy for the (H_2, D_2) exchange reaction. Thus the $Y \rightarrow T \rightarrow Y$ transformation is a viable four-body pathway if such is true.

Although the VB calculated energies may be in error by $\sim(10-15)$ kcal/mole, the VB formulation presented herein should easily possess sufficient accuracy to determine whether or not a $Y \rightarrow T \rightarrow Y$ potential pathway exists. This is implied as a consequence of the semiempirical extended Huckel results of Gimarc on such a pathway, whose barrier is some $60-80 - \frac{\text{kcal}}{\text{mole}}$ less than those previously investigated by ab initio methods (55,56).

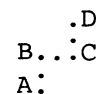
For the VB results it is seen from Table IV and Figures 2 thru 6 that the "Y" conformation energies are less than those of corresponding "T" conformations. Thus, the potential barrier for $Y \rightarrow T \rightarrow Y$ mechanism will be primarily dependent upon the energy of the "T" structure which in this aspect agrees with Gimarc's results. From Figures 2 and 3 the symmetric "T" shapes with $R_1 = R_2 = R_3$ all possess energies greater than -54.801 e.v. corresponding to a potential barrier for the (H_2, D_2)

TABLE IV
COMPARISON OF VB AND HÜCKEL RESULTS FOR TRANS, T, AND Y CONFORMATION

Form	Conformation Dimension	Present ξ	Cal. E (ev)	Extended Hückel ^a E (ev)
Trans ^b	2.46 au	1.01	-56.862	-62.542
T	Symmetric 2.46 au	1.02	-54.319	-61.127
Y	Symmetric 60°; 2.46 au	1.02	-55.736	-62.528

^aReference 2.

^b"Trans" refers to a planar structure of the form



exchange process of at least 161.4 kcal/mole. If the "T" is distorted as shown in Figures 2 and 3, the energy requirement decreases but not to the point where such an intermediate could be a viable transition state for the exchange. These VB results are in accord with those reported by Wilson and Goddard (56) who found no evidence for low energy states of "T" geometry ($R_1 = R_2 = R_3 = 2.2$ a.u., $E = -54.859$ e.v.).

The results obtained in the VB format vividly illustrate that the semiempirical extended Huckel calculation considerably overestimates the energy stability of various (H_2, D_2) conformations. This leads to a plausible four-body mechanism ($Y \rightarrow T \rightarrow Y$) on geometric grounds, being non-plausible on energy grounds when viewed from the relatively more theoretical VB results as compared with the semiempirical extended Huckel results. This point up that, in general, methods, such as Huckel type, that rely primarily or solely upon overlap considerations will tend to overestimate stability. This is due to the fact that the contribution of multicentered repulsion integrals is ignored in such methods. Usually relative stabilities may be obtained qualitatively by such methods but their use to predict reaction potential barriers quantitatively is a hazardous procedure as Gimarc (2) has pointed out and verified herein.

CHAPTER VI

CONCLUSIONS AND RECOMMENDATIONS

The previous section leads us to conclude that a $Y \rightarrow T \rightarrow Y$ four-body mechanism for the (H_2, D_2) exchange reaction is not a low-energy pathway that would make theory compatible with the shock-tube experiments Bauer and Ossa (6), Burcat and Lifshitz (20) and Kern and Nika (23). Also the study verified previous results on various (H_2, D_2) conformations that none yielded a pathway for the (H_2, D_2) exchange reaction consistent on energy grounds with the experimental activation energy.

A four-body reaction mechanism for the (H_2, D_2) exchange reaction has yet to be theoretically found after an exhaustive search of logical pathways containing some degree of symmetry. The VB method used herein is of size to be compatible, computerwise, with a Monte Carol analysis in order to generate a large array of points and corresponding energies for the (H_2, D_2) system. This data could then hopefully be reconcilable with the experimental activation energy and a four-body reaction pathway found from the internuclear distances associated with acceptable energy values.

PART II: $\text{LiH} + \text{H} \rightarrow \text{Li} + \text{H}_2$ AND $\text{LiH} + \text{D} \rightarrow \text{LiD} + \text{H}$ REACTIONS

CHAPTER VII

INTRODUCTION

General Remarks and Purpose of Study

The $\text{LiH} + \text{H} \rightarrow \text{Li} + \text{H}_2$ and the $\text{LiH} + \text{D} \rightarrow \text{LiD} + \text{H}$ are reaction systems which involve the simplest stable heteronuclear diatomic molecule (LiH) and homonuclear molecule (H_2) along with the simplest atom (H) and metal atom (Li) involved in either a hydrogen transfer reaction or hydrogen exchange reaction.

The calculation of a ab initio potential-energy surface (PES) for the (Li, H_2) , (LiH, H) systems as a function of various geometries by means of a quantum mechanical formulation is the starting point for theoretical reaction kinetic studies, for example, using either transition-state theory (69) or quasiclassical trajectories (70,71) on these previously mentioned reactions. Such a calculated PES could be of use in vibronic energy transfer studies and it may also be used to investigate translational-vibrational and translational-rotational energy transfer in these systems.

A valence bond (VB) formalism is used in this study to generate a quantum mechanical PES for various geometries, in particular (C_{2v}) and ($\text{C}_{\infty v}$) for the doublet spin states of the (Li, H_2) and (LiH, H) systems and these are presented in the form of two- and three-dimensional contour maps.

Due to the almost complete lack of both theoretical and experimental studies on these systems along with their importance as typical exchange reactions and likely charge transfer reactions involving a metal component with an open shell configuration, these reactions appear ideal for further study.

The use of a VB formalism herein with its builtin independent-particle type interpretation would be of considerable value to theoretical chemistry. These studies would be of value also to experimental chemistry in order to better plan effective ways to overcome possible experimental difficulties with these systems such as low or high barrier heights.

CHAPTER VIII

HISTORICAL

Experimental

Up to the present time there has been no experimental investigation on the (Li, H_2) and (LiH, H) systems. This is due in large degree to the high temperature region needed to observe the reactive systems and the complication of experimental techniques due to high reactivity of the open shell Li atom. This problem is even more prevalent when examining the above system for energy transfer processes dealing with inelastic scattering such as vibrational or rotational excitation of H_2 by collision with a Li atom.

Work has been done by Teonies and co-workers (72) on the (Li, H_2) system in terms of experimental measurements concerning vibrational and rotational excitation of H_2 by bombardment with Li ions. This was accomplished by utilizing a crossed molecular beam apparatus incorporating a time-of-flight technique to measure the loss in energy of the scattered Li.

In the closed shell system (Li^+, H) one does not have to be concerned with electronic excitation of the Li ions in the investigation of inelastic scattering where as this becomes a real, viable complication for the open shell (Li, H) system.

Semi-Empirical Calculations

The semiempirical calculations in the literature concern another alkali metal, sodium (Na), with H_2 rather than $Li-H_2$ because there exists experimental data (73) on the quenching of excited $Na(2^2P)$ by means of a nonadiabatic energy transfer with H_2 to produce vibrationally excited H_2 and ground state $Na(2^2S)$. In this content semiempirical PES have been formulated to qualitatively explain this above phenomenon and these calculations are being discussed here in light of the great similarity between the $Na-H_2$ and $Li-H_2$ in terms of electronic structures.

Magre and Ri (74) developed PES for the (Na, H_2) system using simple VB theory neglecting any ionic-type wave functions. The London formula (75) was used to obtain PES for both the ground state and first excited state for this system in the linear ($C_{\infty v}$) geometry only. The Coulombic energies and various exchange energies were approximated from Morse curves for the ground state NaH , H_2 and the excited state NaH . The nonadiabatic quenching was not possible from their PES analysis for the ground-state energy did not cross with the excited state energy. They speculated that for the triangular geometry (C_{2v}) the PES of the ground and excited states would cross through an ionic NaH state intermediate thus enabling a nonadiabatic quenching of the sodium D line.

Laidler (76) obtained a PES for the above quenching reaction, which included the ionic state $(Na-H-H)$ PES, by use of the same London formula along with the Coulombic integrals and exchange integrals from Morse type curves for the diatomic molecules that can be formed from H and Na. The results definitely confirm Magee and Ri's speculation that

the quenching proceeds from the upper excited state of Na thru the ionic state intermediate (Na-H-H) and then to the ground state from the observation that the ionic state PES for C_{2v} geometry intersects both the upper (excited) state and the lower (ground) PES of the system.

Mori (77) used a perturbation theory format with various wave functions of a product of a MO on the hydrogen molecule and an atomic orbital of the outer electron on the Na atom along with a charge transfer type wave function where the outer electron on the Na has been transferred to the H molecule, to investigate the quenching reaction involving excited NaH. In solving for the energy for the various PES states, all overlap integrals and integrals between non neighbors are neglected and no real difference between the perturbed and unperturbed Hamiltonian operators is assumed. From analysis of the resulting PES states, with the charge transfer state acting as the state through which nonadiabatic quenching is possible, Mori arrives at the same conclusion as Laidler concerning the quenching mechanism.

Nonempirical Treatment

Mayer and Schielep (78) used the method of Johnston and Parr (79) to calculate activation energies and rate coefficients at 1000 K for both the forward and reverse hydrogen transfer reactions in a linear reaction configuration involving lithium and hydrogen, namely; (1) $Li+H_2 \rightarrow LiH-H$ and (2) $LiH+H \rightarrow LiH_2$ reactions. The method of Johnston and Parr is a nonempirical treatment as it involves no adjustable parameters and used such bond properties as bond energy, vibrational wave numbers, and bond lengths to compute activation energies and rate coefficients.

The activation energies for reaction (1) and (2) respectively at 1000 K were computed to be $51.8 \frac{\text{kcal}}{\text{mole}}$ and $6.1 \frac{\text{kcal}}{\text{mole}}$ and the rate coefficients were $2.04 + 10^3 \frac{\text{cc}}{\text{moles}}$ and $2.69 + 10^{12} \frac{\text{cc}}{\text{mole-sec}}$.

Ab Initio PES Treatment

Krauss (80) was the first to report an ab initio PES calculation on the Li-H system. He employed Roothaan's (81) open-shell method as applied to a Hartree Fock calculation to compute the PES for the 2^2S and 2^2P electronic states of Li with H with the intent of using these PES for theoretical investigation of vibronic energy transfer in the Li H system. The particular vibronic energy transfer concerned was the nonadiabatic quenching of electronically excited Li (2^2P) atoms by energy transfer to the vibrational mode of ground state H_2 .

The analysis of the PES of Krauss yields similar results as those of previously mentioned semiempirical work (74,76) on the excited Na H system in that for the triangular geometry (C_{2v}), Krauss' Hartree Fock ground state PES, corresponding to a charge transfer state ($\text{Li}^+\text{H}-\text{H}$), did cross with the excited state PES at a H-H length of 2.0 a.u. and bisector length from Li to H-H of ≈ 3.3 a.u. No crossing was observed in the linear ($\text{C}_{\infty v}$) geometry. Thus for the C_{2v} geometry, Krauss's results indicate there is no activation energy required for Li atom to be electronically excited by energy transfer from vibrational mode of ground state H_2 and that nonadiabatic quenching of excited Li atom by energy transfer with the vibrational mode of ground state H_2 is plausible from the Hartree Fock MO PES presented.

Wahl and Das (82) used multiconfiguration self-consistent-field methods (MCSCF) to calculate an ab initio PES for the $\text{Li}+\text{H}_2 \rightarrow \text{LiH}+\text{H}$ reac-

tion system. The MCSCF method for this system employs Roothaan's open shell SCF procedure where both the linear MO parameters and the mixing coefficients for various configurations are optimized simultaneously in terms of energy minimization in contrast to a normal SCF-MO-CI calculation where only the mixing coefficients are optimized for fixed molecular orbitals.

In the MCSCF formalism the various MO are orthonormal to each other and the basis sets are composed of Slater type orbitals in contrast to the usual Gaussian type orbitals used as basis sets in MO type calculations. Wahl used STO on the Li atom consisting of 1s, 2s, 3s, 2p-1, 2p+1, 2p₀ functions and 1s, 2s, 2p-1, 2p₀, 2p+1 functions on each H atom.

No specific energy values for the PES were given in the Wahl and DAS paper although they did state that, according to the energy values calculated and the MO character of the wavefunction, the reaction occurs for $\text{Li} + \text{H}_2 \rightarrow \text{Li} + \text{H} + \text{H}$ only when the H_2 internuclear distance increases to between 2.0 and 2.5 a.u. They did not state what reaction geometry gave the lowest barrier height, but it is reasonable that the linear conformation would lead to such. Their results for C_{2v} geometry confirm Krauss' previous findings that indicate a large component of $(\text{Li}^+, \text{H}_2^-)$ character for this geometry.

Goddard and Ladner (83) used the SOGI method to construct a wave function for the $\text{Li} + \text{H}_2 \rightarrow \text{Li} - \text{H} + \text{H}$ system and then constructed the PES for the system in the linear reaction geometry. The SOGI wave function is a spin-coupled and MO optimized wave function done in a SCF format. This SOGI method, which is based on optimum coupling of spin and space orbitals, allows one to look at the resulting wave function in terms of

an independent-particle interpretation as it obviates the Hartree-Fock dilemma as to trying to get correct spin symmetry and proper dissociation occurring as bonds are broken. This is why Goddard has termed this type of wave function as a generalized valence bond (GVB) function even though its one electron orbitals are MO and energies are solved by a SCF methodology. Contracted sets of Gaussian functions are used as basis sets for the MO in their work. The saddle point for the $\text{Li}+\text{H}+\text{H} \rightarrow \text{Li}+\text{H}_2$ was consistent with Hammond's postulate (84) for the quite exothermic reaction (-51.3 kcal/mole, neglecting zero-point energies) in that the linear saddle-point is at $R_{\text{LiH}} = 3.20$ a.u. and $R_{\text{4-H}} = 3.10$ a.u. compared to the Li-H bond length of 3.09 au and H_2 bond length of 1.425 au. The calculated barrier height is 5.1 kcal/mole at the saddle-point which is about $\frac{1}{10}$ the energy of the LiH bond (50.3 kcal/mole). This barrier height is a least 2 kcal/mole higher when they considered the zero-point energy difference of LiH and the linear transition state.

In the reverse reaction: $\text{Li}+\text{H}_2 \rightarrow \text{LiH}+\text{H}$ the barrier height energy is 46.18 kcal/mole and the H_2 bond length changes only very gradually as the Li approaches. Hence it would appear that very few collisions would lead to a scattering path passing near the saddle-point. Thus, even though the total energies may be well above that required to pass over the barrier height, if the H_2 is not vibrationally excited, which enables the reaction cross section to remain quite low, very few collisions will lead to reaction (83)

Goddard's conclusion (83) is that the reverse reaction: $\text{Li}+\text{H}_2 \rightarrow \text{LiH}+\text{H}$ would require vibrationally excited H_2 . For example, for H_2 in the $v=6$ vibrational state the system has 7 kcal/mole more energy than required to go over the reaction barrier. The average value of $R_{\text{H-H}}$

for this vibrational state is 2.19 au which would foster higher reaction cross sections vital for increased probability for the reaction to occur.

By use of his orbital phase continuity principal (OCPE), Goddard (83,85) relates the gerade or ungerade characters of the outer molecular orbital centered on the Li atom and that of the molecular orbitals centered on each H atom with the condition that bonding orbitals will be as orthogonal as possible with the nonbonding orbitals in the transition-state region. From the above he arrived at the conclusion that the $\text{LiH} + \text{H} \rightarrow \text{Li} + \text{H}_2$ reaction should have a low activation energy associated with it, while for the reverse reaction, the activation energy should be much higher. Both are indicated to be so from the barrier heights found from his PES results (83).

Anderson (86) uses 12 points from Goddard's (83) ab initio surface for linear $\text{Li} + \text{H}_2 \rightleftharpoons \text{LiH} + \text{H}$ reaction to construct an analytic expression of the form:

$$W(R_1, R_2) = W_{D1}(R_1) + W_{D2}(R_2) + A \exp[-B(R_1 - (R_2 - D))^2] / (R_1 + R_2)$$

where R_1 and R_2 are the distances from the central nucleus (H) to the other nuclei (H, Li), W_{D1} and W_{D2} are ground state diatomic potential functions for LiH and H_2 , respectively and A, B, C, and D are adjustable parameters which are $A=3.1142$ au, $B=0.02335$ au, $C=3.2172$ au, and $D=3.7384$ au. Such an analytical expression should be useful in one-dimensional scattering work and should also be flexible enough to include modifications to take into account angular dependence of the energy when such ab initio energy points for the nonlinear systems are available such as those found from this study.

CHAPTER IX

METHOD

In this section the valence bond (VB) formalism used in this study to formulate the doublet electronic state of the (Li,H,H) system and its corresponding ground state PES is described. One-electron atomic orbitals multiplied by spin α or β constitute the spin orbitals used as basis functions for the system. The atomic orbitals are STO's and the following are used: 1s and 2s on Li atom, 1s on each H atom. The (Li,H,H) system is a 5 electron system and the following unnormalized product wave function (ϕ), written in the form of Slater determinants to satisfy the antisymmetry property of the electronic system, are used in the context of the VB formulation to obtain the doublet electronic states for the system:

$$\phi_1 = |a(1)\alpha(1)a(2)\beta(2)b(3)\beta(3)c(4)\alpha(4)d(5)2(5)| \quad (33)$$

$$\phi_2 = |a(1)2(1)a(2)B(2)b(3)2(3)c(4)2(4)d(5)B(5)| \quad (34)$$

$$\phi_3 = |a(1)2(1)a(2)B(2)b(3)2(3)d(4)B(4)d(5)2(5)| \quad (35)$$

$$\phi_4 = |a(1)2(1)a(2)B(2)d(3)2(3)d(4)B(4)c(5)2(5)| \quad (36)$$

$$\phi_5 = |a(1)2(1)a(2)B(2)c(3)2(3)c(4)B(4)d(5)2(5)| \quad (37)$$

In the above ϕ 's a is a Slater 1s atomic orbital on Li, b is a Slater 2s atomic orbital on Li, c and d are 1s Slater atomic orbitals centered on each of the H atoms in the system. That is:

$$a = N_1 e^{-\delta_1 r}; \quad b = N_2 e^{-\delta_2 r}; \quad c = N_3 e^{-\delta_3 r}; \quad d = N_4 e^{-\delta_3 r} \quad (38)$$

where N_1, N_2, N_3, N_4 , are the normalization constants for the corresponding Slater orbitals and $\delta_1, \delta_2, \delta_3$ are screening parameters for the Slater orbitals with the screening parameters of the two H atom STO's set equal to each other in order to limit the screening parameters to three in number to reduce the number of different integrals involved.

The first three ϕ 's are nonionic valence-bond functions which yield from the secular equation the two doublet states and quartet state. To obviate this problem (59) we construct two linear combinations of these in order to yield the doublet energy values from the secular equation without the quartet energy state. The resulting unnormalized wave functions which yield the doublet energy state are:

$$\psi_1 = \phi_2 - \phi_3 \quad \text{and} \quad \psi_2 = \phi_3 - \phi_1 \quad (39)$$

and correspond to nonionic doublet VB wave functions for the (Li,H,H) system where ψ_1 and ψ_2 can be pictured as representing a combination of the Li-H₂ and the LiH-H bonding scheme. ψ_1 and ψ_2 differ in which H atom is bonded to the 2s orbital on the Li atom in the LiH-H structure.

Now let $\psi_3 = \phi_4$ and $\psi_4 = \phi_5$. ψ_3 and ψ_4 are ionic valence-bond functions representing the Li⁺H⁻+H doublet ionic bonding scheme.

The total VB wave function is assumed to have the form:

$$\Psi = \sum_{i=1}^4 C_i \psi_i$$

that is, a linear combination of the various nonionic and ionic state ψ 's where the C_i are the coefficients which are minimized by the Variation Principle to yield the corresponding 6x6 secular equation. The

lowest root from the transformed diagonalized Hamiltonian matrix for the system yields the ground-state doublet energy for (Li,H,H) system in the context of the VB formalism used here.

Each of the ψ 's consist of 5x5 Slater determinants, which when combined with another ψ and either the identity operator or the Hamiltonian operator to form the matrix element, will yield upon spin integration a sum of twelve nonzero elements for each $\langle \phi_i | \phi_j \rangle$ and $\langle \phi_i | \hat{H} | \phi_j \rangle$. Six of the terms in the sum will be negative in sign and six will be positive depending whether the permutation is even or odd. That is, for example,

$$\begin{aligned}
 \langle \phi_3 | \hat{H} | \phi_4 \rangle &= \langle aabcd | \hat{H} | aaddc \rangle - \langle aabcd | \hat{H} | addac \rangle \\
 &\langle aabcd | \hat{H} | adcad \rangle - \langle aabcd | \hat{H} | aacdd \rangle - \langle aabcd | \hat{H} | cadda \rangle \\
 &+ \langle aabcd | \hat{H} | caadd \rangle - \langle aabcd | \hat{H} | ddcaa \rangle + \langle aabcd | \hat{H} | ddaac \rangle \\
 &- \langle aabcd | \hat{H} | daabc \rangle + \langle aabcd | \hat{H} | cddaa \rangle \\
 &+ \langle aabcd | \hat{H} | dacda \rangle - \langle aabcd | \hat{H} | cdaad \rangle
 \end{aligned} \tag{40}$$

and

$$\begin{aligned}
 \langle \phi_3 | \phi_4 \rangle &= \langle aabcd | aaddc \rangle - \langle aabcd | addac \rangle \\
 &+ \langle aabcd | adcad \rangle - \langle aabcd | aacdd \rangle - \langle aabcd | cadda \rangle \\
 &+ \langle aabcd | caadd \rangle - \langle aabcd | ddcaa \rangle + \langle aabcd | ddaac \rangle \\
 &- \langle aabcd | daadc \rangle + \langle aabcd | cddaa \rangle \\
 &+ \langle aabcd | dacda \rangle - \langle aabcd | cdaad \rangle.
 \end{aligned} \tag{41}$$

Thus, the overlap matrix elements consist of overlap integrals

between the Slater basis functions. These were obtained from analytically expressions given by Roothaan and coworkers (87).

The individual five electron product integrals containing the Hamiltonian operator (\hat{H}) for the system require first the expression for \hat{H} itself. In atomic units it has the form:

$$\begin{aligned} \hat{H} = & -\frac{1}{2} \nabla_1^2 - \frac{1}{2} \nabla_2^2 - \frac{1}{2} \nabla_3^2 - \frac{1}{2} \nabla_4^2 - \frac{1}{2} \nabla_5^2 - \frac{3}{r_{1A}} - \frac{1}{r_{1B}} - \frac{1}{r_{1C}} - \frac{3}{r_{2A}} \\ & - \frac{1}{r_{2B}} - \frac{1}{r_{2C}} - \frac{3}{r_{3A}} - \frac{1}{r_{3B}} - \frac{1}{r_{3C}} - \frac{3}{r_{4A}} - \frac{1}{r_{4B}} - \frac{1}{r_{4C}} - \frac{3}{r_{3A}} - \frac{1}{r_{3B}} \\ & - \frac{1}{r_{3C}} + \frac{1}{r_{12}} + \frac{1}{r_{13}} + \frac{1}{r_{14}} + \frac{1}{r_{15}} + \frac{1}{r_{23}} + \frac{1}{r_{24}} + \frac{1}{r_{25}} + \frac{1}{r_{34}} + \frac{1}{r_{35}} \\ & + \frac{1}{r_{45}} + \frac{3}{R_{AB}} + \frac{3}{R_{AC}} + \frac{1}{R_{BC}} \end{aligned} \quad (42)$$

where A stands for the Li atom nucleus and B and C represent the two H atom nuclei.

In writing the \hat{H} expression the Born-Oppenheimer approximation (63) is used and no spin coupling or relativistic terms are included. Thus, from the integrals that contain the \hat{H} operator one gets electron kinetic energy integrals; one, two and three-center nuclear-electron attraction integrals; one, two, and three-center electron-electron Coulombic and exchange integrals, along with the nuclear repulsion integrals. The one- and two-center electron kinetic energy integrals, one- and two-center electron nuclear attraction integrals and the one- and two-center Coulombic integrals were all obtained from analytical expressions given by Roothaan and coworkers (87). The two-center electron-electron hybrid integrals were solved analytically based on work by Ruedenberg (88) and Rosen (89). The two-center electron-electron exchange integrals,

except one, were found by first applying Mulliken's approximation (48) which reduces them to a sum of one-and two-center Coulombic integrals which were analytically calculated as previously described. The two center electron-electron exchange integral between the two 1s electrons centered on each H atom was calculated analytically from expression given by Slater (65) in correlation with the use of Hasting's expression (66) for: $\int_x^\infty \frac{1}{\mu} e^{-u} du$ where u is a dummy integration variable and x is equal to $2\delta R$. All the three-center integrals were changed to a sum of two-and one-center integrals by the use of Mulliken's approximation which then were analytically solved. All integrals are listed in the Appendix of the thesis.

The use of permutation rules (59) and the fact that the wave functions are Hermitian allows one to reduce the number of terms one actually has to calculate in this system.

$$\text{(i.e. } \langle aabcd | \hat{H} | badca \rangle = \langle aabcd | \hat{H} | daacb \rangle) \quad (43)$$

But in the end there are 105 terms of the form $\langle aabcd | baacd \rangle$ and $\langle aabcd | \hat{H} | baacd \rangle$, etc., which have to be calculated. The screening parameters, $\delta_1, \delta_2, \delta_3$, are left as adjustable constants in the resulting one-and two-electron integrals so that they too can be varied to minimize the energy for different geometric configurations.

The analytic expressions for the one-and two-center electron integrals were checked from Matsen's VB work (90) on the LiH where numerical values were given for the LiH molecule at its equilibrium value. The 105 terms that present themselves after spin integration on the matrix elements in the secular equation were checked at the Li-H₂, LiH-H, and Li-H-H geometric configurations along with the symmetric

linear geometry (H-Li-H) to see if indeed some of these 105 terms become equal to each other or equal to zero as required from symmetry considerations. Finally the system was put in the LiH-H, Li-H₂ and Li-H-H geometries to see whether the secular equation gave the doublet ground state energies that were compatible with experimental energy values for these asymptotic geometric limits of the (Li,H,H) system.

CHAPTER X

RESULTS AND DISCUSSION

The first value to be presented and discussed here are the appropriate limits for the separate atom and molecule systems: Li-H_2 and LiH-H . These values are given in Table V along with Goddard's results (83) and the experimental limits (91,92). A word here about the LiH-H limit. The H-H distance in the VB method used herein was taken as 21.6 au which is a large enough H-H distance to represent the LiH-H system limit satisfactorily as it is well outside any van der Waal interaction region between the two hydrogen atoms. For HH distances greater than 100 au, the VB calculations herein gave a LiH-H limit energy which was $\approx .1$ eV higher in energy than the saddle-point energy of the linear LiH-H system to be discussed later. For these reasons the energy for LiH-H limit was taken to that corresponding to $R_{\text{H-H}} = 21.6$ au and $R_{\text{LiH}} = 3.30$ au at its equilibrium value. It appears that for $H, H > 100$ au the associated energy for the LiH-H system in comparison to the saddle-point energy of the LiH-H system is an artifact. This is due to the use of Mulliken's approximation for the two-center exchange integrals involving the 1s and 2s orbitals on Li atom with the 1s on the H atom comprising the LiH molecule and their interaction with other terms in the 4×4 secular matrix as extremely large internuclear distances of H,H (100 au) are achieved. For the Li-H_2 system limit no similar discrepancy as above was found for large LiH distances (>20 au).

TABLE V
 COMPARISON OF VB RESULTS WITH GODDARD'S SOGI CALCULATIONS
 AND WITH EXPERIMENT

	$R_{e_{H_2}}$ (au)	$E(R_{e_{H_2}})$
Li + H ₂ system limit: Goddard's results	1.426	-234.0005 e.V.
VB results herein	1.41	-232.7487 e.V.
Experimental	1.4008	-235.4498 e.V.
	$R_{e_{LiH}}$ (au)	$E(R_{e_{LiH}})$
LiH + H system limit: Goddard's results	3.092	-231.7766 e.V.
VB results herein	3.30	-230.4819 e.V.
Experimental	3.015	-233.2179 e.V.

As is seen from Table V the absolute value of Li-H_2 and LiH-H limits for the VB method herein are approximately 3 eV too high for both limits when compared to the experimental values. The calculated exothermic heat of reaction (neglecting zero point energies of H_2 and LiH) for the reaction $\text{LiH+H}\rightarrow\text{Li+H}_2$ is -51.468 kcal. for the VB method. This is within 1 Kcal/mole of that calculated from the experimental energy values for Li-H_2 and LiH-H (91,92) and that found from Goddard's data (83).

The equilibrium internuclear separation of LiH in the LiH-H separated limit was found to be 3.30 au as mentioned previously. This is larger than experimental equilibrium value of 3.015 au or Goddard's value of 3.092 au. This is a consequence of the use of Mulliken's approximation for the two-center exchange integrals involving the 1s and 2s orbitals of the Li atom with the 1s orbital on the H atom comprising the LiH molecule. Mulliken's approximation is proportional to overlap integral square so these two-center exchange integrals will have a higher value at the experimental equilibrium internuclear distance than the analytical values of such. Thus, in order to lower the energy of these electron-electron type integrals, thereby lowering the system energy, the equilibrium distance of $R_{\text{Li-H}}$ does increase to the VB found value of 3.30 au. The equilibrium value of the H-H bond distance in the Li-H_2 separated limit (1.41 au) is in excellent agreement with both the experimental H-H equilibrium bond distance (1.4008 au) and Goddard's value (1.426 au). This is to be expected due to the fact that all nonzero integrals which are present in such a configuration are analytically obtained along with the fact that the VB method should yield good correlation here with the experimental value due to the Li-H_2

limit representing a primarily covalent bonding type situation.

The VB result for the Li+H+H limit was found to be -229.058 ev. This was the first limit found of the three mentioned (LiH-H and Li-H₂ being the others) and was used in the initial stages of checking for computer program errors.

In all the above work and subsequent work to be discussed the best values the screening parameters in the 1s and 2s orbitals on the lithium atom that resulted in minimized system energy were the Slater values (60) for each, namely: 2.70 for 1s of Li, 0.65 for 2s of Li. The best value for the screening parameter in the 1s orbital on the H atoms were found to be 1.16 for H-H distance <1.6 au, 1.08 for H-H> 1.6 au but <1.8 au, 1.0 for H-H distance> 1.8 au.

The first potential-energy surfaces to be discussed are those related to likely reaction geometries for the reaction: LiH+H→Li+H₂. The three geometries studied were the linear configuration, a configuration with the H-H bond inclined 45° relative to the horizontal line containing the LiH bond, and the configuration with the H-H bond inclined 90° relative to the horizontal line containing the LiH bond. These are pictured in Figures 24 thru 27. The contour line values are listed in Table IX. Thus, one has a straight line, an obtuse triangle, and right triangle formed, respectively from the above three reaction surfaces studied. The saddle point and associated barrier height energies relative to the LiH-H limit are given in Table VI. One sees that the linear configuration gives the lowest barrier-height energy (6.2 kcal/mole). Agreement with Goddard's value (83) of 5.1 Kcal/mole for this configuration is good. The LiH and H-H internuclear distances at the saddle point, 3.50 au and 3.14 respectively, compare favorably with Goddard's values

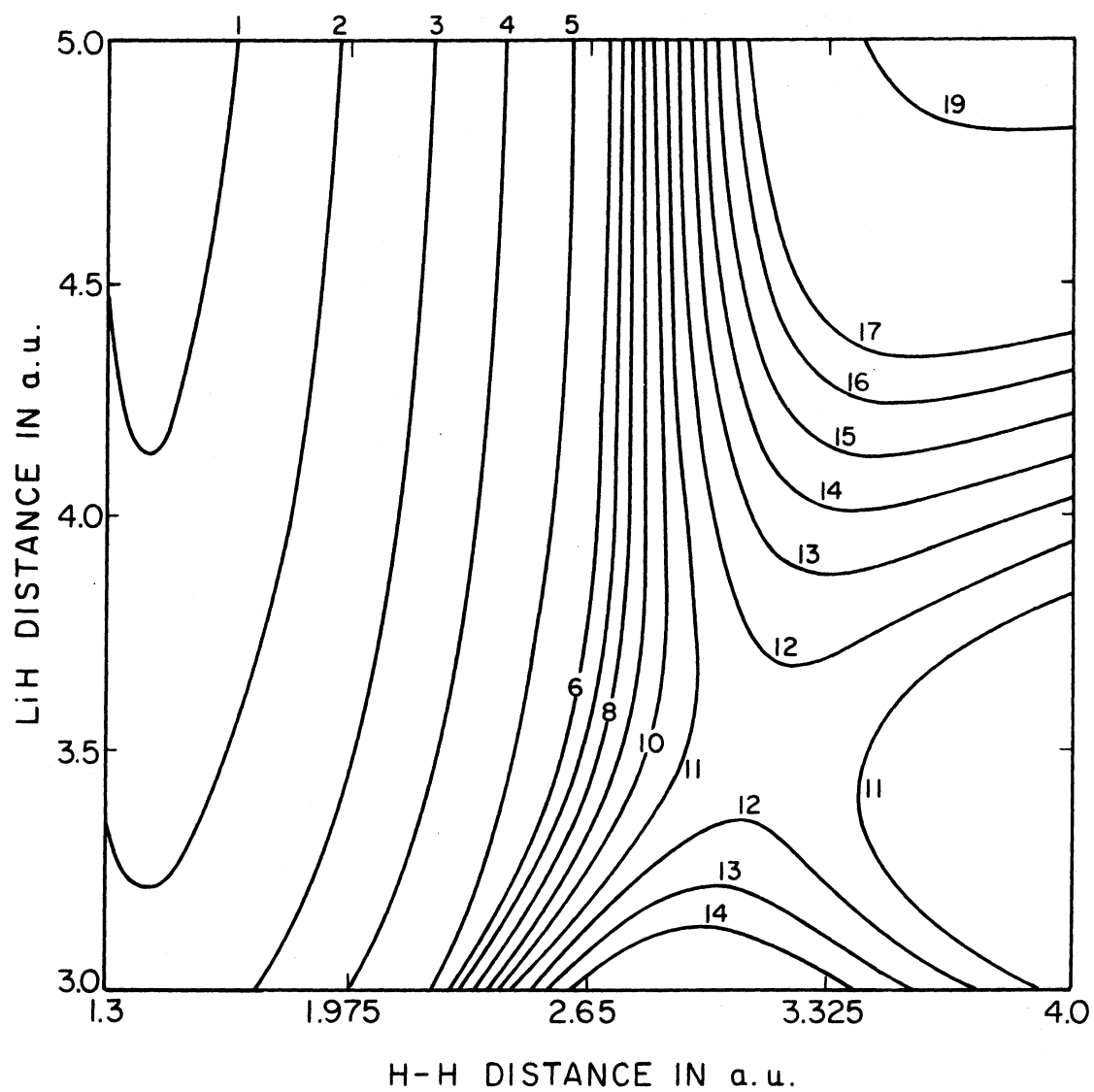


Figure 24. PES for Li-H-H in 135° Obtuse Triangle Configuration

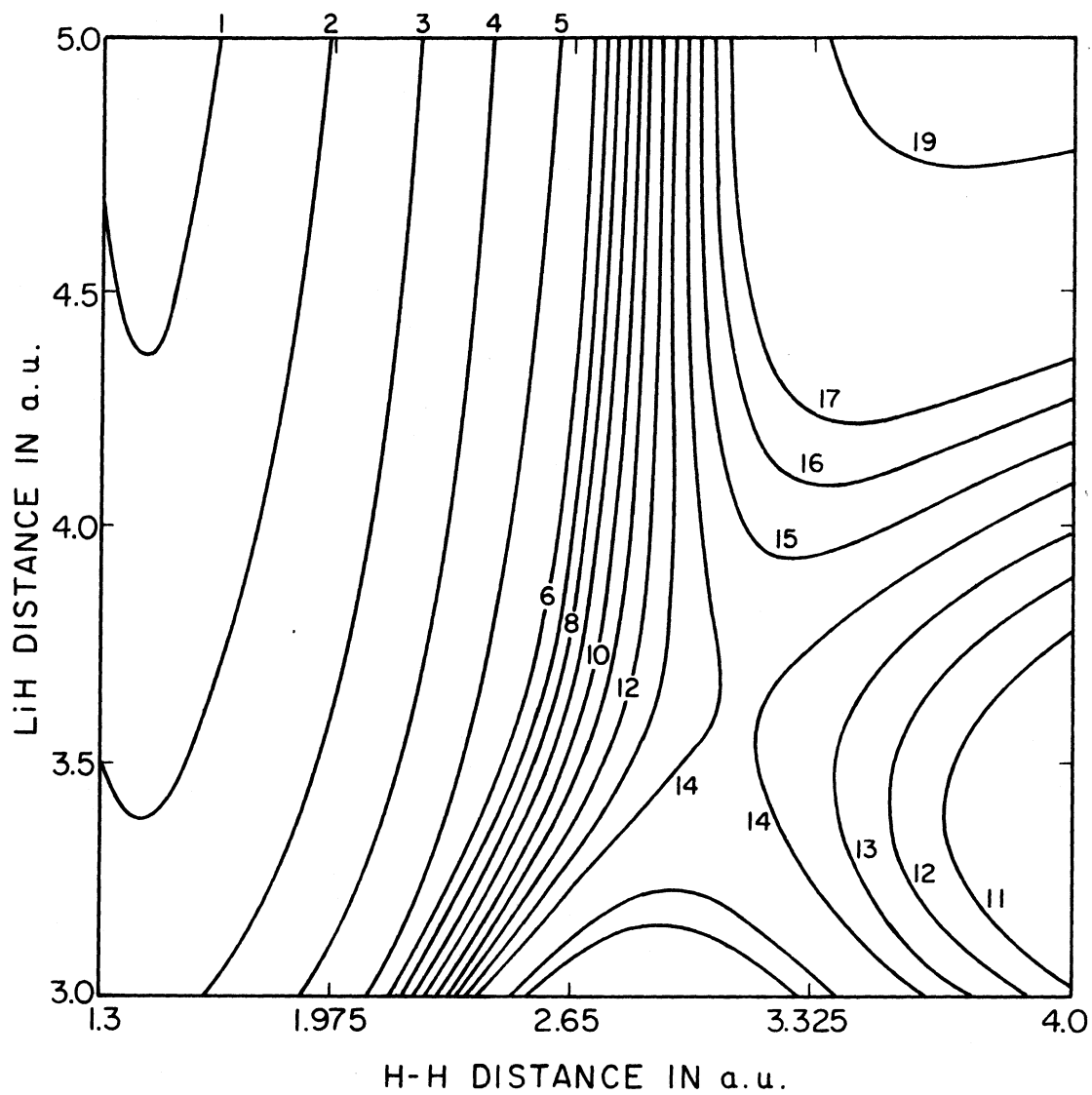


Figure 25. 135 Degree VB Surface for Li-H-H

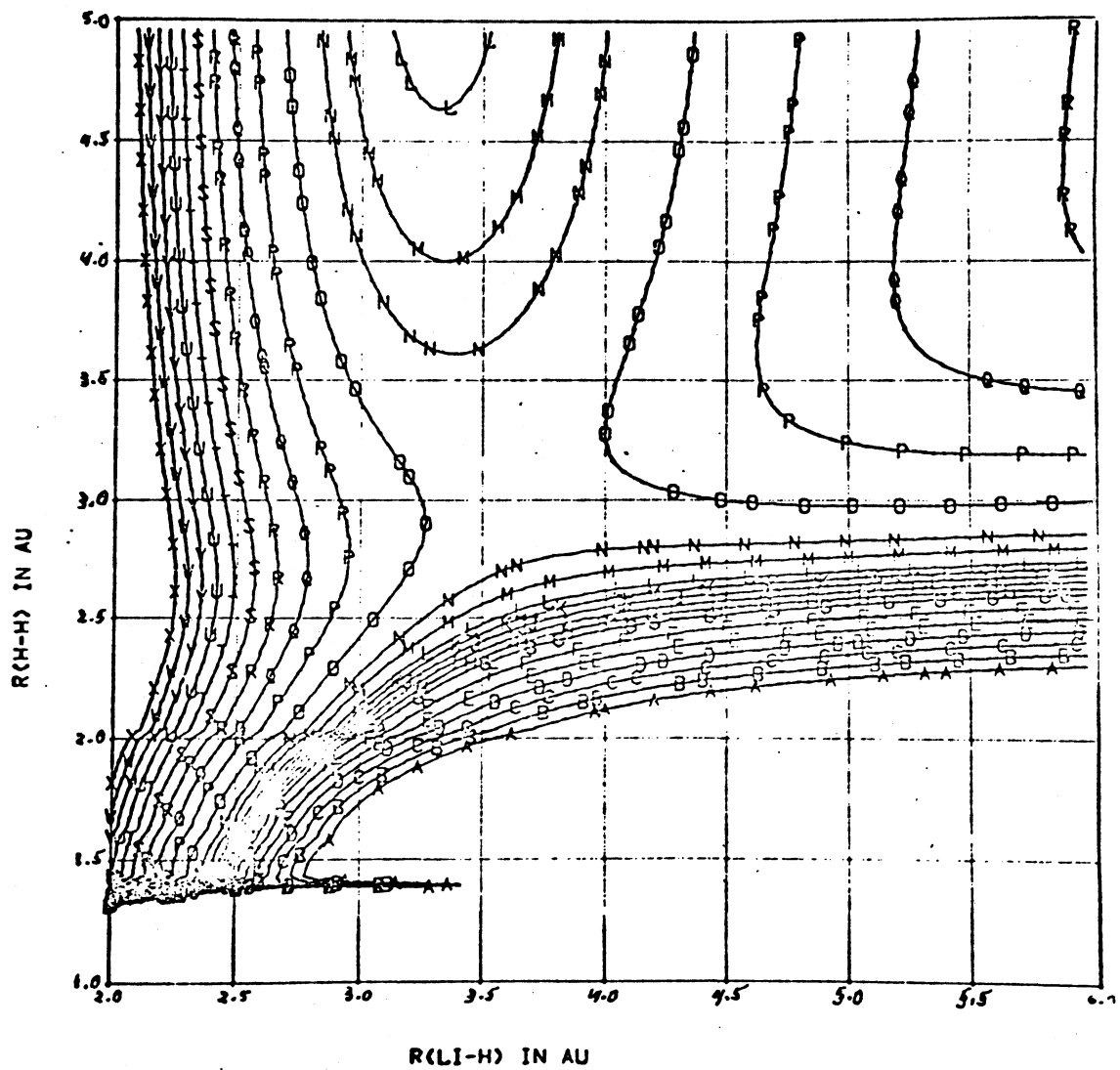


Figure 26. 90 Degree VB Surface for Li-H-H

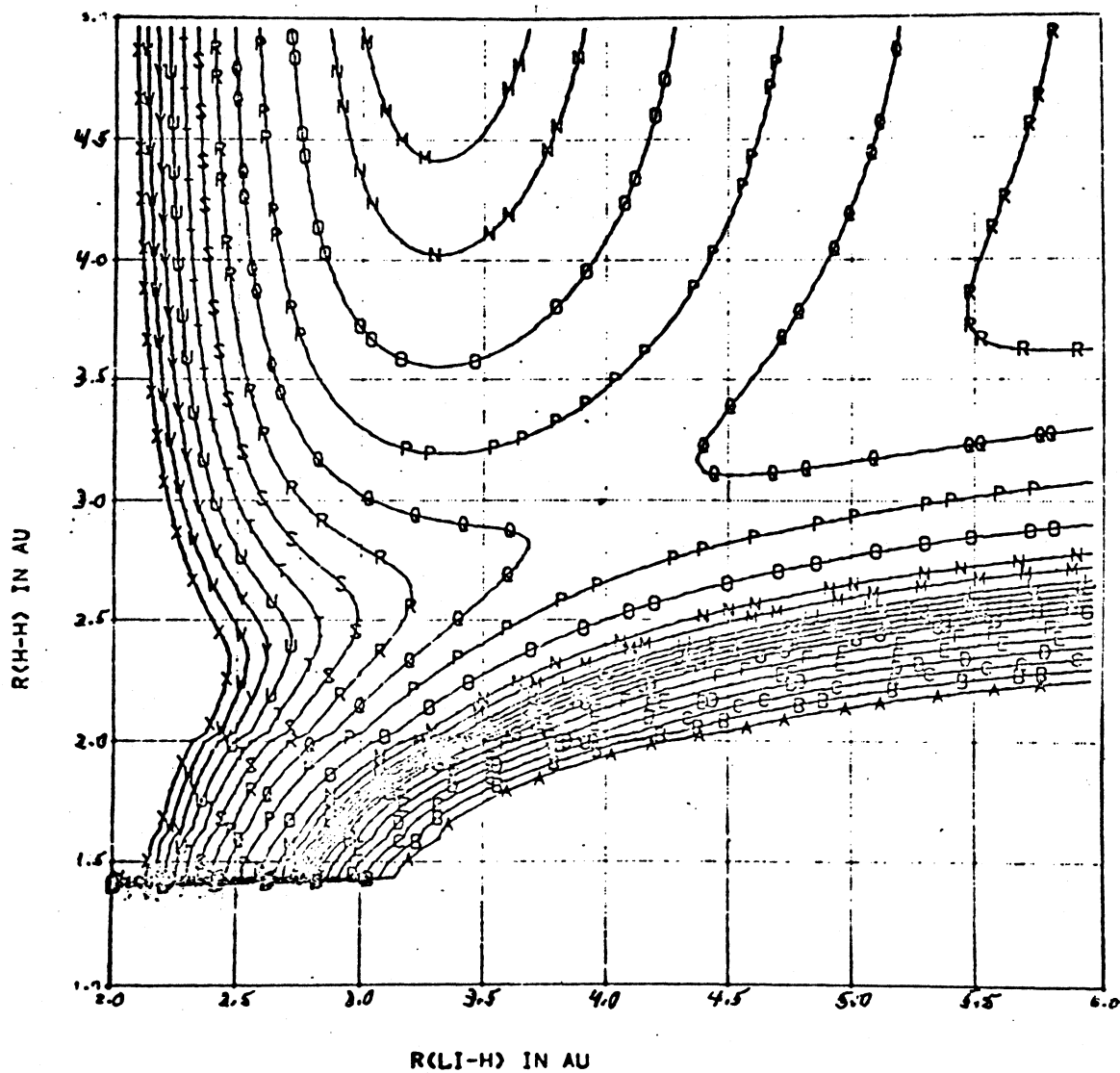


Figure 27. 135 Degree VB Surface for H-Li-H

TABLE VI

BARRIER HEIGHT ENERGIES AND SADDLE POINTS FOR $\text{LiH}+\text{H} \rightarrow \text{Li}+\text{H}_2$
REACTION FOR VARIOUS CONFIGURATIONS

Configuration	Barrier Energy* (Kcal/mole)	Saddle Points
Linear (Li-H-H)	6.2	$R_{\text{LiH}} = 3.5 \text{ a.u.}$ $R_{\text{H-H}} = 3.14 \text{ a.u.}$
Obtuse triangle (Li-H ^H)	8.4	$R_{\text{LiH}} = 3.53 \text{ a.u.}$ $R_{\text{H-H}} = 3.04 \text{ a.u.}$
Right triangle (Li-H ^H)	≈ 17.0	$R_{\text{LiH}} \approx 4.0 \text{ a.u.}$ $R_{\text{H-H}} \approx 3.0 \text{ a.u.}$

*Relative to $\text{LiH}+\text{H}$ separated limit of -230.4819 e.V.

BARRIER HEIGHT ENERGIES AND SADDLE POINTS FOR $\text{Li}+\text{H}_2 \rightarrow \text{LiH}+\text{H}$
REACTION FOR VARIOUS CONFIGURATIONS

Configuration	Barrier Energy ⁺ (Kcal/mole)	Saddle Points
Linear Li-H-H	58.5	$R_{\text{LiH}} = 3.5 \text{ a.u.}$ $R_{\text{H-H}} = 3.14 \text{ a.u.}$
Obtuse Li-H ^H	60.7	$R_{\text{LiH}} = 3.53 \text{ a.u.}$ $R_{\text{H-H}} = 3.04 \text{ a.u.}$
Right triangle Li-H ^H	≈ 69.3	$R_{\text{LiH}} \approx 4.0 \text{ a.u.}$ $R_{\text{H-H}} \approx 3.0 \text{ a.u.}$

⁺Relative to $\text{Li}+\text{H}_2$ separated limit of -232.7487 e.V.

($R_{\text{LiH}} = 3.20$ au, $R_{\text{H-H}} = 3.1$ au). Also one can see that going from the linear configuration to the right triangle configuration the barrier-height energy increases by a factor of 3; the R_{LiH} distance increases from 3.5 au to 4.0 au; and the $R_{\text{H-H}}$ distance declines slightly from 3.14 au to 3.0 au. This is a manifestation that as the three atoms get relatively closer together as they go from a linear configuration to one of a right triangle there will be more significant electron-electron repulsion terms and nuclear-nuclear repulsion terms present. These are compensated for by the increase in the saddle-point distance of LiH with only nominal decrease in H-H distance. The saddle-point values associated with the 90° VB surface for Li-H-H (right triangle configuration) were determined by extrapolation to the saddle-point region from the use of Figure 27. The saddle-point values associated with the linear and obtuse triangle conformations of the Li-H-H system were found exactly from a point grid analysis in the saddle-point region. A comparison, given in Table VII, of the VB results with a recent full CI calculation by Raff (93) for the linear Li-H-H configuration indicates that the average absolute difference between the two is 7.0 Kcal/mole. This is quite good considering the limited basis set in the VB method.

Like that of Goddard's PES (83) for the linear Li-H-H system, we see from Figure 24 that starting at the LiH end and proceeding along the reaction path that the LiH bond length increases slowly as the H atom comes closer. This would indicate that vibrational excitation is not expected to be important in overcoming the barrier height as translational energy alone should be adequate (94). The barrier height for the reverse reaction $\text{Li}+\text{H}\rightarrow\text{LiH}+\text{H}$ is 58.5 kcal for the linear configuration in reference to the $\text{Li}+\text{H}_2$ system limit energy of -232.7487 e.v.

TABLE VII

COMPARISON OF VB AND CI RESULTS FOR Li+H+H COLLINEAR SURFACE

R(1) a.u.	R(2) a.u.	R(3) a.u.	E(VB) KCAL/MOLE	E(CI) KCAL/MOLE	DIFFERENCE
3.10	3.14	6.24	8.662955	-.662663	9.345618
3.70	3.14	6.84	6.680540	3.192404	3.488136
3.30	3.14	6.44	6.945601	-.163271	7.108872
3.00	3.14	6.14	10.139468	-.398938	10.538406
3.00	3.00	6.00	10.650329	-.769223	11.419552
3.30	3.00	6.30	7.024703	-.874350	7.899053
3.50	3.00	6.50	6.185324	.308075	5.877249
3.00	3.35	6.35	8.962304	.929575	8.032729
3.30	3.35	6.65	6.232828	.436644	5.796184
3.50	3.35	6.85	6.047615	2.295172	3.752443
3.00	3.60	6.60	7.449313	.240602	7.208711
3.30	3.60	6.90	5.067035	.937412	4.129623
3.50	3.60	7.10	5.123933	2.789697	2.334236
3.15	3.60	6.75	5.803294	.214638	5.588656
3.19	3.50	6.69	6.047600	1.329157	4.718443
3.19	3.75	6.94	4.786960	.664706	4.122254
3.00	3.50	6.50	8.043720	-.023432	8.067152
3.00	3.75	6.75	6.618676	.139648	6.479028
3.50	3.75	7.25	4.527182	2.752049	1.775133
3.50	3.50	7.00	5.518760	2.232243	3.286517
2.80	3.75	6.55	10.634363	1.011103	9.623260
2.80	3.50	6.30	12.238776	.890427	11.348349
4.50	3.60	8.10	12.938518	16.711930	-3.773412
2.80	2.70	5.50	15.460360	-.338883	15.799242
3.19	2.70	5.89	6.371726	-3.943527	10.315253
3.19	1.80	4.99	-21.226045	-30.341495	9.115451
3.70	1.80	5.50	-28.936682	-34.937066	6.000384
4.50	2.25	6.75	-15.001585	-15.890923	.809338
3.70	2.25	5.95	-10.682909	-15.141223	4.458314
3.19	2.25	5.44	-3.848730	-12.205879	8.357169
4.50	2.70	7.20	1.109236	2.591980	-1.482744
3.70	2.70	6.40	2.263349	-2.533072	4.796421
4.50	1.80	6.30	-34.997399	-37.921918	2.924518
4.50	3.14	7.64	10.416530	12.220552	-1.804022
2.80	1.80	4.60	-10.591285	-22.946342	12.355057
2.50	2.70	5.20	29.832909	8.253579	21.579330
2.50	3.75	6.25	22.766542	9.207892	13.558650

AVERAGE ABSOLUTE DIFFERENCE =
7.001863 kcal/mole

Both E(VB) and E(CI) values are barrier height energies relative to the Li-H+H limit energy.

This barrier height and those for the other configurations are listed in Table VI. Also, as in Goddard's PES for the linear (Li-H₂) system (83), the H₂ bond length changes only very gradually as the Li atom approaches and does not lead naturally to the saddle point (Figure 24). This would appear to indicate that H₂ will have to be in an excited vibrational state. If the H₂ is in a low vibrational state, for example the $v = 0$ state, which has a classical turning point for H₂ of ≈ 1.75 au, very few collisions would lead to a scattering path passing near the saddle point (83).

Two-dimensional contour plots of the various LiH-H conformation are presented in Figures 24 thru 27. In Figures 31 thru there are presented perspective three-dimensional energy plots for the various Li-H-H conformations.

Results for various reaction surfaces for the LiH+D \rightarrow LiD+H exchange reaction are now presented in Figures 28-30. It was found that for conformations where the H-Li-H bond angle was 90° or greater that no saddle point was found but there existed a slight well relative to the LiH-H energy limit. The point at the minimum of the well and their associated configurations and energies are presented in Table VIII. Recent work by Raff (93) using a full CI format on these surfaces reveal no wells. Hence these very slight wells are an artifact in this study as a result of the use of Mulliken's approximation along with the fact that very little H-H bonding is occurring in those configurations where the H-Li-H bond angle is 90° or greater while appreciable bonding resonance centered on the LiH bond is present. The VB formulation used here is not as responsive to studying cases as above where there is little H-H bonding and appreciable LiH resonant bonding (ionic included)

contrary to previously discussed Li-H-H configurations where there is appreciable H-H bonding as well as LiH bonding.

TABLE VIII
WELL ENERGIES AND ASSOCIATED POINTS FOR VARIOUS
H $\overset{R}{\text{---}}$ Li $\overset{R'}{\text{---}}$ H CONFIGURATIONS

Configuration	Minimum Well Energy (kcal/mole)	Internuclear Distance at Minimum Well Energy
Linear (H-Li-H)	-1.6	R = R' = 3.55 a.u.
135° obtuse triangle (H-Li ^H)	-1.5	R = R' = 3.55 a.u.
Right triangle (H-L ^H)	-0.3	R = R' = 3.57 a.u.

*relative to the LiH+H separated limit of -230.4819 e.v.

However the results do show as the H-Li-H angle is decreased from 180° the system energy increases as one would expect, denoting a less energetically favorable reaction pathway for the D+LiH → LiD+H exchange reaction. For the H-Li-H configuration where the H-Li-H bond angle is 45° and the LiH distances are comparable to those in Table VIII, the corresponding energy (-229.211 e.v.) is considerably higher than that of the LiH+H energy illustrating what was said previously concerning the amount of H-H and LiH bonding being present.

The various H-Li-H surfaces are given in Figures 28 thru 30. The corresponding contour line values are given in Table X. The most notable feature of these surfaces beside the shallow well is the re-

TABLE IX
ENERGY CONTOUR VALUES FOR FIGURES 24 AND 25

Line No.	Energy Value
1	-232.30 e.V.
2	-231.80
3	-231.30
4	-230.90
5	-230.60
6	-230.45
7	-230.40
8	-230.36
9	-230.32
10	-230.28
11	-230.24
12	-230.20
13	-230.16
14	-230.12
15	-230.08
16	-230.04
17	-230.00
18	-229.90
19	-229.80
20	-229.70

TABLE X
 CONTOUR VALUES FOR FIGURES 26 THRU 30

Identification				Contour Value*
A	A	A	A	-15.000 Kcal/mole
B	B	B	B	-13.000
C	C	C	C	-11.000
D	D	D	D	- 9.000
E	E	E	E	- 7.000
F	F	F	F	- 5.000
G	G	G	G	- 3.000
H	H	H	H	- 2.000
I	I	I	I	- 1.000
J	J	J	J	- 0.000
K	K	K	K	- 1.000
L	L	L	L	- 2.000
M	M	M	M	- 4.000
N	N	N	N	- 6.000
O	O	O	O	10.000
P	P	P	P	15.000
Q	Q	Q	Q	20.000
R	R	R	R	25.000
S	S	S	S	30.000
T	T	T	T	35.000
U	U	U	U	40.000
V	V	V	V	45.000
W	W	W	W	50.000
X	X	X	X	55.000

*Relative to Li-H+H system limit energy.

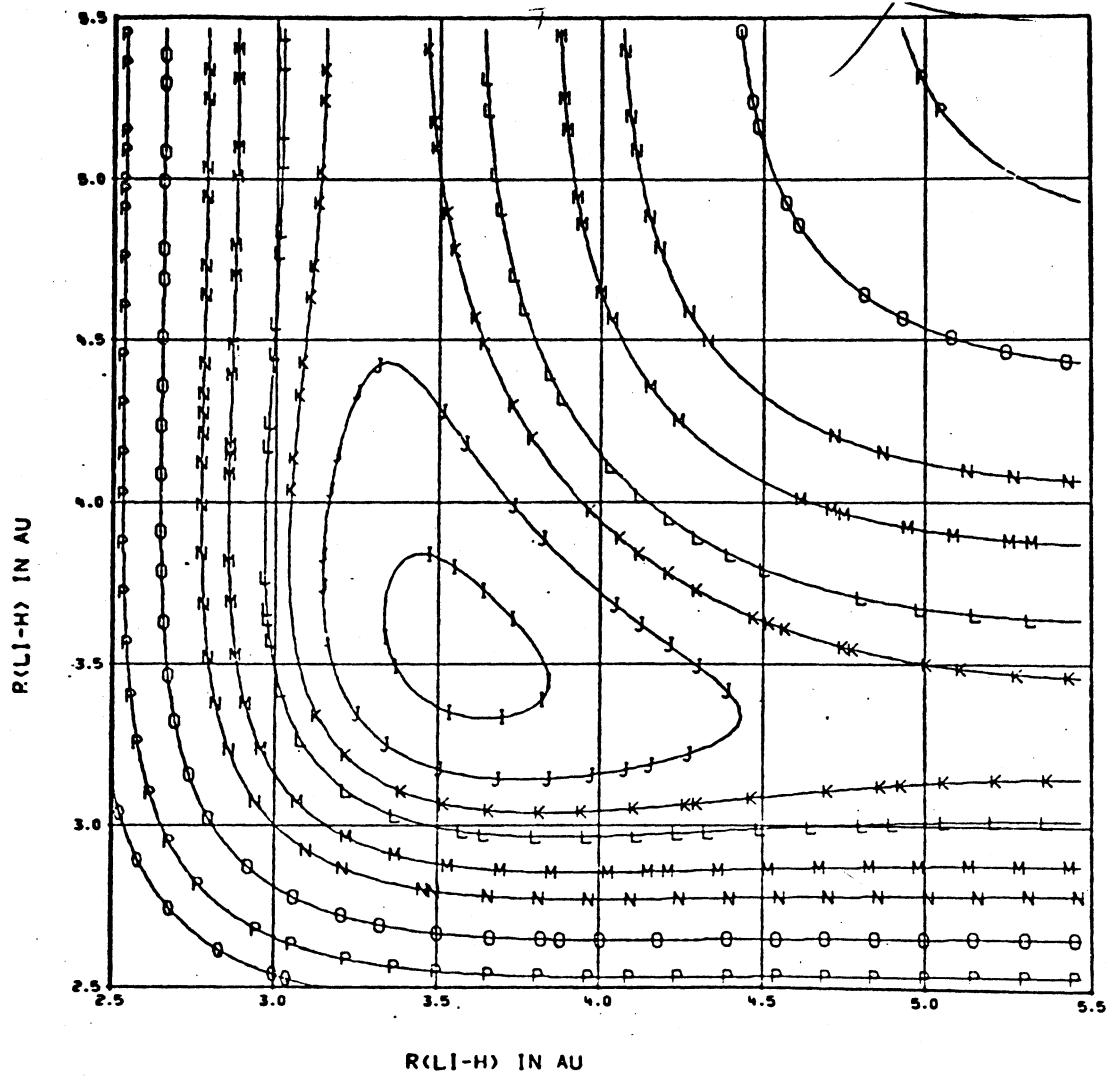


Figure 28. 135 Degree VB Surface for H-Li-H

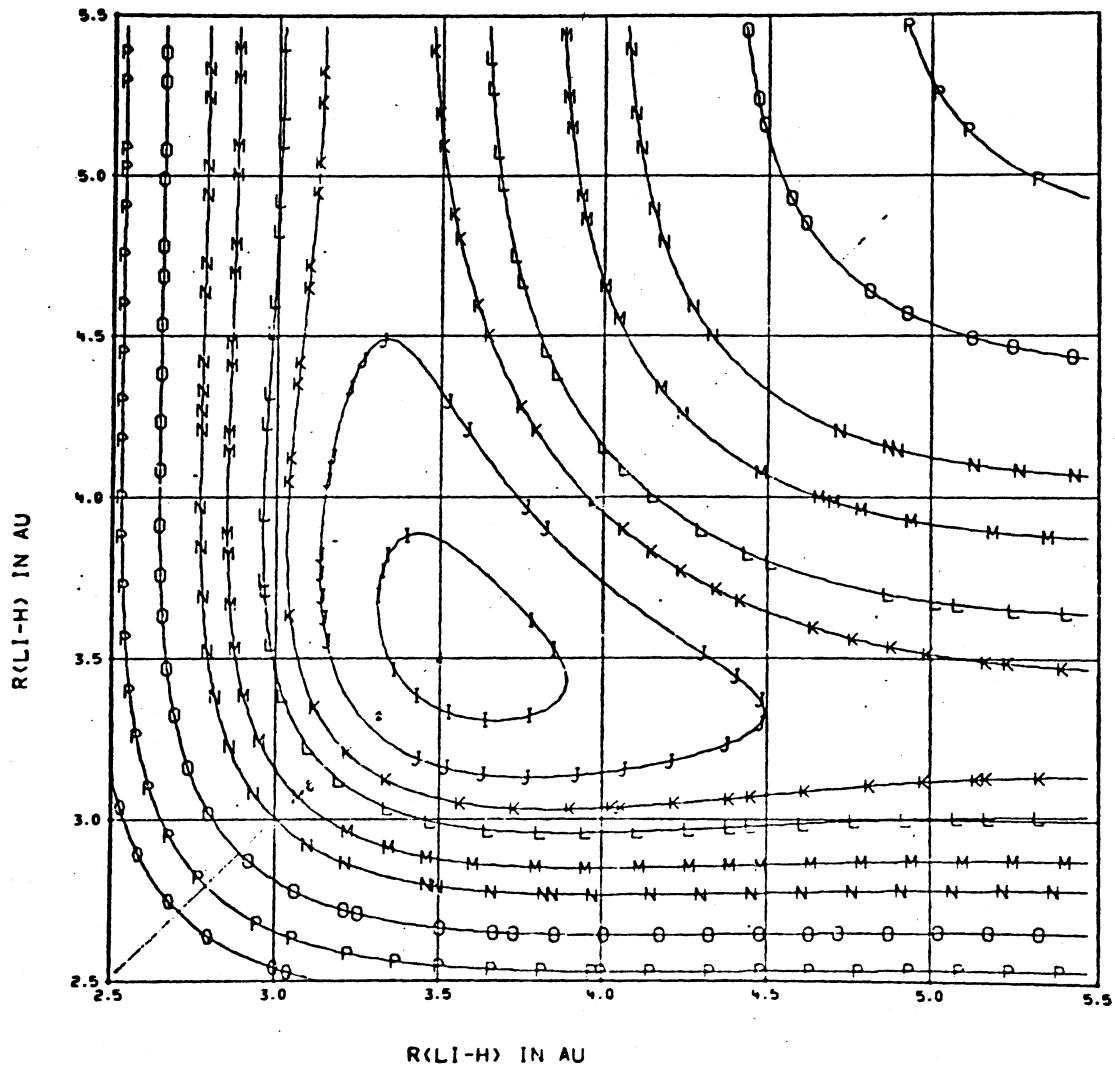


Figure 29. Collinear VB Surface for H-Li-H

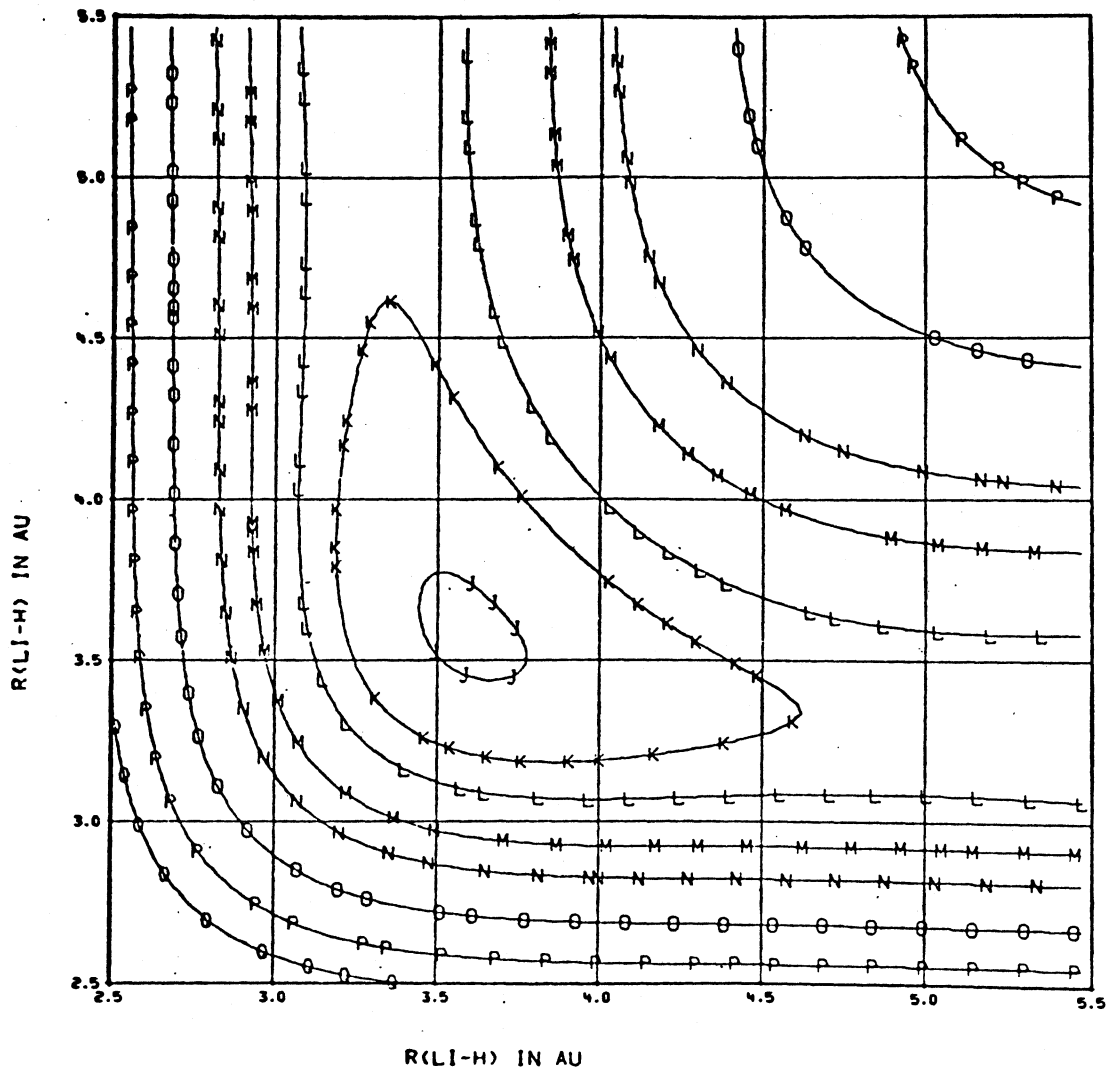


Figure 30. 90 Degree VB Surface for H-Li-H



Figure 31. 3-D Plot of Li-H-H in Linear Configuration



Figure 32. 3-D Plot of Li-H-H in 135 Obtuse Triangle Configuration

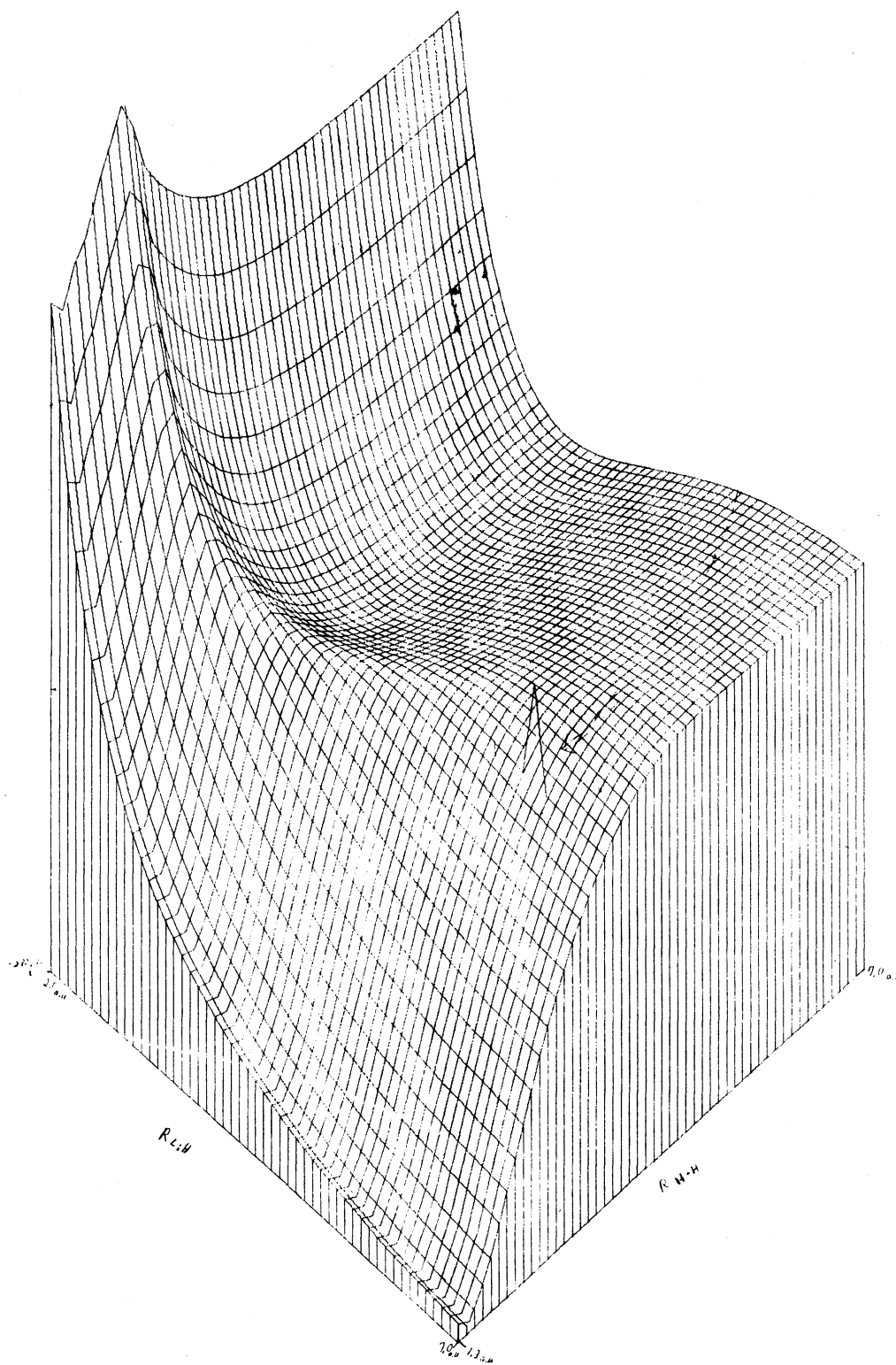


Figure 33. 3-D Plot of Li-H-H in Right Triangle Configuration

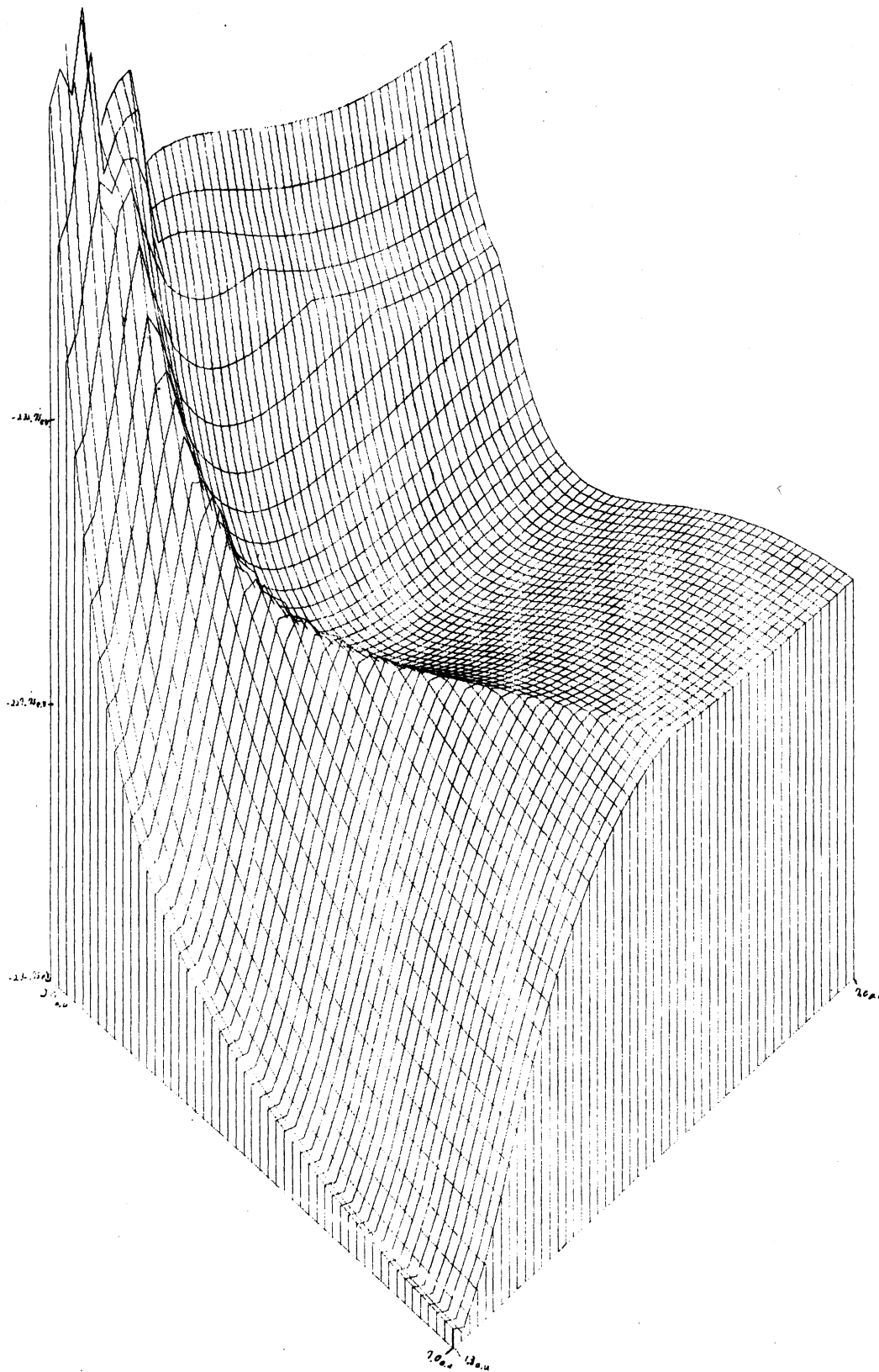


Figure 34. 3-D Plot of Li-H-H in 45 Acute Triangle Configuration

flective symmetry of the surfaces around the 45° line which indeed should be the case for these surfaces.

CHAPTER XI

CONCLUSIONS AND RECOMMENDATIONS

From the PES for the $\text{LiH}+\text{H} \rightarrow \text{Li}+\text{H}_2$ reaction it appears that the linear configuration has the lowest barrier-height energy in comparison to the obtuse triangle and right triangle configurations. This is true also for the reverse reaction $\text{Li}+\text{H}_2 \rightarrow \text{LiH}+\text{H}$. It appears that vibrational excitation of LiH is not needed in the LiH+H reactant system whereas H_2 vibrational excitation is needed in the $\text{Li}+\text{H}_2$ reactant system as indicated by the PES for the linear configuration. The barrier-height energies for the above two reactant systems in the linear configuration agree favorably with the a priori calculated activation energies for such (78).

A relative comparison of the results of this study indicate that on barrier-height energy considerations alone, the hydrogen-exchange reaction ($\text{LiH}+\text{D} \rightarrow \text{LiD}+\text{H}$) requires less energy than either the hydrogen displacement ($\text{LiH}+\text{H} \rightarrow \text{Li}+\text{H}_2$) or hydrogen addition ($\text{Li}+\text{H}_2 \rightarrow \text{LiH}+\text{H}$) reactions.

Although some artifacts appear in this study, the overall good comparison with a full CI calculation indicates that an important value of this VB study and ones in the future would be to use such to locate saddle-point regions of systems first in much less computer time than that required by a full CI type calculation. These regions then could be explored fully by the more sophisticated and complete CI method.

Thus, the VB method would be used as a screening procedure for more complete and computer time consuming methods.

A SELECTED BIBLIOGRAPHY

- (1) Freihaut, B., and L. M. Raff, *J. Chem. Phys.*, 58, 1202 (1973).
- (2) Gimarc, B. M., *J. Chem. Phys.*, 53, 1623 (1970).
- (3) Glasstone, S., K. J. Laidler, and H. Eyring, *The Theory of Rate Processes*, McGraw-Hill, New York (1941).
- (4) Karplus, M., and L. M. Raff, *J. Chem. Phys.*, 41, 1267 (1964).
- (5) Karplus, M., R. N. Porter, and R. D. Sharma, *J. Chem. Phys.*, 41, 3259 (1965).
- (6) Bauer, S. H., and E. Ossa, *J. Chem. Phys.*, 45, 434 (1966).
- (7) Farkas, A., and L. Farkas, *Proc. Roy. Soc. (London)*, A 152 124 (1935).
- (8) Baato, G., G. Careri, A. Cimino, E. Molinari, and G. G. Volpi, *J. Chem. Phys.*, 24, 783 (1956).
- (9) Niki, T., Ph.D. Thesis, University of Detroit (1971) and Mains, G. J., private communication.
- (10) Satton, E. A., *J. Chem. Phys.*, 36, 2923 (1962).
- (11) Rink, J. P., *J. Chem. Phys.*, 36, 1398 (1962).
- (12) Natl. Bur. Std. (U.S.) No. 564 (1956).
- (13) Natl. Bur. Std. (U.S.) Monograph No. 20 (1961).
- (14) Myerson, A. L., and W. S. Watts, *J. Chem. Phys.*, 49, 425 (1968).
- (15) Wilson, C. W., Jr., and W. A. Goddard III, *J. Chem. Phys.*, (51) 716 (1969).
- (16) Bauer, S. H., A. Lifshitz, and C. Lifshitz, *J. Am. Chem. Soc.* 87, 143 (1965).
- (17) Kiefer, J. H., and R. W. Latz, *J. Chem. Phys.*, 44, 658, 668 (1966).
- (18) Moreno, J. B., *Phys. Fluids*, 9, 431 (1966).

- (19) Bauer, S. H., D. Marshall, and T. Baer, J. Am. Chem. Soc. 87, 5514 (1965).
- (20) Burcat, A. and A. Lifshitz, J. Chem. Phys., 47, 3079 (1967).
- (21) Lewis, A., and S. H. Bauer, J. Am. Chem. Soc., 90, 5390 (1968).
- (22) Poulson, L. L., J. Chem. Phys., 53, 1987 (1970).
- (23) Kern, R. D., and G. G. Nika, J. Phys. Chem., 75, 1615 (1971).
- (24) Kern, R. D., and G. G. Nika, J. Phys. Chem., 75, 2541 (1971).
- (25) Bauer, S. H., D. M. Lederman, E. L. Resler, Jr., and E. R. Fisher, Int. J. Chem. Kinetics, 5, 93 (1973).
- (26) Jaffe, S. B., and J. B. Anderson, J. Chem. Phys., 51, 1057 (1969).
- (27) Sullivan, J. H., J. Chem. Phys., 46, 736 (1967).
- (28) Raff, L. M., R. N. Porter, D. L. Thompson, and L. B. Sims, J. Am. Chem. Soc., 92, 3208 (1970).
- (29) Raff, L. M., Lewis Stivers, R. N., Porter, D. L. Thompson and L. B. Sims, J. Chem. Phys., 52, 3449 (1970).
- (30) Bishop, W. P., and L. M. Dorfman, J. Chem. Phys., 52, 3210, (1970).
- (31) Eyring, H., J. Am. Chem. Soc., 53, 2537 (1931).
- (32) London, F., Z. Electrochem., 35, 552 (1929).
- (33) Benson, S. W., and G. R. Haugen, J. Am. Chem. Soc., 87, 4036 (1965).
- (34) Abrams, R. R., J. C. Patel, and F. O. Ellison, J. Chem. Phys., 49, 450 (1968).
- (35) Morokuma, R., L. Pedersen, and M. Karplus, J. Am. Chem. Soc., 89, 5064 (1967).
- (37) Sato, S., J. Chem. Phys., 23, 592, 2465 (1955).
- (38) Kolos, W., and C. C. J. Roothaan, Rev. Mod. Phys., 32, 219 (1960).
- (39) De Boer, J. Physica, 9, 363 (1942).
- (40) Margenau, H., Phys. Rev., 64, 131 (1943).
- (41) Margenau, H., Phys. Rev., 90, 1021 (1953).
- (42) Taylor, R., Proc. Phys. Soc. (London), A64, 249 (1951).

- (43) Griffing, V., and A. Macek, *J. Chem. Phys.*, 23, 1029 (1955).
- (44) Griffing, V., and J. F. Vanderslice, *J. Chem. Phys.*, 23, 1035 (1955).
- (45) Roothaan, C. C. J., *Rev. Mod. Phys.*, 23, 69 (1951).
- (46) Barker, R. E., R. L. Snow, and H. Eyring, 23, 1686 (1955).
- (47) Rufta, A. R., and V. Griffing, *J. Chem. Phys.*, 36, 1389 (1962).
- (48) Mulliken, R. S., *J. Chem. Phys.*, 46, 475 (1949).
- (49) Magnasco, V., and G. F. Musco, *J. Chem. Phys.*, 46, 4015 (1960).
- (50) Magnasco, V., and G. F. Musco, *J. Chem. Phys.*, 47, 1723 (1971).
- (51) Lowdin, P. O., *J. Chem. Phys.*, 18, 365 (1950).
- (52) Mcweeny, R., *Proc. Roy. Soc. (London)*, A223, 63, 306 (1954).
- (53) Conroy, H., and G. Malli, *J. Chem. Phys.*, 50, 5049 (1969).
- (54) Schwartz, W. E., and L. J. Schaad, *J. Chem. Phys.*, 48, 4709 (1968).
- (55) Shavitt, T., and M. Rubenstein, *J. Chem. Phys.*, 51, 716 (1969).
- (56) Wilson, C. W., Jr., and W. A. Goddard, III., *J. Chem. Phys.*, 51, 716 (1969).
- (57) Wilson, C. W., Jr., and W. A. Goddard, III., *J. Chem. Phys.*, 56, 5913 (1972).
- (58) Goddard, III., W. A., *Phys. Rev.*, 157, 81 (1967).
- (59) Slater, J. C., *Phys. Rev.*, 38, 1109 (1931).
- (60) Eyring, H., J. Walters, and G. E. Kimball, Quantum Chemistry, John Wiley and Sons, New York (1944).
- (61) Pauling, L., and E. B. Wilson, Jr., Introduction of Quantum Mechanics, McGraw-Hill, New York (1935).
- (62) Porter, R. N., and L. M. Raff, *J. Chem. Phys.*, 50, 5216 (1969).
- (63) Born, M., and J. R. Oppenheimer, *Ann. d. Phys.*, 84, 457 (1927).
- (64) Rosen, N., *Phys. Rev.*, 38, 2099 (1931).
- (65) Slater, J. C., Quantum Theory of Molecules and Solids, Vol. 1, McGraw-Hill, New York (1963).

- (66) Hastings, Jr., C., Approximations for Digital Computers, Princeton University Press, Princeton, N.J. (1955).
- (67) Companion, A. L., and R. G. Parr, *J. Chem. Phys.*, 35, 2268 (1961).
- (68) Wang, S. C., *Phys. Rev.*, 31, 519 (1928).
- (69) Glasstone, S., K. J. Laidler and H. Eyring, The Theory of Rate Processes, McGraw-Hill, New York (1941).
- (70) Karplus, M., R. N. Porter, and R. D. Sharma, *J. Chem. Phys.* 41, 3259 (1965).
- (71) Karplus, M., and L. M. Raff, *J. Chem. Phys.*, 41, 1267 (1964).
- (72) Toennies, J. P., R. David, and M. Faubel, *Chem. Phys. Lett.*, 18, (1973).
- (73) Mohler, F. I., *Phys. Rev.*, 29, 419 (1927).
- (74) Magee, J. L., and T. Ri., *J. Chem. Phys.*, 9, 638 (1941).
- (75) London, F., *Z. Electrochem.*, 35, 552 (1929).
- (76) Laidler, K. J., *J. Chem. Phys.*, 10, 34 (1942).
- (77) Mori, Y., *Bull. Chem. Soc. Japan*, 35, 1584 (1962).
- (78) Mayer, S. W., and L. Schielep, *J. Phys. Chem.*, 72, 236 (1968).
- (79) Johnston, H. S., and C. Parr, *J. Am. Chem. Soc.*, 85, 2544 (1963).
- (80) Krauss, M., *Journal of Research of N.B.S.*, 72A, 553 (1968).
- (81) Roothaan, C. C. J., *Rev. Mod. Phys.*, 32, 179 (1960).
- (82) Wahl, A. C., and G. Das, Proceedings of Conference on Potential Energy Surfaces in Chemistry, IBM Research Laboratory, W. A. Lester, Jr., Ed., 73 (1971).
- (83) Ladner, R. C., and W. A. Goddard, III., *Theoret. Chem. Acta*, to be published.
- (84) Hammond, G. S., *J. Am. Chem. Soc.*, 77, 334 (1955).
- (85) Ladner, R. C., and W. A. Goddard, III., *J. Am. Chem. Soc.*, 93, 6750 (1971).
- (86) Anderson, A. B., *Chem. Phys. Lett.*, 18, 303 (1973).
- (87) Roothaan, C. C. J., *J. Chem. Phys.*, 19, 1445 (1951).
- (88) Ruedenberg, K., C. C. J. Roothaan, and W. Jaunzemis, *J. Chem. Phys.*

24, 201 (1956).

- (89) Rosen, N., Phys. Rev., 38, 255 (1931).
- (90) Matsen, F. A., J. Miller, R. H. Friedman, and R. P. Hurst, J. Chem. Phys., 17, 1385 (1957).
- (91) Herzberg, G., Spectra of Diatomic Molecules, D. Van Nostrand Co., New York (1952).
- (92) Bender, C. F., and E. R. Davidson, J. Phys. Chem., 70, 2675 (1966).
- (93) Raff, L. M., unpublished results.
- (94) Polaryi, J. C., and W. H. Wong, J. Chem. Phys., 51, 1439 (1969).

APPENDIX A

FOR H₄ SYSTEM STUDY

List of integrals and their analytic solution

- 1) $\langle a | -\frac{1}{2}\bar{V}_1^2 | a \rangle = \delta^2 + \delta \langle a | \frac{1}{r_{1a}} | a \rangle$
- 2) $\langle a | \frac{1}{r_{1A}} | a \rangle = \delta$
- 3) $\langle a | \frac{1}{r_{1A}} | b \rangle = \delta e^{-\delta R} (\delta R + 1)$
- 4) $\langle a | \frac{1}{r_{1B}} | a \rangle = \frac{1}{R} - e^{-2\delta R} (\delta R + 1)/R$
- 5) $\langle ab | \frac{1}{r_{12}} | ab \rangle = \frac{1}{R} - \frac{e^{-2\delta R}}{R} ((\delta R)^3/6 + 3(\delta R)^2/4 + 11\delta R/8 + 1)$
- 6) $\langle ab | \frac{1}{r_{12}} | ba \rangle = .2\delta ((-e^{-2\delta R}) (-3.125 + 5.75 (2\delta R) + \frac{10}{3} (2\delta R)^2)$
 $+ (612\delta R) (Y^2 (G + \ln(2\delta R)) - W^2$
 $(\text{Ei}(-4\delta R)) + 2YW (\text{Ei}(-2\delta R)))$

where

$$Y = e^{-\delta R} (1 + \delta R + \frac{1}{3} (\delta R)^2)$$

$$W = e^{\delta R} (1 - \delta R + \frac{1}{3} (\delta R)^2)$$

$$G = .57721566$$

$$\text{Ei}(-4\delta R) = \int_{4\alpha R}^{\infty} \frac{1}{u} e^{-u} du$$

$$\text{Ei}(-2\delta R) = \int_{2\delta R}^{\infty} \frac{1}{u} e^{-u} du$$

$$7) \langle aa | \frac{1}{r_{12}} | aa \rangle = \frac{5}{8} \delta$$

$$8) \langle a | b \rangle = (1 + \delta R + \frac{1}{3} (\delta R)^2) e^{-\delta R}$$

APPENDIX B

FOR H_4 STUDY

Example of Mullikens Approximation in simplifying three and four center integrals.

$$1) \quad \langle a | \frac{1}{r_{1c}} | b \rangle \approx \frac{\langle a | b \rangle}{2} (\langle a | \frac{1}{r_{1c}} | a \rangle + \langle b | \frac{1}{r_{1c}} | b \rangle)$$

$$2) \quad \langle ab | \frac{1}{r_{12}} | cd \rangle \approx \frac{\langle a | c \rangle \langle b | d \rangle}{4} (\langle ab | \frac{1}{r_{12}} | ab \rangle + \langle ad | \frac{1}{r_{12}} | ad \rangle \\ + \langle bc | \frac{1}{r_{12}} | bc \rangle + \langle cd | \frac{1}{r_{12}} | cd \rangle)$$

$$3) \quad \langle ac | \frac{1}{r_{12}} | ad \rangle \approx \frac{\langle c | d \rangle}{2} (\langle ac | \frac{1}{r_{12}} | ac \rangle + \langle ad | \frac{1}{r_{12}} | ad \rangle)$$

APPENDIX C

FOR Li+H+H SYSTEM STUDY

OVERLAP INTEGRALS

$$\langle a | b \rangle$$

$$\langle a | c \rangle$$

$$\langle a | d \rangle$$

$$\langle c | d \rangle$$

$$\langle b | c \rangle$$

$$\langle b | d \rangle$$

EXCHANGE INTEGRALS

$$\langle ac | \frac{1}{r_{12}} | ca \rangle$$

$$\langle ad | \frac{1}{r_{12}} | da \rangle$$

$$\langle bd | \frac{1}{r_{12}} | db \rangle$$

$$\langle bc | \frac{1}{r_{12}} | ab \rangle$$

$$\langle ad | \frac{1}{r_{12}} | ab \rangle$$

$$\langle ac | \frac{1}{r_{12}} | cb \rangle$$

$$\langle cd | \frac{1}{r_{12}} | dc \rangle$$

COULOMB INTEGRALS

$$\langle ac | \frac{1}{r_{12}} | ac \rangle$$

$$\langle ad | \frac{1}{r_{12}} | ad \rangle$$

HYBRID INTEGRALS

$$\langle aa | \frac{1}{r_{12}} | ac \rangle$$

$$\langle aa | \frac{1}{r_{12}} | ad \rangle$$

COULOMB INTEGRALS

$$\langle bd | \frac{1}{r_{12}} | bd \rangle$$

$$\langle bc | \frac{1}{r_{12}} | bc \rangle$$

$$\langle ac | \frac{1}{r_{12}} | bc \rangle$$

$$\langle ad | \frac{1}{r_{12}} | bd \rangle$$

$$\langle cd | \frac{1}{r_{12}} | cd \rangle$$

HYBRID INTEGRALS

$$\langle aa | \frac{1}{r_{12}} | bc \rangle$$

$$\langle aa | \frac{1}{r_{12}} | bd \rangle$$

$$\langle ab | \frac{1}{r_{12}} | ac \rangle$$

$$\langle ab | \frac{1}{r_{12}} | ad \rangle$$

$$\langle ab | \frac{1}{r_{12}} | bc \rangle$$

$$\langle ab | \frac{1}{r_{12}} | bd \rangle$$

$$\langle bb | \frac{1}{r_{12}} | bd \rangle$$

$$\langle bb | \frac{1}{r_{12}} | bc \rangle$$

$$\langle ab | \frac{1}{r_{12}} | cb \rangle$$

$$\langle ab | \frac{1}{r_{12}} | db \rangle$$

$$\langle bd | \frac{1}{r_{12}} | dd \rangle$$

$$\langle ad | \frac{1}{r_{12}} | dd \rangle$$

COULOMB INTEGRALS

HYBRID INTEGRALS

$$\langle ac | \frac{1}{r_{12}} | cc \rangle$$

$$\langle bc | \frac{1}{r_{12}} | cc \rangle$$

$$\langle cd | \frac{1}{r_{12}} | dd \rangle$$

$$\langle cd | \frac{1}{r_{12}} | cc \rangle$$

ONE CENTER INTEGRALS

TWO CENTER INTEGRALS

THREE CENTER INTEGRALS

$$\langle aa | \frac{1}{r_{12}} | aa \rangle$$

$$\langle a | \frac{1}{r_{1A}} | c \rangle$$

$$\langle a | \frac{1}{r_{1c}} | c \rangle$$

$$\langle cc | \frac{1}{r_{12}} | cc \rangle = \langle dd | \frac{1}{r_{12}} | dd \rangle$$

$$\langle a | \frac{1}{r_{1A}} | d \rangle$$

$$\langle a | \frac{1}{r_{1b}} | d \rangle$$

$$\langle ab | \frac{1}{r_{12}} | ba \rangle$$

$$\langle c | \frac{1}{r_{1c}} | d \rangle$$

$$\langle b | \frac{1}{r_{1c}} | c \rangle$$

$$\langle bb | \frac{1}{r_{12}} | ba \rangle$$

$$\langle b | \frac{1}{r_{1A}} | c \rangle$$

$$\langle b | \frac{1}{r_{1B}} | d \rangle$$

$$\langle a | \frac{1}{r_{1A}} | a \rangle$$

$$\langle b | \frac{1}{r_{1A}} | d \rangle$$

$$\langle c | \frac{1}{r_{1A}} | d \rangle$$

$$\langle a | \frac{1}{r_{1A}} | b \rangle$$

$$\langle c | -\frac{1}{2}\nabla^2 | d \rangle$$

$$\langle aa | \frac{1}{r_{12}} | cd \rangle$$

$$\langle b | \frac{1}{r_{1A}} | b \rangle$$

$$\langle a | -\frac{1}{2}\nabla^2 | c \rangle$$

$$\langle ab | \frac{1}{r_{12}} | cd \rangle$$

$$\langle c | \frac{1}{r_{1B}} | c \rangle = \langle d | \frac{1}{r_{1C}} | d \rangle$$

$$\langle b | -\frac{1}{2}\nabla^2 | c \rangle$$

$$\langle bd | \frac{1}{r_{12}} | cb \rangle$$

ONE CENTER INTEGRALS

TWO CENTER INTEGRALS

THREE CENTER INTEGRALS

$$\langle a | -\frac{1}{2}\nabla^2 | a \rangle$$

$$\langle a | -\frac{1}{2}\nabla^2 | d \rangle$$

$$\langle ab | \frac{1}{r_{12}} | dc \rangle$$

$$\langle b | -\frac{1}{2}\nabla^2 | b \rangle$$

$$\langle b | -\frac{1}{2}\nabla^2 | d \rangle$$

$$\langle ac | \frac{1}{r_{12}} | cd \rangle$$

$$\langle b | -\frac{1}{2}\nabla^2 | a \rangle$$

$$\langle c | \frac{1}{r_{1A}} | c \rangle$$

$$\langle ad | \frac{1}{r_{12}} | cd \rangle$$

$$\langle c | -\frac{1}{2}\nabla^2 | c \rangle = \langle d | -\frac{1}{2}\nabla^2 | d \rangle$$

$$\langle d | \frac{1}{r_{1A}} | d \rangle$$

$$\langle bd | \frac{1}{r_{12}} | cd \rangle$$

$$\langle d | \frac{1}{r_{1B}} | d \rangle$$

$$\langle ac | \frac{1}{r_{12}} | dc \rangle$$

$$\langle d | \frac{1}{r_{1C}} | c \rangle$$

$$\langle bc | \frac{1}{r_{12}} | dc \rangle$$

$$\langle a | \frac{1}{r_{1B}} | a \rangle$$

$$\langle ad | \frac{1}{r_{12}} | dc \rangle$$

$$\langle b | \frac{1}{r_{1B}} | b \rangle$$

$$\langle bc | \frac{1}{r_{12}} | cd \rangle$$

$$\langle b | \frac{1}{r_{1C}} | b \rangle$$

$$\langle ac | \frac{1}{r_{12}} | bd \rangle$$

$$\langle a | \frac{1}{r_{1C}} | a \rangle$$

$$\langle bd | \frac{1}{r_{12}} | dc \rangle$$

$$\langle a | \frac{1}{r_{1B}} | b \rangle$$

$$\langle ac | \frac{1}{r_{12}} | ad \rangle$$

$$\langle a | \frac{1}{r_{1C}} | b \rangle$$

$$\langle bc | \frac{1}{r_{12}} | bd \rangle$$

$$\langle a | \frac{1}{r_{1B}} | c \rangle$$

ONE CENTER INTEGRALS

TWO CENTER INTEGRALS

THREE CENTER INTEGRALS

$$\langle a | \frac{1}{r_{1C}} | d \rangle$$

$$\langle c | \frac{1}{r_{1B}} | d \rangle$$

$$\langle b | \frac{1}{r_{1B}} | c \rangle$$

$$\langle b | \frac{1}{r_{1C}} | d \rangle$$

VITA

Bart Harold Freihaut

Candidate for the Degree of

Doctor of Philosophy

Thesis: STUDIES OF VALENCE-BOND BASED QUANTUM MECHANICAL POTENTIAL-ENERGY SURFACES: PART I: $H_2 + D_2$ EXCHANGE REACTION - PART II: $LiH + H \rightarrow Li + H_2$ AND $LiH + D \rightarrow LiD + H$ REACTIONS

Major Field: Chemistry

Biographical:

Personal Data: I was born on January 28, 1943 in St. Louis, Mo., of Quentin and Dorothy Freihaut. I graduated in June, 1961 from Christian Brothers High School in Clayton, Mo. I attended Christian Brothers College in Memphis, Tenn., graduating cum laude with a B.S. in engineering chemistry in June, 1965. I attended graduate school at Oklahoma State University, Stillwater, Oklahoma in Sept. 1965 majoring in physical chemistry, where I will graduate from, in January, 1976 with a Doctor of Philosophy in Chemistry. I married Leticia Birao on August 12, 1973 and on June 18, 1974 twin girls, Beverly and Lorraine were born.

Professional Experience: My work experience includes that of a graduate teaching assistant in freshman chemistry labs and in physical chemistry labs, process chemical engineer for two years with Shell Oil Co., instructor at St. Gregory's College, Shawnee, Oklahoma for one year, research chemist at Community Blood Center in Kansas City, Mo., for 1½ years, instructor in the School of Technology at Oklahoma State University for one semester, and process engineer with Ethyl Corporation.

Professional Affiliations: I am a member in the Phi Lambda Upsilon Honorary Chemical Society, the American Chemical Society, Who's Who Among Students in American Colleges and Universities.